

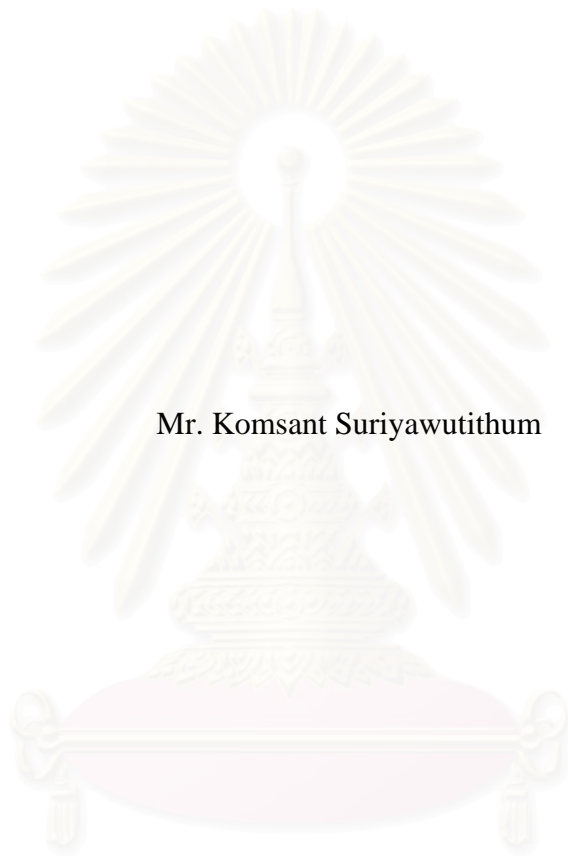
การเตรียมหลุมอัดและหลุมผลิตแวนอนเพื่อให้ได้ประสิทธิภาพสูงสุด



นายคมสันต์ สุริยาอุทัยธรรม

สถาบันวิทยบริการ
จุฬาลงกรณ์มหาวิทยาลัย
วิทยานิพนธ์นี้เป็นส่วนหนึ่งของการศึกษาตามหลักสูตรปริญญาวิศวกรรมศาสตรมหาบัณฑิต
สาขาวิชาวิศวกรรมปิโตรเลียม ภาควิชาวิศวกรรมเหมืองแร่และปิโตรเลียม
คณะวิศวกรรมศาสตร์ จุฬาลงกรณ์มหาวิทยาลัย
ปีการศึกษา 2551
ลิขสิทธิ์ของจุฬาลงกรณ์มหาวิทยาลัย

OPTIMAL COMPLETION FOR HORIZONTAL INJECTOR AND PRODUCER



Mr. Komsant Suriyawutithum

A Thesis Submitted in Partial Fulfillment of the Requirements
for the Degree of Master of Engineering Program in Petroleum Engineering

Department of Mining and Petroleum Engineering

Faculty of Engineering

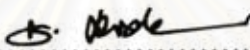
Chulalongkorn University

Academic Year 2008

Copyright of Chulalongkorn University

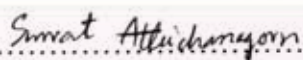
Thesis Title OPTIMAL COMPLETION FOR HORIZONTAL
 INJECTOR AND PRODUCER
By Mr. Komsant Suriyawutithum
Field of Study Petroleum Engineering
Thesis Advisor Assistant Professor Suwat Athichanagorn, Ph.D.

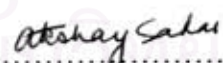
Accepted by the Faculty of Engineering, Chulalongkorn University in
Partial Fulfillment of the Requirements for the Master's Degree


..... Dean of the Faculty of Engineering
(Associate Professor Boonsom Lerthirunwong, Dr.Ing.)

THESIS COMMITTEE


..... Chairman
(Associate Professor Sarithdej Pathanasetpong)


..... Advisor
(Assistant Professor Suwat Athichanagorn, Ph.D.)


..... Examiner
(Akshay Sahni, Ph.D.)

สถาบันวิจัยวิศวกรรม
จุฬาลงกรณ์มหาวิทยาลัย

คมสันต์ สุริยวณิชธรรม: การเตรียมหลุมอัดและหลุมผลิตแนวนอนเพื่อให้ได้ประสิทธิภาพสูงสุด (OPTIMAL COMPLETION FOR HORIZONTAL INJECTOR AND PRODUCER)
 อ.ที่ปรึกษาวิทยานิพนธ์หลัก: ผศ. ดร. สุวัฒน์ อธิชนากร, 113 หน้า.

หลุมแนวนอนถูกนำมาใช้ในการเพิ่มประสิทธิภาพการผลิตไฮโดรคาร์บอนในกระบวนการอัดน้ำแทนที่มาเป็นเวลานานแล้ว เนื่องจากให้ประสิทธิภาพการกวาดได้ดีกว่าหลุมแนวตั้ง ในการศึกษาการไล่ด้วยน้ำหลายครั้งมีการจำลองหลุมแนวนอนโดยไม่คำนึงถึงความเสียดทานซึ่งทำให้ได้ประสิทธิภาพเกินจริง เนื่องจากแรงเสียดทานในส่วนแนวนอนจะทำให้เกิดความดันที่แตกต่างมากระหว่างภายในหลุมกับแหล่งกักเก็บบริเวณช่วงต้น และความดันที่แตกต่างน้อยที่บริเวณปลายของหลุมอัดน้ำและหลุมผลิตแนวนอนทำให้เกิดระนาบของน้ำที่ไม่สม่ำเสมอ ซึ่งเป็นผลให้ประสิทธิภาพการกวาดลดลงและน้ำเข้ามาถึงหลุมผลิตเร็วขึ้น ในการรักษาระนาบของน้ำให้สม่ำเสมอนั้น ต้องมีการออกแบบช่วงเปิดและปิดในการเตรียมหลุมอย่างระมัดระวัง การเตรียมหลุมที่ทำให้เกิดระนาบของน้ำที่สม่ำเสมอนั้นเรียกว่าการเตรียมหลุมที่ได้ประสิทธิภาพสูงสุด

ในการศึกษานี้ใช้โปรแกรมจำลองแหล่งกักเก็บเพื่อหาการเตรียมหลุมที่ได้ประสิทธิภาพสูงสุด โดยใช้แบบจำลองหลุมแบบหลายส่วนในแหล่งกักเก็บแบบเนื้อเดียวกัน การจำลองถูกคำนวณขึ้นภายใต้อัตราการไหลและอัตราส่วน โมบิลิตีของของไหลที่ถูกอัดและถูกผลิตต่างๆ เพื่อหาว่า ที่สภาวะใดที่การเตรียมหลุมที่ได้ประสิทธิภาพสูงสุดมีผลต่อการเพิ่มการผลิตมาก ผลจากการจำลองบ่งชี้ว่า การเตรียมหลุมให้ได้ประสิทธิภาพสูงสุคนั้นดีกว่าการเตรียมหลุมแบบเปิดเท่ากันทุกช่วงในกรณีที่มีอัตราการไหลมากและในกรณีที่มีอัตราส่วน โมบิลิตีมาก

สถาบันวิทยบริการ จุฬาลงกรณ์มหาวิทยาลัย

ภาควิชา วิศวกรรมเหมืองแร่และปิโตรเลียม ลายมือชื่อนิสิต.....คมสันต์ สุริยวณิชธรรม.....
 สาขาวิชา วิศวกรรมปิโตรเลียม ลายมือชื่อ.ที่ปรึกษาวิทยานิพนธ์หลัก.....สม อธิชนากร.....
 ปีการศึกษา 2551

4971603021 : MAJOR PETROLEUM ENGINEERING

KEYWORDS: FLOW DISTRIBUTION/ WATERFLOODING / HORIZONTAL WELL / WELL COMPLETION / HORIZONTAL INJECTOR / HORIZONTAL PRODUCER

KOMSANT SURIYAWUTITHUM.: OPTIMAL COMPLETION FOR HORIZONTAL INJECTOR AND PRODUCER. THESIS ADVISOR: ASST. PROF. SUWAT ATHICHANAGORN, Ph.D., 113 pp.

Horizontal wells have long been used to improve hydrocarbon recovery efficiency in waterflooding process because they provide better sweep efficiency than conventional vertical wells. Many waterflooding studies modeled the horizontal wells as non-friction wells, which overestimated the well performance. Due to friction pressure loss along the horizontal section, there exists a high pressure difference between the wellbore and the reservoir near the heel and low pressure difference near the toe of the injector and producer, generating a non-uniform water front. This results in reduction of areal sweep efficiency and early breakthrough. In order to keep the flood front uniform, the well cannot be uniformly completed but must be carefully designed for closed and open intervals. The completions that give rise to uniform front of water flowing out of the injector to the producer are referred to as optimal completion.

In this study, a reservoir simulator was used to develop the optimal completion along the horizontal length via multi-segment well model in a homogeneous reservoir. A methodology to develop such completion is described. Several simulation runs were performed under different operating flow rates and mobility ratios of the injected and produced fluids to determine which conditions the optimal completion has high impact on recovery improvement. The simulation results indicate that optimal completion is recommended over conventional completion with equally completed intervals when in case with high operating flow rate and high mobility ratio.

Department: Mining and Petroleum Engineering Student's Signature: *[Signature]*
 Field of Study: Petroleum Engineering Advisor's Signature: *[Signature]*
 Academic Year: 2008

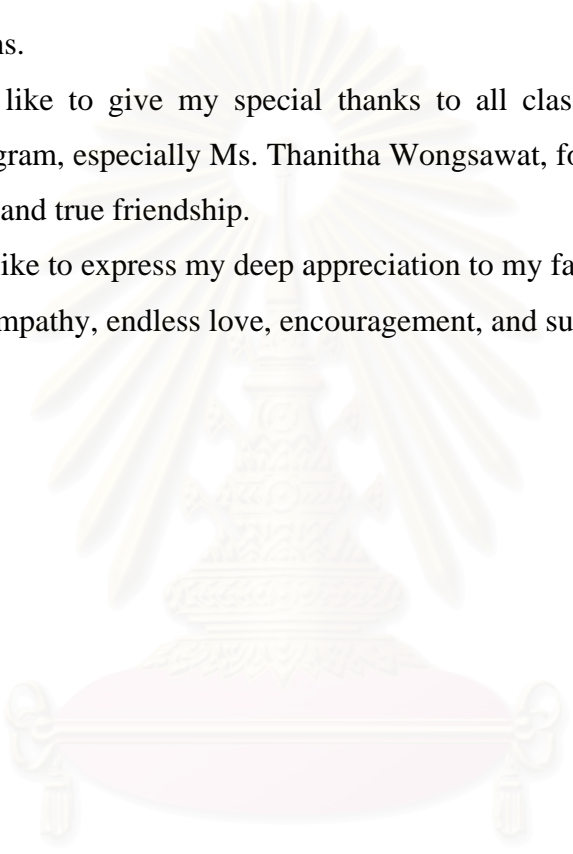
ACKNOWLEDGEMENTS

I would like to express my appreciation to my advisor, Dr. Suwat Athichanagorn, for giving knowledge of petroleum engineering and invaluable guidance during this study.

I wish to thank the thesis committee members for their comments and recommendations.

I would like to give my special thanks to all classmates in the petroleum engineering program, especially Ms. Thanitha Wongsawat, for invaluable discussions, encouragement, and true friendship.

I would like to express my deep appreciation to my family and my friends who give me their sympathy, endless love, encouragement, and support



สถาบันวิทยบริการ
จุฬาลงกรณ์มหาวิทยาลัย

CONTENTS

	Page
Abstract (Thai)	iv
Abstract (English)	v
Acknowledgements	vi
Contents	vii
List of Tables	x
List of Figures	xi
List of Abbreviations	xvii
Nomenclature	xviii
 CHAPTER	
I Introduction	1
1.1 Outline of Methodology.....	2
1.2 Thesis Outline.....	3
 II Literature Review	 4
 III Theories and Concepts	 7
3.1 Horizontal Wells.....	7
3.1.1 Horizontal Well Completions.....	7
3.1.2 Pressure Drop through a Horizontal Well.....	9
3.2 Waterflooding.....	10
3.2.1 Fluid Displacement.....	10
3.2.2 Conventional Waterflooding.....	13
3.2.3 Waterflooding with Horizontal Wells.....	14
3.3 Reservoir Simulation.....	15
3.3.1 Multi-segment Well Model.....	15
3.3.2 LGR Model.....	18
 IV Development of Optimal Completion	 19
4.1 Model Description.....	19

CHAPTER	Page
4.1.1 Reservoir Model.....	20
4.1.2 Local Grid Refinement.....	21
4.1.3 Horizontal Well Model.....	22
4.1.4 Fluid and SCAL Properties.....	25
4.2 Simulation Study.....	26
4.2.1 Compare the Performance between Direct and Inverted Line Drive Patterns	27
4.2.2 Development of Optimal Completion.....	31
4.2.3 Comparison of Optimal Completion and Equally Open Completion.....	49
V Effect of Flow Rate and Mobility Ratio.....	54
5.1 Optimal Completion with Different Flow Rates.....	54
5.1.1 Effect on Optimal Flow Distribution and Open Interval.....	55
5.1.2 Effect on Sweep Efficiency at Breakthrough.....	57
5.1.3 Effect on Watercut and Recovery Efficiency at Abandonment.....	62
5.1.4 Effect on Bottomhole Pressure.....	65
5.2 Optimal Completion with Different Mobility Ratios.....	67
5.2.1 Effect on Optimal Flow Distribution and Open Interval.....	69
5.2.2 Effect on Sweep Efficiency at Breakthrough.....	71
5.2.3 Effect on Watercut and Recovery Efficiency at Abandonment.....	75
5.2.4 Effect on Bottomhole Pressure.....	77
VI Conclusions and Remarks.....	80
6.1 Conclusions.....	80
6.2 Remarks.....	81
References.....	83
Appendices.....	85
Appendix A.....	86

CHAPTER	Page
Appendix B.....	103
Vitae.....	113



สถาบันวิทยบริการ
จุฬาลงกรณ์มหาวิทยาลัย

LIST OF TABLES

		Page
Table 4.1	Reservoir model description and reservoir properties.....	20
Table 4.2	Well conditions.....	23
Table 4.3	Fluid properties.....	26
Table 4.4	Base case conditions.....	27
Table 4.5	Comparison of reference flow profiles between before and after normalization.....	39
Table 4.6	The normalized reference flow fraction profiles after symmetrical adjustment.....	40
Table 4.7	The normalized reference flow fraction profiles after subtracting by 0.1.....	40
Table 4.8	Comparison of the target flow distribution for injection rate of 6,000 RB/D with different profile factors.....	44
Table 4.9	Comparison of the target flow distribution for production rate of 3,000 RB/D with different profile factors.....	44
Table 4.10	Waterflooding performance at breakthrough for different flow profiles.....	47
Table 4.11	Summary of compare case conditions.....	49
Table 4.12	Comparison of waterflooding performance for different completions.....	50
Table 4.13	Comparison of open interval fraction for different completions....	52
Table 5.1	Summary of the sweep efficiency at breakthrough obtained from different completions and operating flow rates.....	61
Table 5.2	Summary of the sweep efficiency at breakthrough obtained from different completions and mobility ratios.....	74

LIST OF FIGURES

	Page
Figure 2.1 Comparison of sweep efficiencies.....	5
Figure 2.2 The waterflooding pattern and well geometry.....	5
Figure 3.1 Sample of wire wrapped screen.....	8
Figure 3.2 Different completion methods for horizontal wells.....	8
Figure 3.3 Completion assembly schematic inflow control system in horizontal well.....	9
Figure 3.4 Different flow profiles for horizontal wells.....	10
Figure 3.5 Relative permeability curve for oil and water.....	11
Figure 3.6 Stable and unstable displacement in the horizontal plane.....	12
Figure 3.7 Gravity tonguing.....	12
Figure 3.8 Flooding patterns.....	13
Figure 3.9 Comparison of flooded areas for $M = 10, 1$ and 0.1 for direct line drive pattern.....	14
Figure 3.10 Well orientation of different flooding patterns.....	14
Figure 3.11 Waterflooding by infill drilled horizontal wells.....	15
Figure 3.12 Structure of multi-segment well model.....	16
Figure 3.13 Flow components in multi-segment well model.....	16
Figure 3.14 The concept of LGR model.....	18
Figure 4.1 Reservoir model.....	20
Figure 4.2 Local Grid Refinement near horizontal producer.....	21
Figure 4.3 Cemented and perforated completion used in the simulation.....	22
Figure 4.4 Multi-segment well model represent the cased and perforated horizontal wells.....	22
Figure 4.5 Location of producer and injector.....	24
Figure 4.6 Relative permeability curve.....	25
Figure 4.7 Well location compared between 2 patterns.....	26
Figure 4.8 Saturation distribution at breakthrough using direct line drive pattern.....	28

Figure 4.9	Saturation distribution at breakthrough using inverted line drive pattern.....	29
Figure 4.10	Comparison of water front development by the two patterns.....	30
Figure 4.11	Flow distribution along the horizontal well model without friction loss consideration.....	31
Figure 4.12	Flow regime along the horizontal wells.....	32
Figure 4.13	Saturation distribution at breakthrough when using non-friction well model.....	36
Figure 4.14	Saturation distribution at breakthrough when using frictional well with flow distribution emulating the non-friction well model...	36
Figure 4.15	Development of water front by non-ideal friction-free model.....	37
Figure 4.16	Comparison between saturation distribution at breakthrough obtained from two studies.....	38
Figure 4.17	Normalized reference flow fraction profile.....	40
Figure 4.18	The plots of flow fraction offset versus location in a unit-length horizontal section for injector and producer.....	41
Figure 4.19	Comparison of flow fraction offset profiles for the injector between different profile factors.....	42
Figure 4.20	Comparison of flow fraction offset profiles for the producer between different profile factors.....	43
Figure 4.21	Saturation distribution at breakthrough for profile factor of 2.....	45
Figure 4.22	Saturation distribution at breakthrough for profile factor of 3.....	45
Figure 4.23	Saturation distribution at breakthrough for profile factor of 4.....	46
Figure 4.24	Saturation distribution at breakthrough for profile factor of 5.....	46
Figure 4.25	Saturation distribution at breakthrough for profile factor of 6.....	47
Figure 4.26	Development of water front by optimal completion.....	48
Figure 4.27	Saturation distribution at breakthrough for profile factor of 5 in direct line drive pattern.....	49
Figure 4.28	Comparison of flow distributions at the producer for equally open and optimal completion.....	50
Figure 4.29	Comparison between watercut profiles for different completions....	51

Figure 4.30	Comparison between recover efficiency profile for different completions.....	51
Figure 4.31	Comparison between BHP history for different completions.....	52
Figure 5.1	The normalized reference flow fraction profiles for different operating flow rates.....	55
Figure 5.2	Comparison between optimal flow distributions at the producers for different flow rates.....	56
Figure 5.3	Comparison between optimal completions strategies at the producers for different flow rates.....	56
Figure 5.4	Comparison between average pressure profiles for different operating flow rates.....	57
Figure 5.5	Comparison of recovery at breakthrough for different operating flow rates	58
Figure 5.6	Saturation distribution at breakthrough using optimal completion for operating rate of 6,000 RB/D.....	59
Figure 5.7	Saturation distribution at breakthrough using optimal completion for operating rate of 8,000 RB/D.....	59
Figure 5.8	Saturation distribution at breakthrough using optimal completion for operating rate of 10,000 RB/D.....	60
Figure 5.9	Saturation distribution at breakthrough using optimal completion for operating rate of 12,000 RB/D.....	60
Figure 5.10	Comparison of saturation distribution at breakthrough when operating at 12,000 RB/D with different completions.....	62
Figure 5.11	Watercut profile obtained from optimal completion for different operating flow rates.....	63
Figure 5.12	Recovery efficiency obtained from optimal completion for different operating flow rates.....	63
Figure 5.13	Comparison of recovery factor at abandonment for different completions at various operating flow rates.....	64
Figure 5.14	Comparison of producer's BHP history for different operating flow rates.....	65

Figure 5.15	Comparison of injector's BHP history for different operating flow rates.....	66
Figure 5.16	Difference of producer's BHP before breakthrough between equally open completion and optimal completion for different operating flow rates.....	67
Figure 5.17	The normalized reference flow fraction profiles for different mobility ratios.....	68
Figure 5.18	Comparison between saturation distributions at breakthrough Obtained from non-friction well model for different mobility ratio..	68
Figure 5.19	Comparison between optimal flow distribution at producers for different mobility ratios.....	69
Figure 5.20	Comparison between optimal completion strategies at producers for different mobility ratios.....	70
Figure 5.21	Comparison of pressure drop components at producers for different mobility ratios.....	71
Figure 5.22	Saturation distribution at breakthrough using optimal completion for mobility ratio of 1.....	72
Figure 5.23	Saturation distribution at breakthrough using optimal completion for mobility ratio of 3.....	72
Figure 5.24	Saturation distribution at breakthrough using optimal completion for mobility ratio of 5.....	73
Figure 5.25	Saturation distribution at breakthrough using optimal completion for mobility ratio of 10.....	73
Figure 5.26	Comparison of saturation distribution at breakthrough when mobility ratio is 10 for different completions.....	74
Figure 5.27	Watercut profiles for different mobility ratios.....	75
Figure 5.28	Recovery factors at 90% watercut for different mobility ratios.....	76
Figure 5.29	Comparison of recovery factor at abandonment for different completions at various mobility ratios.....	77
Figure 5.30	Comparison of producer's BHP history for different mobility ratios.....	78

Figure 5.31	Difference of producer's BHP before breakthrough between equally open completion and optimal completion for different mobility ratios.....	79
Figure B1	Comparison of watercut and recovery profile obtained from the Base case and the optimal completion for the operating flow rate Of 6,000 RB/D and mobility ratio of 1.....	103
Figure B2	Comparison of watercut and recovery profile obtained from the Base case and the optimal completion for the operating flow rate Of 8,000 RB/D and mobility ratio of 1.....	104
Figure B3	Comparison of watercut and recovery profile obtained from the Base case and the optimal completion for the operating flow rate Of 10,000 RB/D and mobility ratio of 1.....	105
Figure B4	Comparison of watercut and recovery profile obtained from the Base case and the optimal completion for the operating flow rate Of 12,000 RB/D and mobility ratio of 1.....	106
Figure B5	Comparison of watercut and recovery profile obtained from the Base case and the optimal completion for the operating flow rate Of 6,000 RB/D and mobility ratio of 3.....	107
Figure B6	Comparison of watercut and recovery profile obtained from the Base case and the optimal completion for the operating flow rate Of 6,000 RB/D and mobility ratio of 5.....	108
Figure B7	Comparison of watercut and recovery profile obtained from the Base case and the optimal completion for the operating flow rate Of 6,000 RB/D and mobility ratio of 10.....	109
Figure B8	Saturation distribution at breakthrough time for equally open completion in direct line drive pattern with operating flow rate of 6,000 RB/D and mobility ratio of 1.....	110
Figure B9	Saturation distribution at breakthrough time for equally open completion in inverted line drive pattern with operating flow rate of 6,000 RB/D and mobility ratio of 1.....	111

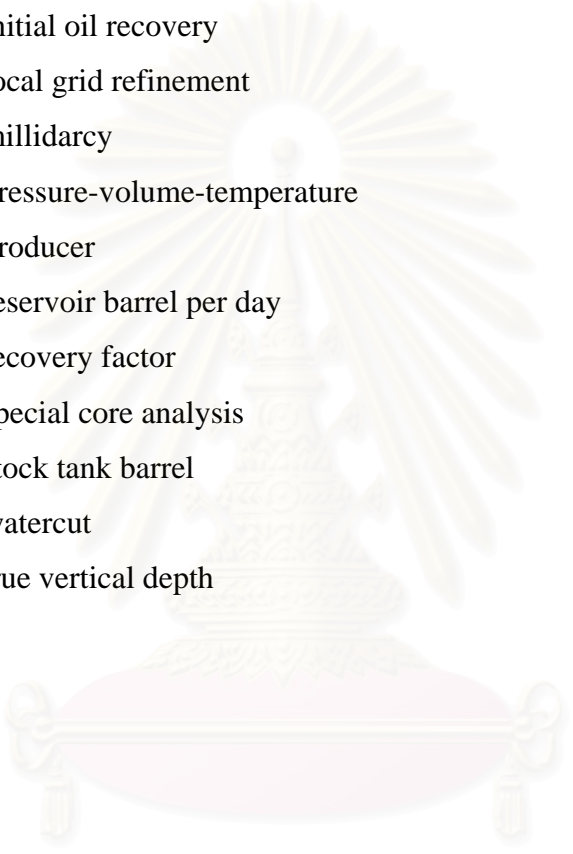
Figure B10 Saturation distribution at breakthrough time for optimal completion in inverted line drive pattern with operating flow rate of 6,000 RB/D and mobility ratio of 1.....	112
---	-----



สถาบันวิทยบริการ
จุฬาลงกรณ์มหาวิทยาลัย

LIST OF ABBREVIATIONS

BHP	bottomhole pressure
cp	centipoises
INJ	injector
IOR	initial oil recovery
LGR	local grid refinement
md	millidarcy
PVT	pressure-volume-temperature
PROD	producer
RB/D	reservoir barrel per day
RF	recovery factor
SCAL	special core analysis
STB	stock tank barrel
WCT	watercut
TVD	true vertical depth



สถาบันวิทยบริการ
จุฬาลงกรณ์มหาวิทยาลัย

NOMENCLATURE

$\frac{dp}{dL}$	pressure drop per unit length
k	absolute permeability
k_r	relative permeability
k_{ro}	relative permeability of oil
k_{rw}	relative permeability of water
k_w	permeability of water
L	distance between injector and producer
L_w	horizontal section length
M	mobility ratio
p	pressure
S_w	water saturation
S_{wc}	connate water saturation
W	pattern width

GREEK LETTERS

Φ	porosity
μ	viscosity
μ_o	oil viscosity
μ_w	water viscosity

CHAPTER I

INTRODUCTION

The use of horizontal well technology improves the overall efficiency of various recovery processes. Using horizontal wells in a waterflooding process, higher sweep efficiency for less cost can be achieved when compared to the use of vertical wells.

Horizontal wells are generally used to improve recovery by increasing reservoir drainage area, increasing production rate and delaying water and gas coning. In waterflooding processes, these advantages of horizontal wells provide better sweep efficiency, and production and injection rate than conventional vertical wells.

There have been many works studying the effect of horizontal flooding on recovery efficiency. However, many studies modeled the horizontal wells as infinite conductivity or non-friction sections, which resulted in better performance compared to friction well models. The reason is the pressure loss along the horizontal wells may significantly affect on the recovery efficiency. Due to the friction pressure loss along the horizontal section of the well, high drawdown pressure near the heel generally exists. Accordingly, non uniform distribution of the well bore pressure along the horizontal section of the well generates a non uniform flow profile. This results in reduction of sweep efficiency and early breakthrough.

From previous reservoir simulation studies, it was found that more than 90% sweep efficiency can be obtained when using horizontal producer and injector, without frictional pressure loss consideration. The key to this appealing result is non-friction horizontal well generates uniform flux along the horizontal section.

This thesis focuses on maximizing sweep efficiency by carefully designing appropriate completion intervals. The different completion techniques, such as slotted liner and Inflow Control Devices (ICD), can be designed to achieve the same flow profile established in this study.

1.1 Outline of Methodology

The concept of this thesis comes from the uniform flow profile when flooding with non-friction wells in the simulation. By using Multi-segment well, the flow rate in each segment of the horizontal section can be obtained. So we can emulate this flow profile by using the well model with friction loss consideration and improve the flow profile by adjusting the perforation intervals to get the optimal completion. Finally, we compare the results with different flooding scenarios to see how the sweep efficiency and recovery can be improved.

A waterflooding process with the injectors at the bottom and producers at the top will be simulated using ECLIPSE 100 reservoir simulator. The multi-segment well model was selected to model both the producers and injectors. The procedure for this study is as follows:

1. Build reservoir and wells model to represent a flooding pattern.
2. Design initial completion interval as equally open completion.
3. Run the simulations with the direct and inverted line drive patterns to determine the most preferable pattern.
4. Run the simulation with the well model without pressure loss consideration and record the flow rate from each segment to establish the target flow distribution.
5. Run the simulation with the well model with friction loss consideration and record flow rate from each segment.
6. Adjust the open interval of each segment based on the observed flow rates from step 5 to obtain the completion strategy that gives the target flow distribution in step 4. Then, record the saturation distribution, sweep efficiency, and recovery factor.
7. Adjust the perforation intervals based on the saturation distribution in step 6 to obtain the completion strategy that gives the highest sweep efficiency.

1.2 Thesis Outline

This thesis consists of 6 chapters as outlined below:

Chapter 1 introduces the main idea and concepts of this work

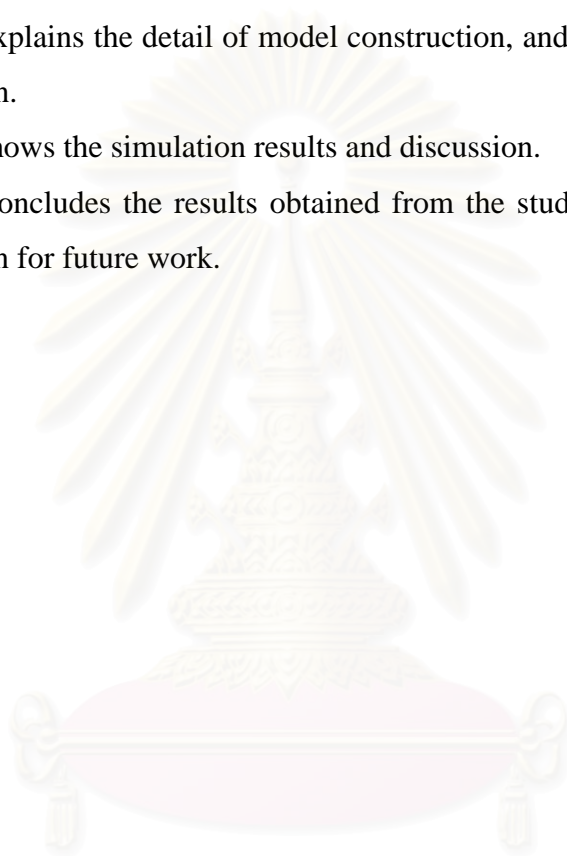
Chapter 2 reviews previous studies on waterflooding using horizontal wells, and some techniques to equalize the flow profile in the horizontal section.

Chapter 3 describes the basic principles of waterflooding, frictional flow, well completion, and some reservoir simulation concept.

Chapter 4 explains the detail of model construction, and reservoir conditions used in the simulation.

Chapter 5 shows the simulation results and discussion.

Chapter 6 concludes the results obtained from the study and makes remarks for recommendation for future work.



สถาบันวิทยบริการ
จุฬาลงกรณ์มหาวิทยาลัย

CHAPTER II

LITERATURE REVIEW

Waterflooding was started by using vertical wells in many fields. The performance when using vertical wells has been studied in various scenarios such as different flooding patterns, mobility ratio, flow rate, etc. However, using horizontal wells as injectors and producers should take into account the pressure loss due to friction along the horizontal sections.

Some related works on waterflooding using horizontal wells are reviewed in this chapter. Several numerical simulation and field studies, which are different in concepts and techniques are described.

Ferriara *et al.*⁽¹⁾ modeled a 40-acre five-spot pattern to compare performance when using both vertical producer and injector with alternative use of horizontal wells as producer and injector. The effect of many parameters such as mobility ratio, k_v/k_h , elevation of horizontal injector, completion interval length, and reservoir thickness were studied. Results from this work showed that the mobility ratio and completion interval length significantly affect water-flooding efficiency, while other parameters have less impact. Note that the horizontal system results in a much better recovery than a vertical system.

Popa *et al.*⁽²⁾ ran various simulations with different flooding patterns, one of those with direct line drive pattern using horizontal wells as injector and producer. Figure 2.1 compares the sweep efficiencies for different patterns and well models. Comparison between the direct line drive pattern with and without friction loss consideration shows the sweep efficiency difference of 33% at water breakthrough. In case of no friction consideration, the sweep efficiency is about 99%. The reason is the pressure loss due to friction along the horizontal well causes the heel to have lower pressure for the producer and higher pressure for the injector. Then, the tendency of water preferentially moves from the heel of the injector to the heel of the producer. Popa *et al.*⁽²⁾ recommended using the inverted line drive pattern as it yields better sweep efficiency than direct line drive pattern.

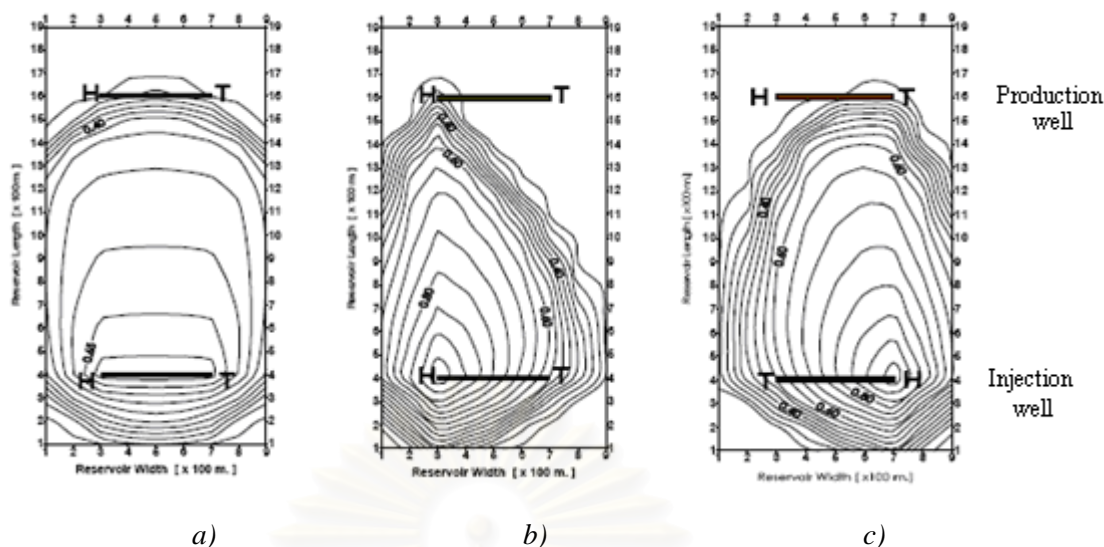


Figure 2.1: Comparison of sweep efficiencies ⁽²⁾

- a) Non-friction well model.
- b) Frictional well in direct line drive line drive pattern
- c) Frictional well in inverted line drive pattern

Mukminov ⁽³⁾ considered the ratio between the length of horizontal well (L_w) and pattern width (W) as the main parameter in his study. Figure 2.2 illustrates this ratio. The sweep efficiencies at breakthrough were highest when the ratio is one (full completion). Again, this work recommended using inverted line drive line drive pattern.

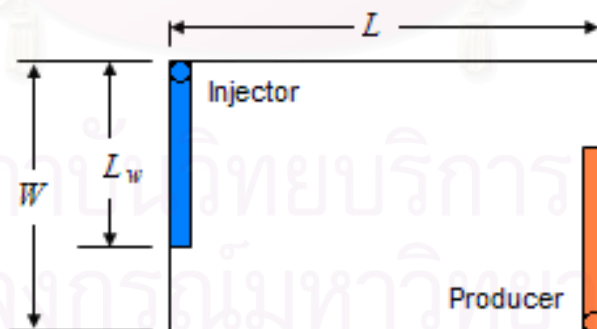


Figure 2.2: The waterflooding pattern and well geometry

Weatermark ⁽⁴⁾ studied waterflooding in a heterogeneous reservoir, as indicated by the extreme contrast in permeability and the apparent influence of natural fractures. Many patterns were simulated to compare their sweep efficiencies. The conclusion was that horizontal wells should be aligned parallel to the major fracture

orientation to maximize oil recovery. This agrees with the principle that oil recovery will be maximized with the most uniform flow profile when flooding with horizontal wells.

In practice, to connect the well with the reservoir, cased/perforated or slotted liner completions can be applied. Furul *et al.*⁽⁵⁾ presented the optimization of horizontal well completion design with these options. The criteria to select the completion type are damage around the wellbore, fluid viscosity, flow rate, strength of formation, etc. Note that perforation in long horizontal wells can be practiced with overbalance perforation.

Asheim *et al.*⁽⁶⁾ proposed the method to compute the optimal perforation profile based on models for inflow performance and flow along the wellbore. The objective of this work is to design the perforation density that creates uniform inflow profile. However, they commented that it might reduce injectivity or productivity.

A new technology that combines Inflow Control Device (ICD) with horizontal wells has been applied to control flow rate along the horizontal section. It is an alternative way to create uniform flow profile to delay water or gas coning. This application was studied by Ratterman *et al.*⁽⁷⁾. Horizontal wells were completed with ICD integrated with sand screen or debris filter to equalize longitudinal inflow, regardless of permeability variation and location in the wellbore. The simulations and field case histories showed economic improvement of oil recovery.

This thesis studies on waterflooding performance when using horizontal wells that create the optimal flow profile. The completion method selected for this study is cased and perforated completion.

CHAPTER III

THEORIES AND CONCEPTS

This chapter presents the basic principles and theories concerning horizontal well application, waterflooding, and reservoir simulation. First, the basic concepts concerning in horizontal well are introduced. Next, the mechanism of conventional waterflooding (vertical wells) is described for fundamental understanding. Then, the concept of waterflooding with horizontal wells is explained. The multi-segment well model is selected to model the horizontal wells in this work. It is most suitable for monitoring flow rate and adjusting the perforation in each section.

3.1 Horizontal Wells

Horizontal wells can be applied in any recovery scheme: primary, secondary, and enhanced. The objective is to increase the economic recovery of oil and gas. Sample of horizontal wells are alternative infill drilling in later phases, reducing water or gas coning, increasing productivity in low permeability reservoir, and improving waterflood efficiency by placing the injectors and producers in parallel.

3.1.1 Horizontal Well Completions

There are various completion options for horizontal wells. These completion aspects are described below:

1. *Openhole*: This completion is inexpensive but is limited to competent rock formations. It is difficult to stimulate and control either injection or production.
2. *Slotted or Perforated Liner*: Liners can be run to protect the borehole from collapse and provide a convenient path to insert tools in horizontal well. Slots may limit the sand control with their sizes, but wire wrapped screen (Figure 3.1) can effectively handle sand problem in horizontal wells. The main disadvantage of this completion is that effective well stimulation can be difficult due to the open annular space between liner and well. Selective production and injection are difficult.

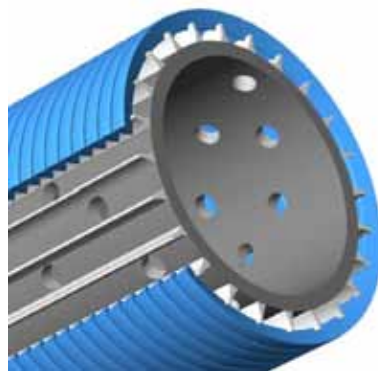


Figure 3.1: Sample of wire wrapped screen ⁽⁹⁾

3. *Liner with Partial Isolations*: External Casing Packers (ECPs) can be installed outside the liner to divide a long horizontal wellbore into several sections. This provides zone isolation allowing selective production or stimulation.
4. *Cemented and Perforated liner*: It is possible to cement and perforate medium and long radius wells. However, in cementing, free water in cement segregates near the top portion of well while heavier cement settles at the bottom. This can result in poor cement job.

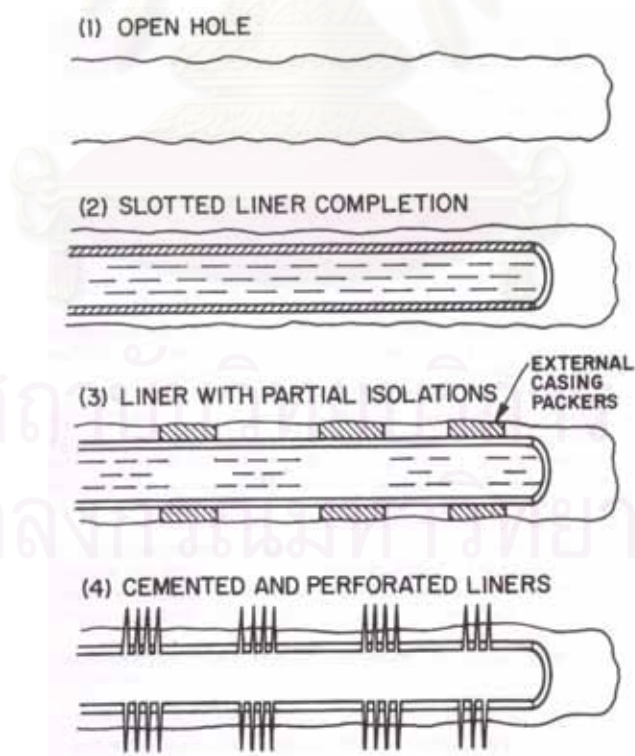


Figure 3.2: Different completion methods for horizontal wells ⁽¹⁰⁾

Another completion technique combining Inflow Control Device (ICD) with a sand screen has been applied in horizontal wells. This technique is used to delay water and gas coning by creating uniform flux along the horizontal well. Figure 3.3 illustrates the completion assembly of ICD system in the horizontal well. Each ICD unit controls the inflow with the principle of choke restriction. Then, the flow profile along the horizontal well can be designed.

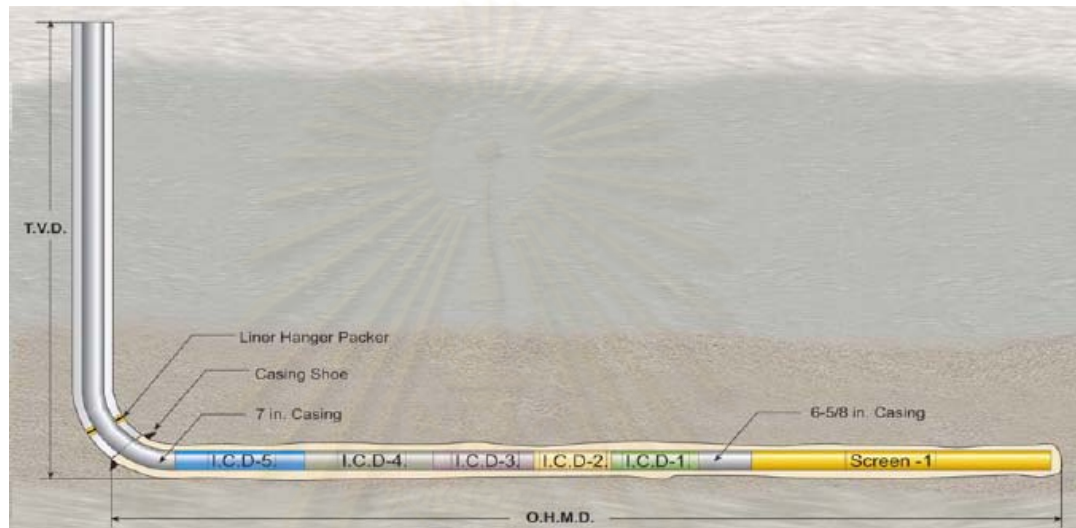


Figure 3.3: Completion assembly schematic Inflow Control System in horizontal well ⁽⁷⁾

3.1.2 Pressure Drop in a Horizontal Well

Flow in horizontal well can be represented as that in horizontal pipe, the equation for calculating pressure drop can be written as

$$\frac{dp}{dL} = \left(\frac{dp}{dL} \right)_{gravity} + \left(\frac{dp}{dL} \right)_{friction} + \left(\frac{dp}{dL} \right)_{acceleration}$$

where $\frac{dp}{dL}$ represents pressure drop per unit length.

The gravity term is a function of fluid density and change in elevation. The acceleration term is a function of fluid density and the change in the squares of flow rate. The friction term is a function of fluid density, fluid viscosity, pipe diameter, pipe roughness, and flow rate. Generally, the pressure drop due to gravity in horizontal pipe is negligible. In some cases, the pressure drop due to acceleration is also negligible.

There are different flow profiles for horizontal well as shown in Figure 3.4. In a typical horizontal well, the pressure drop along the horizontal well causes a high drawdown at the heel. Thus, the inflow (or injection) rate near the heel is higher than that away from the heel. The infinite-conductive well with uniform wellbore pressure does not induce a totally uniform flow profile due to larger exposure to reservoir at both ends. If the well completion is carefully designed, a uniform flux entry may be achieved. In any case, different well-boundary conditions and reservoir heterogeneity may cause the flow profile to be different from what is shown in Figure 3.4.

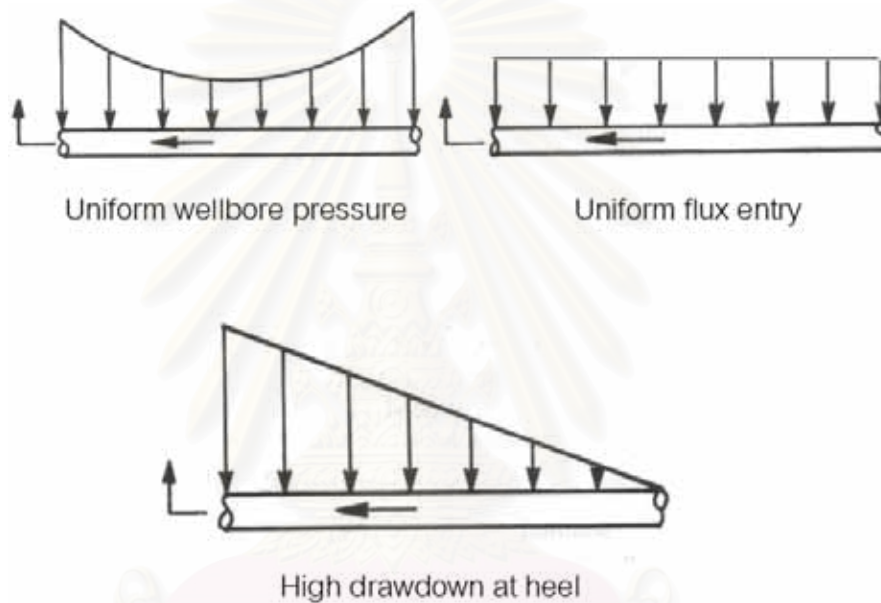


Figure 3.4: Different flow profiles for horizontal wells ⁽¹¹⁾

3.2 Waterflooding

Waterflooding is the most widely applied IOR process. Water is injected into the reservoir to displace and sweep oil towards the production well. It is necessary to understand the mechanism of fluid displacement in the reservoir and waterflooding process in order to optimize waterflooding performance.

3.2.1 Fluid displacement

During fluid displacement in the reservoir, both gravity and viscous forces play a major role in determining the shape of the displacement front. The viscous force will encourage water to flow through the reservoir faster than oil, while gravity forces will encourage water to remain at the lowest point in the reservoir.

In the reservoir, there is always connate water present; two fluids are competing for the same pore space. The permeability of one of the fluids is then described by its “relative permeability” (k_r), which is a function of saturation of the fluid as shown in Figure 3.5.

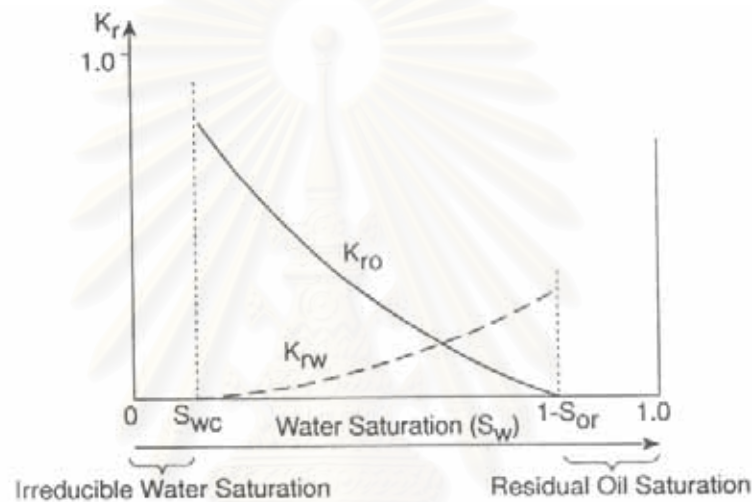


Figure 3.5: Relative permeability curve for oil and water⁽¹³⁾

For a given water saturation (S_w), the permeability to water (k_w) can be determined from the absolute permeability and the relative permeability as follows:

$$k_w = k \cdot k_{rw}$$

The mobility of a fluid is defined as the ratio of its permeability to viscosity:

$$\text{Mobility} = \frac{k \cdot k_r}{\mu}$$

When water is displacing oil in the reservoir, the mobility ratio determines which fluid can move more preferentially through the pore space. The mobility ratio for water displacing oil is defined as:

$$\text{Mobility ratio (M)} = \frac{k_{rw}/\mu_w}{k_{ro}/\mu_o}$$

If the mobility ratio is greater than 1.0, it means water can move faster than oil through the reservoir. This causes “Unstable Displacement” which can be described as viscous fingering as shown in Figure 3.6.

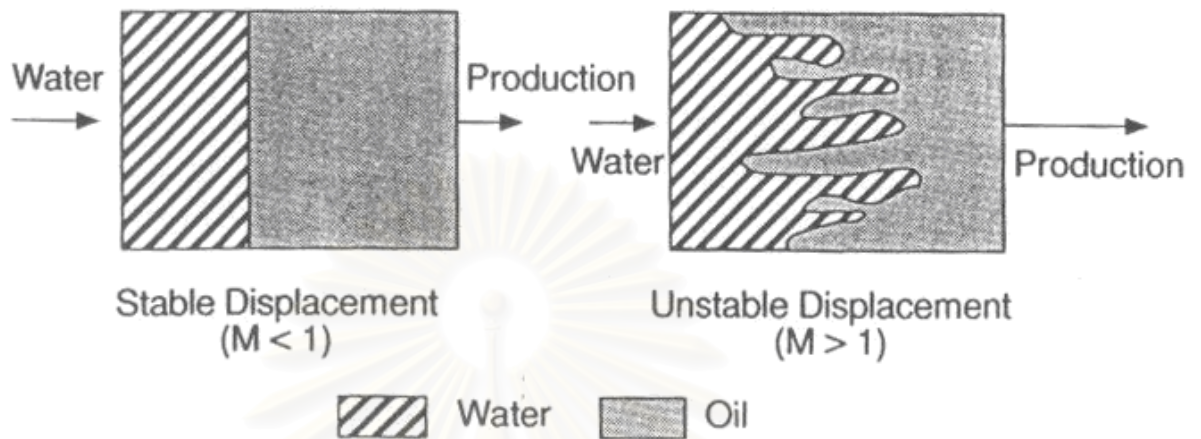


Figure 3.6: Stable and Unstable displacement in the horizontal plane ⁽¹³⁾

Unstable displacement is clearly less preferable, since water reaches the producer much earlier than in stable situation, and some oil may be left unrecovered at abandonment.

Consider the water displacing oil in a dipping reservoir, at low injection rates the displacement is stable; the gravity force is dominating the viscous forces. At higher injection rates, the viscous forces dominates, and the water underruns the oil, forming a so-called “gravity tongue”. This is less favorable situation since water will break through early. The steeper the dip angle, the more influence the gravity force will have. Figure 3.7 compares between stable and unstable situation.

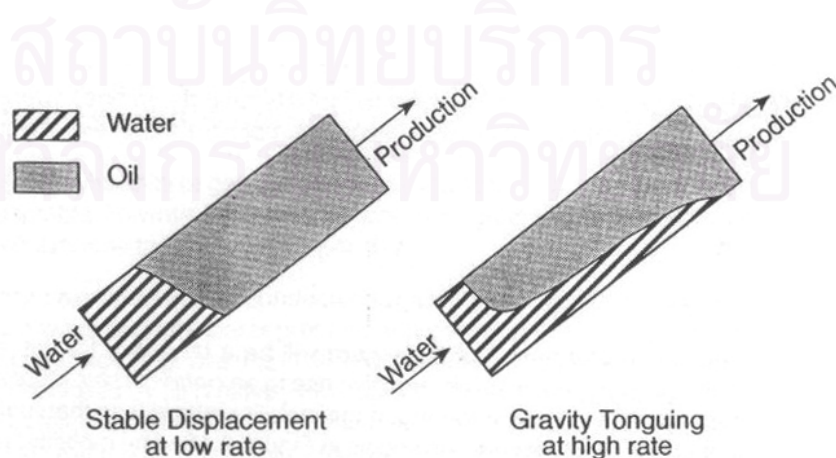


Figure 3.7: Gravity tonguing ⁽¹³⁾

3.2.2 Conventional Waterflooding

The displacement process is typically conducted in patterns where specific configuration of injectors and producers is repeated across the field. Figure 3.8 illustrates common flooding patterns used in waterflooding.

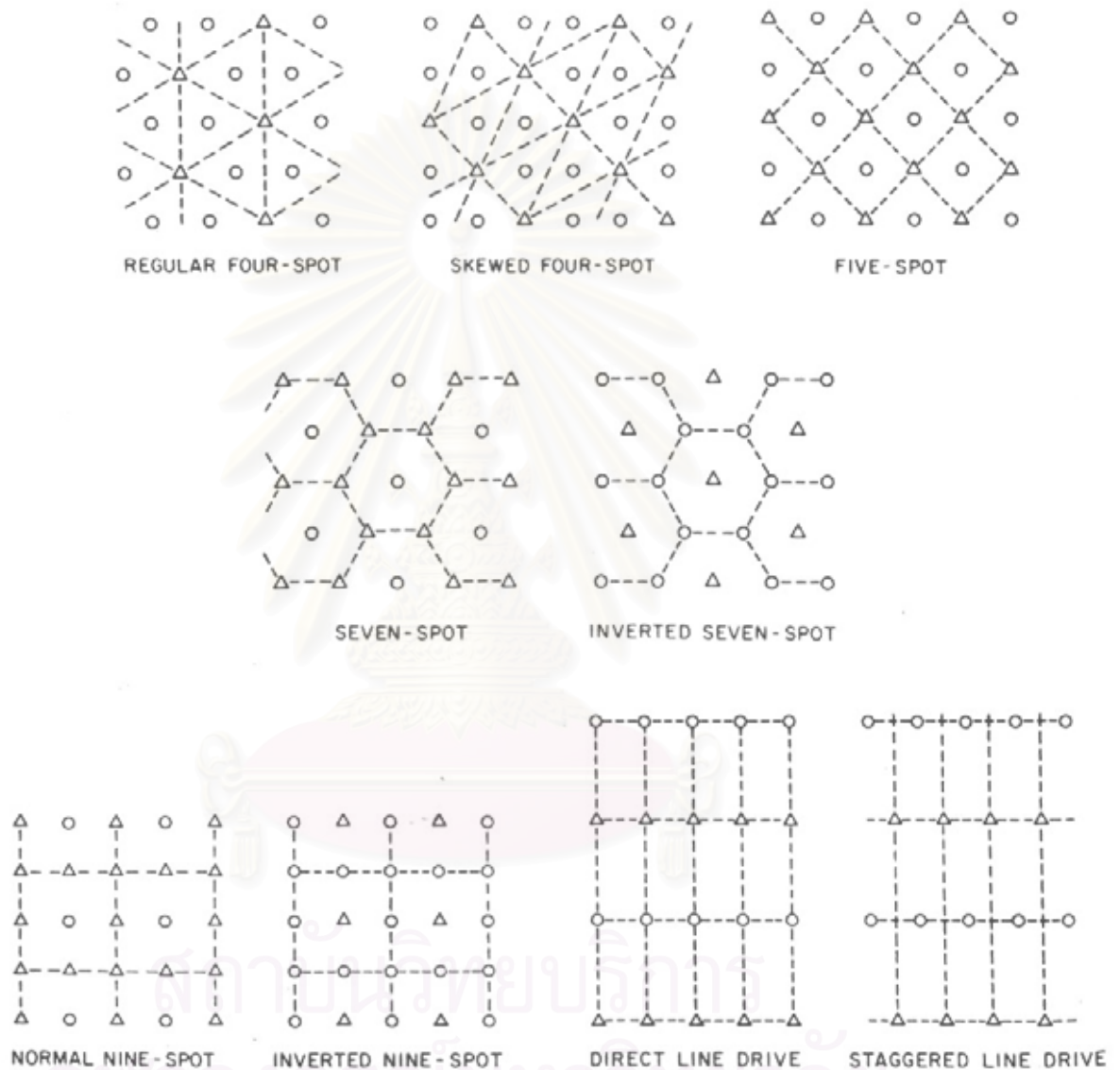


Figure 3.8: Flooding patterns⁽¹⁴⁾

The performance of waterflooding can be determined by the swept area between injectors and producers within the pattern. Pattern geometry and viscous forces are the main factors used to determine the sweep efficiency. Figure 3.9 compares the sweep efficiency at breakthrough of direct line drive pattern with various mobility ratios. A

low mobility ratio gives more sweep efficiency than a high mobility ratio due to more displacement efficiency.

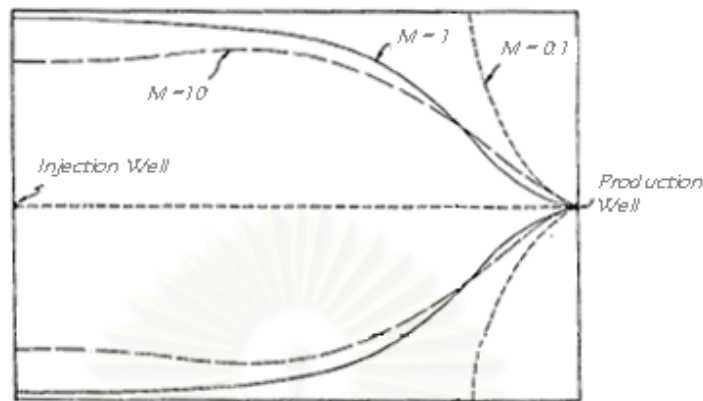


Figure 3.9: Comparison of flooded areas for $M = 10, 1$ and 0.1 for direct line drive pattern⁽¹⁵⁾

3.2.3 Waterflooding with Horizontal Wells

Horizontal wells may be used in waterflooding processes as injectors and producers in different flooding patterns. In water-flooding with horizontal wells, more patterns can be studied by changing well orientation or combination of horizontal and vertical wells. Two simplest patterns which are direct and inverted line drive are shown in Figures 3.10A and 3.10B. Both patterns are different in the orientation of the injector and producer. The direct line drive places both injector and producer the same direction while the inverted line drive places them in the opposite direction.

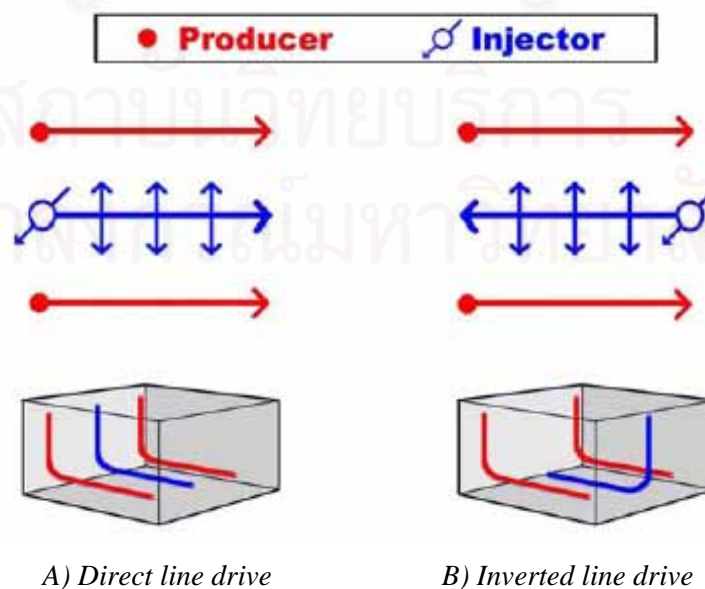


Figure 3.10: Well orientation of different flooding patterns⁽³⁾

Infill drilling with horizontal wells may be applied by drilling and recompleting the existing vertical wells. It is usually more economic than drilling new horizontal wells. The patterns of infill drilled horizontal wells depend on the existing patterns. Figure 3.11 illustrates this application. From the figure, the pattern of existing vertical well is five-spot pattern, then the inverted line drive pattern is applied in the waterflooding with horizontal well.

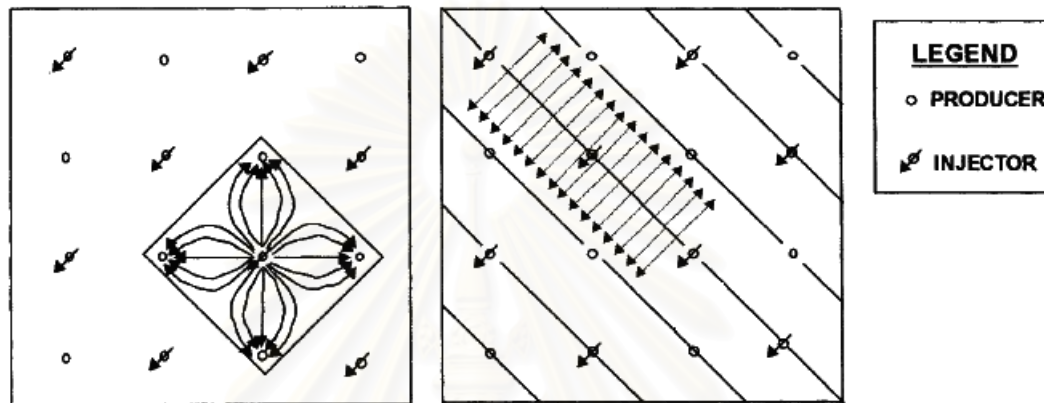


Figure 3.11: Waterflooding by infill drilled horizontal wells ⁽³⁾

3.3 Reservoir Simulation

In order to study the behavior of waterflooding process, we used ECLIPSE 100 reservoir simulator⁽⁸⁾ since it has the multi-segment well model and the local grid refinement (LGR) that can handle specific requirements in this thesis.

3.3.1 Multi-segment Well Model

In order to determine the completion that leads to uniform flux between injector and producer, we must be able to compute and adjust the flow rate in each section along the horizontal section. Thus, the well has to be divided into segments. The multi-segment well model is capable of handling this requirement.

1. *Segment Structure:* Each segment consists of a **node** and a **flowpath** to its parent segment's node. A segment's node is positioned at the end away from the wellhead (Figure 3.12). Each node lies at a specified depth and has a nodal pressure which is determined by the well model calculation. Flow from the formation through grid-block-to-well connections also enters the well at segment nodes (Figure 3.13). Each segment also has a specified length, diameter, roughness, and area. These attributes are properties of its flowpath

and are used in the friction and acceleration pressure loss calculations. Also, associated with each segment's flowpath are the flow rates of oil, water and gas, which are determined by the well model calculation.

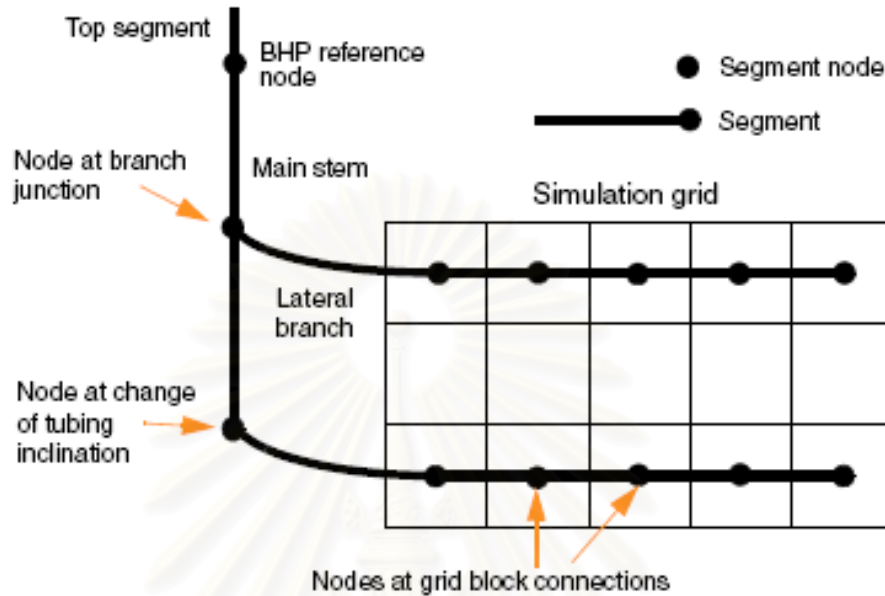


Figure 3.12: Structure of multi-segment well model⁽⁸⁾

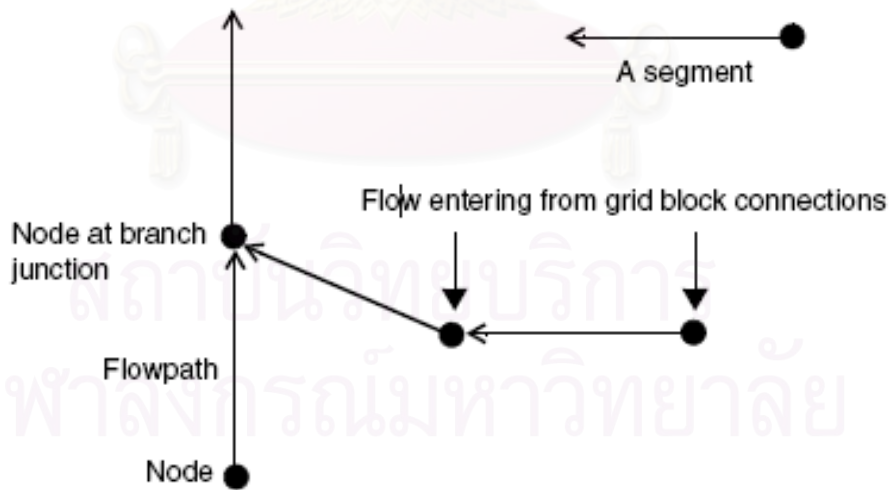


Figure 3.13: Flow components in multi-segment well model⁽⁸⁾

2. *Inflow Performance*: The flow of fluid between a grid block and its associated segment's node is given by the inflow performance relationship

$$q_{pj} = T_{wj} M_{pj} (P_j + H_{cj} - P_n - H_{nc})$$

where

q_{pj} is the volumetric flow rate of phase p in connection j at stock tank condition.

T_{wj} is the connection transmissibility factor

M_{pj} is the phase mobility at the connection.

P_j is the pressure in the grid block containing the connection.

H_{cj} is the hydrostatic pressure head between the connection's depth and the center depth of the grid block.

P_n is the pressure at the associated segment's node n .

H_{nc} is the hydrostatic pressure head between the segment node n and the connection's depth.

3. *Frictional Pressure Loss Calculation*: The calculation of the frictional pressure loss is based on the correlation of Hagedorn and Brown.

$$\Delta P_f = \frac{C_f f L w^2}{A^2 D \rho}$$

where

f is the Fanning friction factor

L is the length of the segment

w is the mass flow rate of the fluid mixture through the segment

A is the segment's area of cross-section for flow

D is the segment's diameter

ρ is the in-situ density of the fluid mixture

C_f is a unit conversion constant

2.679E-15 (METRIC), 5.784E-14 (FIELD)

4. *Acceleration Pressure Loss Calculation:* The acceleration pressure loss across a segment is the difference between the velocity head of the mixture flowing across the segment's outlet junction and the velocity heads of the mixture flowing through all its inlet junctions.

$$\Delta P_a = H_{vout} - \sum_{inlets} H_{vin}$$

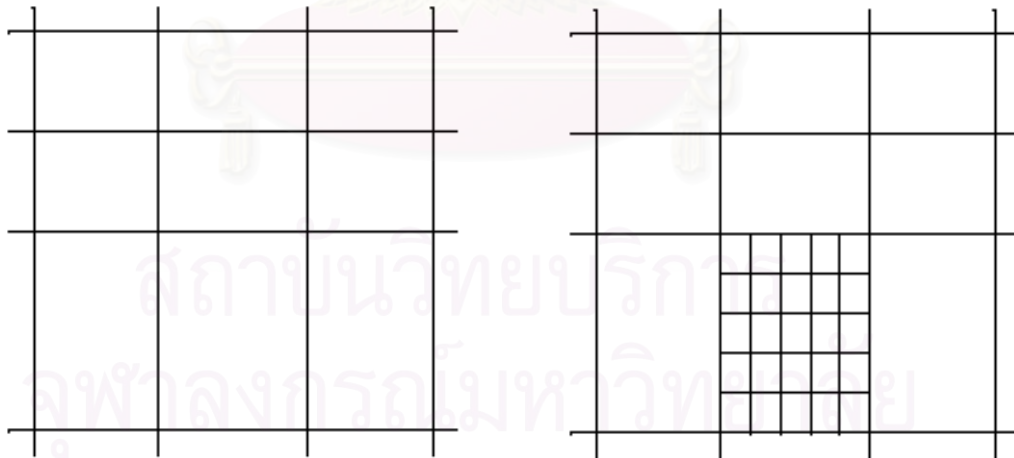
The velocity head of the mixture flowing through a junction is

$$H_v = \frac{0.5C_f w^2}{A^2 \rho}$$

For the outlet junction flow, A is the cross-sectional area of the segment. For inlet junction flows, A is the maximum of the cross-sectional areas of the segment and the inlet segment.

3.3.2 LGR Model

This thesis studies on breakthrough of flooded water. For more accurate results, it usually requires more grids to see the change in water saturation around the wellbore. Local Grid Refinement (LGR) can handle this requirement. The concept of LGR is to refine the local grid into several small grids as shown in Figure 3.14A and B.



A) Global Cartesian grid

B) Refined Cartesian grid

Figure 3.14 The concept of LGR model ⁽⁸⁾

CHAPTER IV

DEVELOPMENT OF OPTIMAL COMPLETION

As mentioned before, this thesis studies the performance of waterflooding using horizontal wells under different completion scenarios in order to determine the best completion practice. In doing so, we constructed a hypothetical reservoir model in ECLIPSE 100 reservoir simulator. The model can handle several requirements such as

1. Completion in selected intervals along the horizontal well with different open interval lengths.
2. Computation of inflow or outflow of each completion along the horizontal well in order to obtain the flow distribution along the horizontal well.
3. Refinement of the reservoir grid blocks at specific locations.

This chapter describes the construction of reservoir and well models. The reservoir and well properties were hypothetically constructed for the purpose of result comparison. First, the models with waterflooding pattern used in Popa² were set up as the based cases. Then, several simulations were run to determine the optimal completion.

4.1 Model Description

The hypothetical model is a simple rectangular reservoir with two horizontal producers at opposite sides and one horizontal injector in the middle. Since waterflooding performance such as sweep efficiency and breakthrough time must be determined accurately, grids nearby the producers need to be refined using local grid refinement (LGR). The ECLIPSE script for base case is provided in Appendix A.

4.1.1 Reservoir Model

The reservoir model consists of 18x39x5 grid blocks which are generally 160x160x20 ft for each block as shown in Figure 4.1. In the rows that the horizontal wells are placed, the y-grid sizes are reduced to 80 ft in order to refine the grid size around the wellbore (yellow grids). Two horizontal producers are placed at the edge of the reservoir and one injector is placed at the middle. The model is homogenous reservoir, and the reservoir properties are shown in Table 4.1

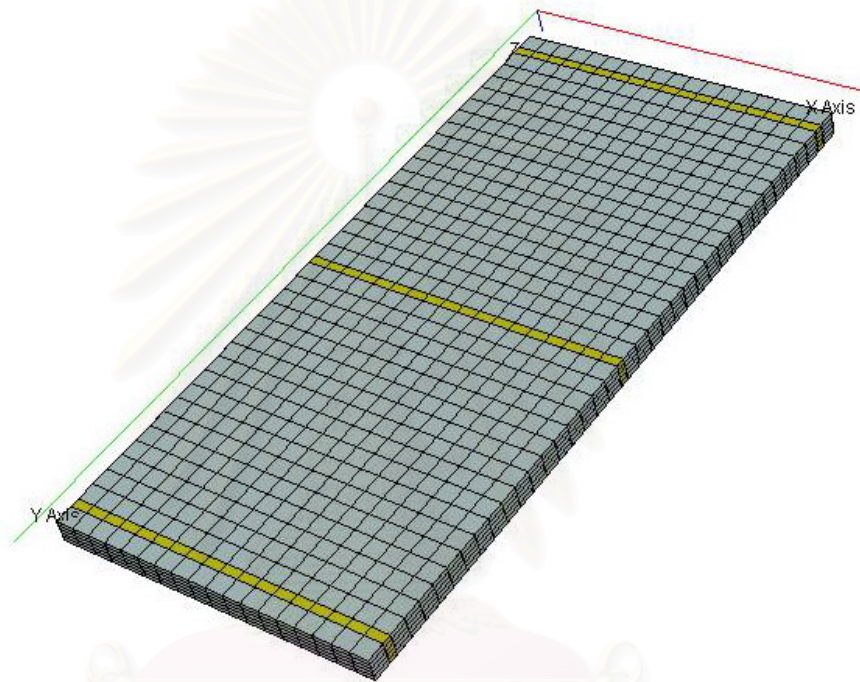


Figure 4.1: Reservoir model

Table 4.1: Reservoir model description and reservoir properties

Number of grids	18x39x5
Grid size	160x160*x20 ft
Porosity	0.2
Initial water saturation	0.2
Horizontal permeability	1,000 md
Vertical permeability	100 md
Datum depth	3,500 ft
Initial pressure @ TVD	1,500 psia
Reservoir temperature	150 °F

*3 rows have Y-grid sizes of 80 ft

4.1.2 Local Grid Refinement

In order to accommodate rapid changes around the horizontal producers, particularly when the water breaks through, the grids around the horizontal producer are locally refined. The $14 \times 3 \times 5$ global grids near the producers are refined into $28 \times 6 \times 5$ local grids. Figure 4.2 shows the location of these two zones of locally refined grids.

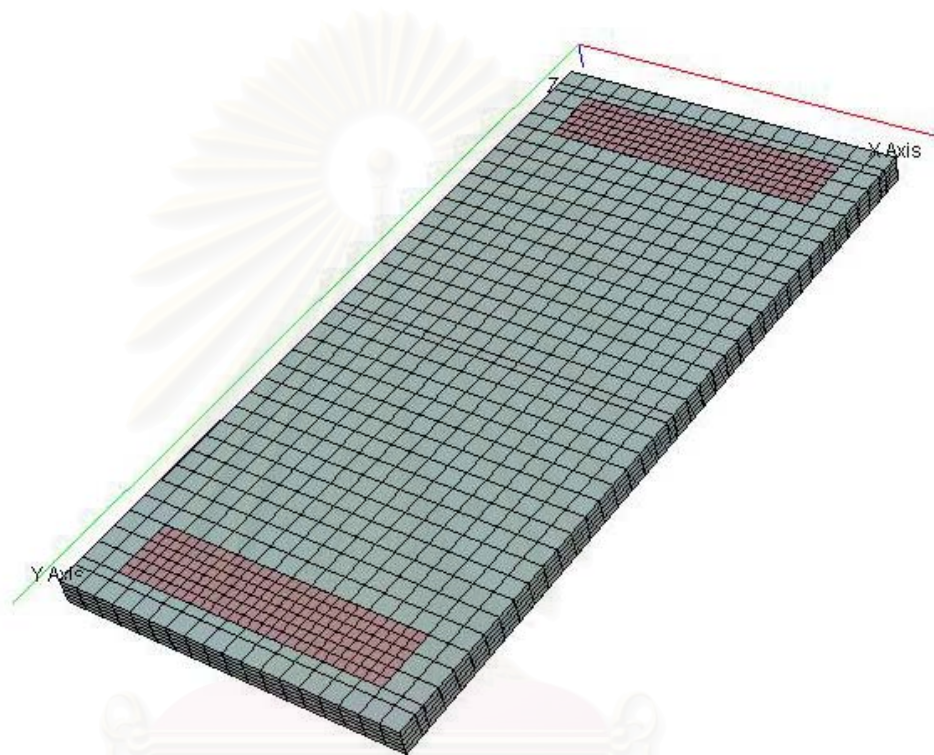


Figure 4.2: Local Grid Refinement near horizontal producers

สถาบันวิทยบริการ
จุฬาลงกรณ์มหาวิทยาลัย

4.1.3 Horizontal Well Model

The type of completion of horizontal wells used in our simulation study is cemented and perforated completion. This kind of completion consists of open (perforated) and closed intervals alternately completed along the horizontal well as shown in Figure 4.3.

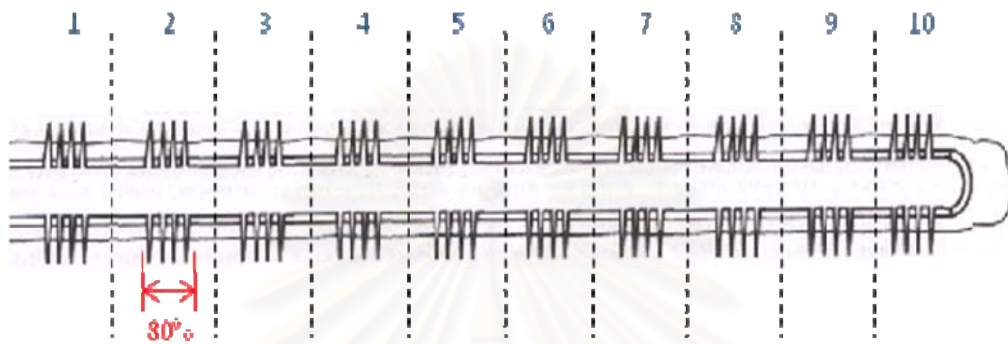


Figure 4.3: Cemented and perforated completion used in the simulation

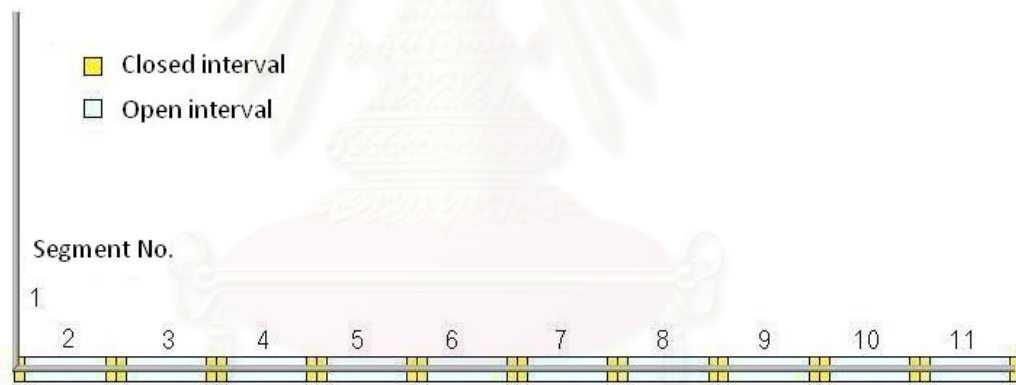


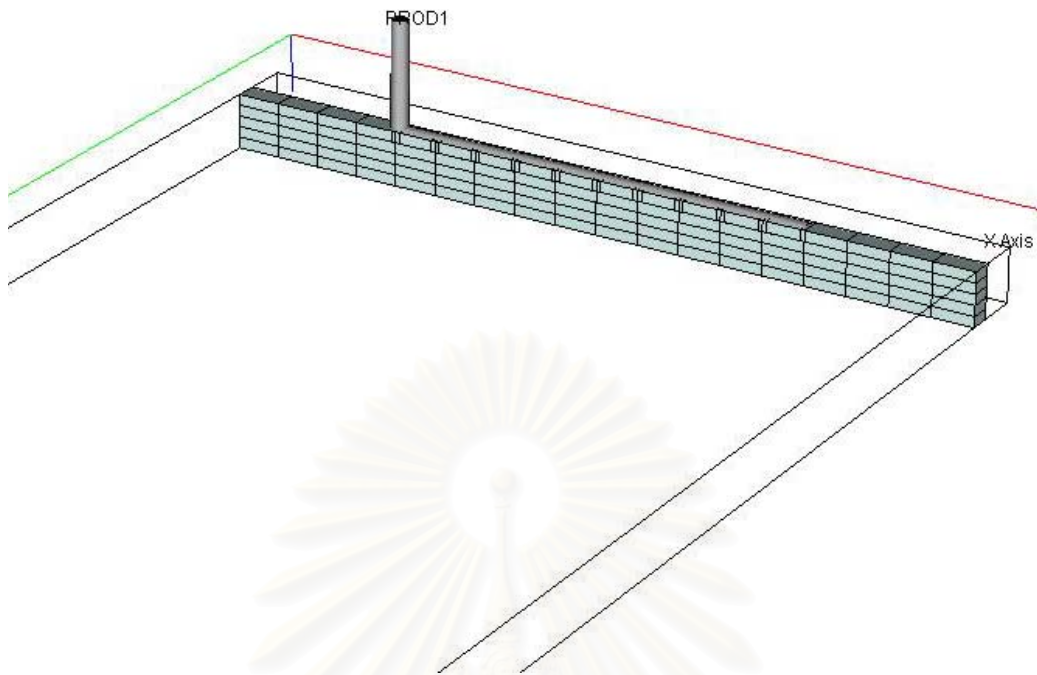
Figure 4.4: Multi-segment well model representing the cased and perforated horizontal wells

By using multi-segment well model, the horizontal wells are divided into 11 segments with one vertical segment (top segment) and 10 horizontal segments. The model of multi-segment well is illustrated in Figure 4.4. The first segment's node represents the bottom hole node. The 10 horizontal segments represent the perforated intervals of the horizontal wells. The reservoir grids penetrated by the horizontal wells are locally refined into three grids: the middle local grids are opened and connected to the reservoir while two local grids at the two edges are closed.

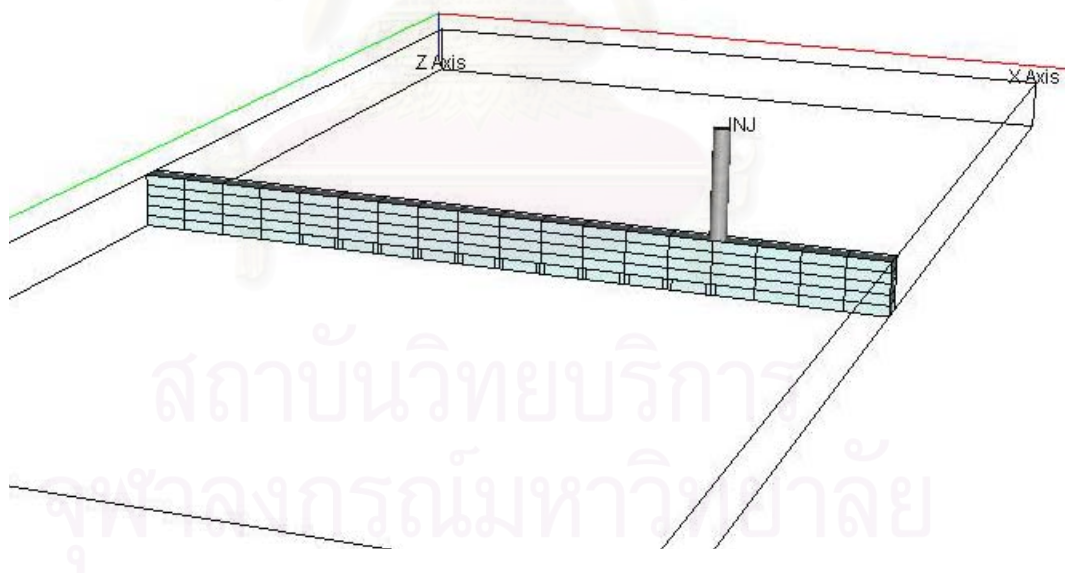
The open fraction of each segment representing perforation fraction can be adjusted in the model. For base case, the length of all opened local grids is set to be 80 percent of the length of the segment. Then, the length of each closed local grid is 10 percent of the segment length. The skin factor for all perforation is assumed to be zero. Two horizontal producers are placed in the top layer and a horizontal injector is placed in the bottom layer as shown in Figure 4.5. We use the same wellbore radius and relative roughness as used in Popa². The well conditions are described in Table 4.2.

Table 4.2: Well conditions

Horizontal length	1600 ft
Distance between injector and producers	2,640 ft
No. of well segments	11 segments
No. of perforated nodes	10 nodes
Well radius (horizontal)	0.164 ft
Maximum BHP (injector)	7,000 psi
Minimum BHP (producer)	500 psi
Skin factor	0.0
Relative roughness	10^{-3}



A) *The horizontal producer is placed in the top layer*



B) *The horizontal injector is placed in the bottom layer*

Figure 4.5: Location of producer and injector

4.1.4 Fluid and SCAL Properties

The initial fluids in the reservoir consist of oil and water. The initial water saturation is equal to 0.2 as the connate water. The type of oil used in the simulation is dead oil. The oil viscosity is kept constant in order to keep the mobility ratio constant in each case. For the base cases, unit mobility ratio is used. The fluid properties are listed in Table 4.3. To define the relative permeability, the Corey correlation is used assuming the following values:

Irreducible water saturation (S_{wc})	20%
Residual oil saturation (S_{or})	20%
Water curve exponent (N_w)	3
Oil curve exponent (N_o)	1.5
Maximum water relative permeability	0.5
Maximum oil relative permeability	0.5
Water relative permeability at S_{wc}	0.5
Oil relative permeability at S_{or}	0.5

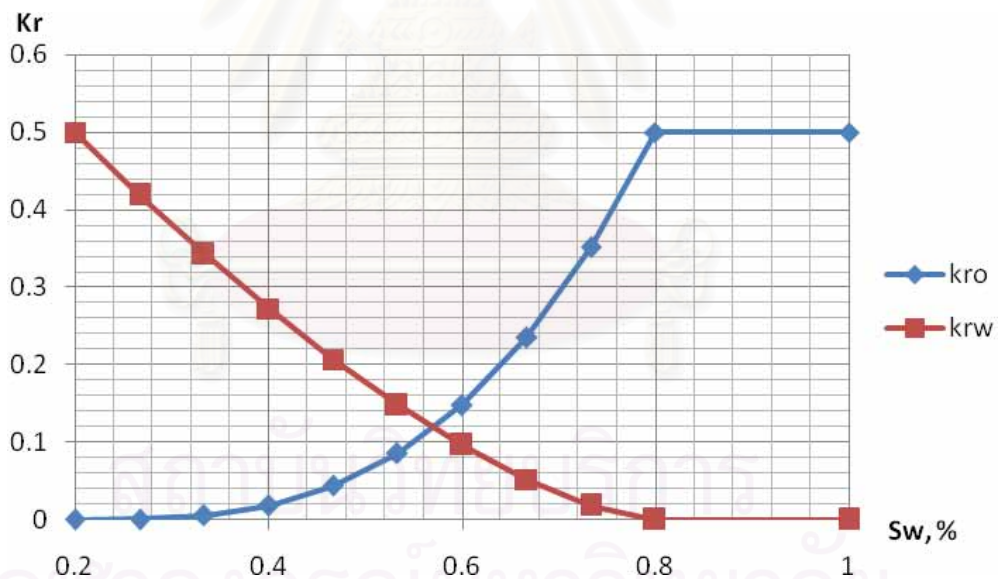


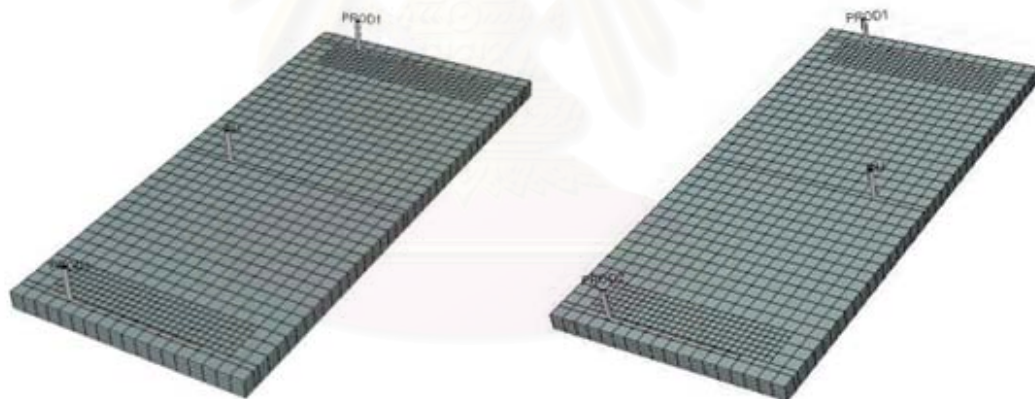
Figure 4.6: Relative permeability curve

Table 4.3: Fluid properties

Oil density	54.9 lb/ft ³
Water density	62.4 lb/ft ³
Oil viscosity	1 cp
Water viscosity	1 cp
B _o at initial pressure	1.05 Rb/STB
B _w at initial pressure	1.01 Rb/STB

4.2 Simulation Study

The simulations were performed using two simple patterns for waterflooding with horizontal wells: direct line drive pattern in which horizontal injector and producer are aligned in the same direction and inverted line drive pattern in which horizontal injector and producer are aligned in the opposite direction. Figure 4.7 depicts the difference between the two patterns.



A) Direct line drive pattern

B) Inverted line drive pattern

Figure 4.7: Well location compared between 2 patterns

The default completion of 80 percent open interval is set as the maximum open interval completion and used to simulate the base cases. The horizontal injector and producers are first modeled as non-friction well model. After that the open interval of the frictional horizontal injector and producers are adjusted to generate the same flow distribution as non-friction well model since it is expected to generate the highest sweep efficiency by creating uniform water front.

4.2.1 Comparison of Performance between Direct and Inverted Line Drive Patterns

Both direct and inverted line drive patterns were run to verify which pattern gives a better performance and would be used as the base case. The mobility ratio of one was used in the simulation. The injection and production were controlled by reservoir rate as listed in Table 4.5.

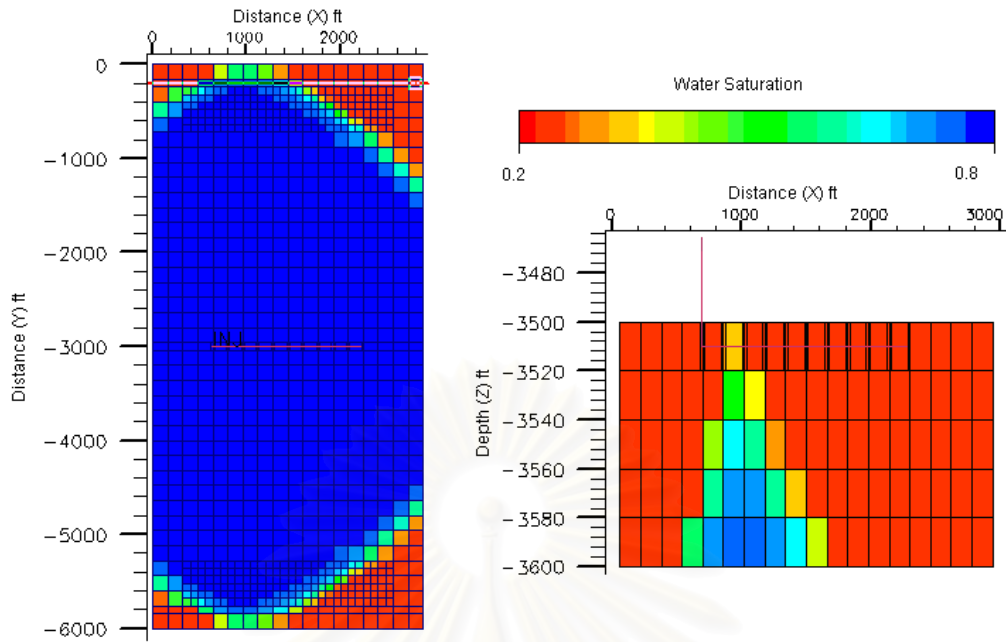
Table 4.4: Base cases conditions

Injection rate	6,000 RBPD
Production rate	2 x 3,000 RBPD
Mobility ratio	1.0

Case 1: Waterflooding with frictional horizontal wells with maximum open completion, direct line drive pattern

The first case is the direct line drive pattern. According to Popa², this pattern causes early water breakthrough due to the tendency that the injected water moves preferentially from the heel of injector to the heel of producer.

Our simulation gives the same result as Popa². Figure 4.8 illustrates the water saturation distribution at breakthrough when using direct line drive pattern. Figure 4.8A shows that the water tends to displace oil on the heel side. Figure 4.8B shows the development of water coning around the producer's heel. In this study, the sweep efficiency is determined by accounting for the swept area between the injector and producer where the water saturation increases from the initial saturation and then averaging the swept area from each layer. After 3,979 days of water injection, the water breaks through, and the sweep efficiency is about 83% with the recovery factor of 48.1%.

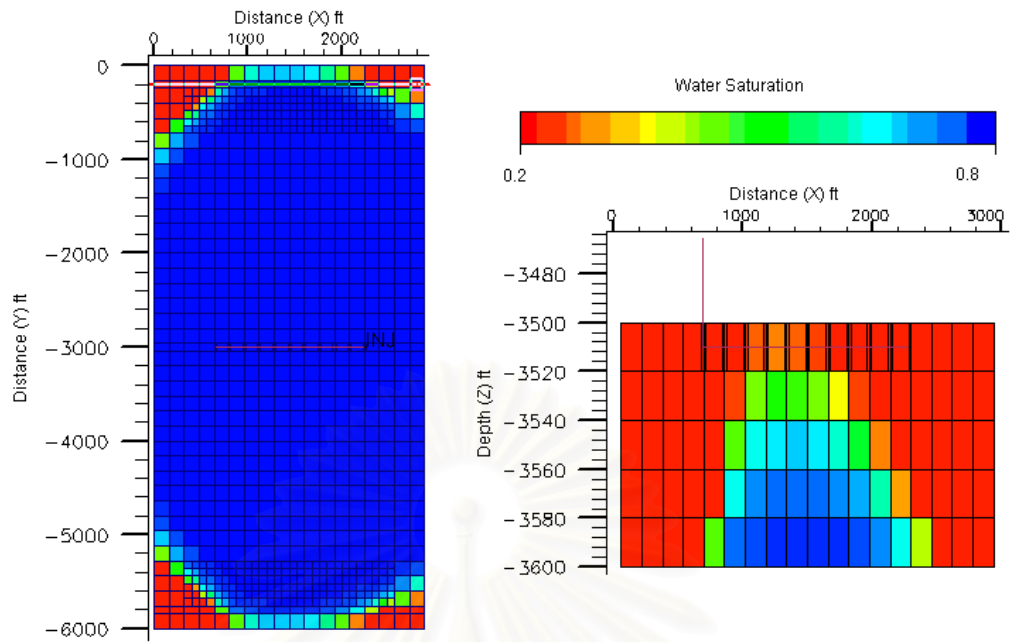


A) Top view of reservoir (bottom layer) B) Side view of reservoir at producer

Figure 4.8: Saturation distribution at breakthrough using direct line drive pattern

Case 2: Waterflooding with frictional horizontal wells with maximum open completion, inverted line drive pattern

Running with inverted line drive pattern results in the same trend as illustrated by Popa². Placing the heels of the injector and producers in the opposite direction (which is inverted line drive pattern) results in a better sweep efficiency. The inverted line drive pattern generates a more even water front and delays water breakthrough time. The improvement in sweep efficiency is depicted in Figure 4.9. The water breakthrough time is delayed to 4,436 days, and the sweep efficiency is increased to 87% with recovery factor of 53.7%. The location where the water breakthrough spreads out over a long distance along the horizontal producer.

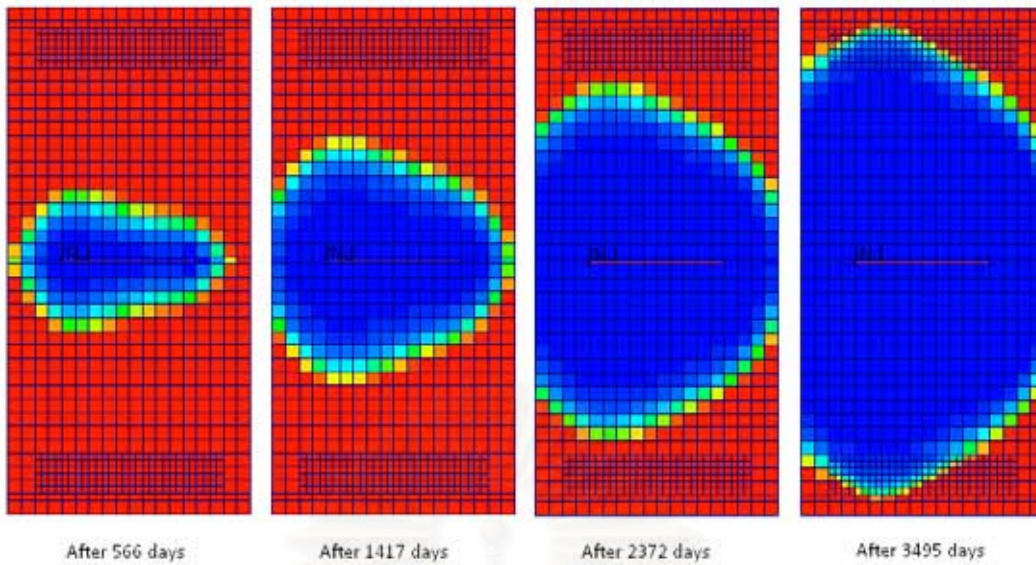


A) Top view of reservoir (Bottom layer)

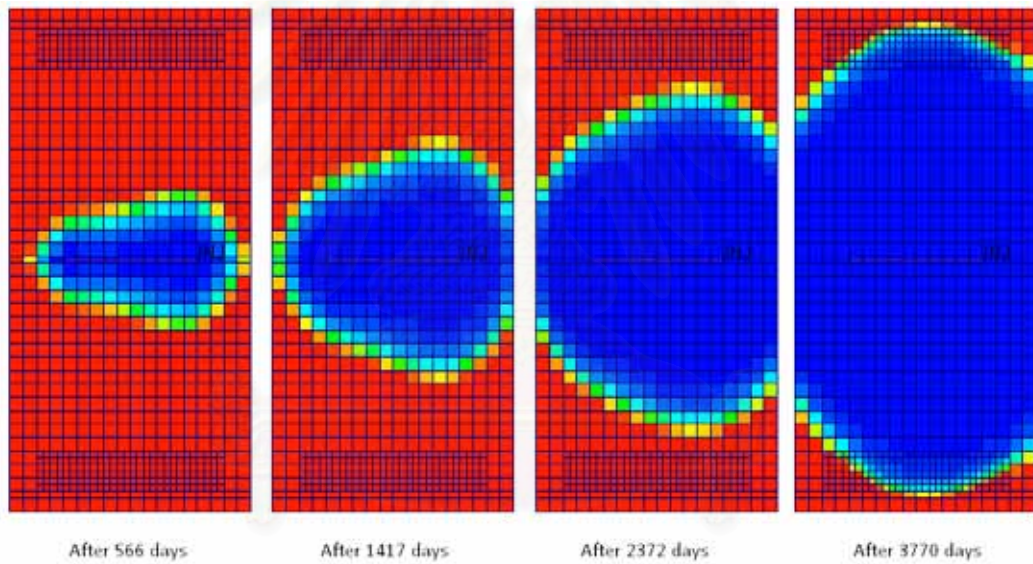
B) Side view of reservoir at producer

Figure 4.9: Saturation distribution at breakthrough using inverted line drive pattern

Figure 4.10 illustrates the development of water front when using the two patterns. The water fronts obtained from both line drive patterns with maximum open completion are not uniform. The result shows that the inverted line drive pattern gives better sweep efficiency than the direct line drive pattern. Then, we focus on determining the optimal completion using the inverted line drive pattern only.



A) Development of water front by direct line drive pattern with maximum open completion



B) Development of water front by inverted line drive pattern with maximum open completion

Figure 4.10: Comparison of water front development by the two patterns

จุฬาลงกรณ์มหาวิทยาลัย

4.2.2 Development of Optimal Completion

In Popa⁽²⁾, the horizontal well model without friction loss consideration along the horizontal section gives higher sweep efficiency than the model with friction loss. The reason is that the horizontal injector and producer represented by non-friction well model generate uniform flow distribution along the horizontal section. Then, the water front is almost parallel to the horizontal wells.

In this study, the uniform front will be emulated by finding appropriate open/closed fraction of each interval to account for the friction loss in the well. The inverted line drive pattern was used in the development of such completion. The procedure to obtain the target flow distribution starts from modeling all horizontal wells **without friction** loss consideration with maximum open interval and determining the flow rate before breakthrough for all segments. Figure 4.11 illustrates the flow distribution generated by non-friction horizontal well model. Since there are two producers and only one injector, the injection rate is double of the production rate.

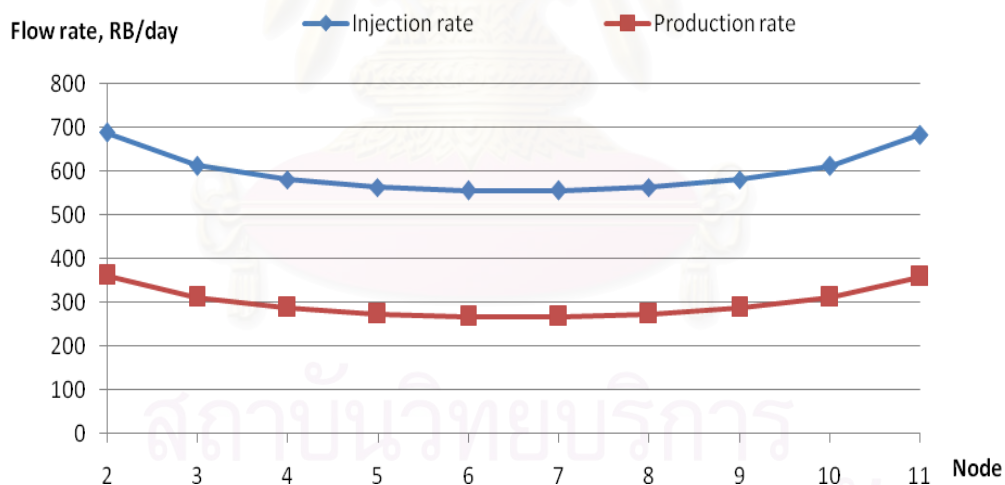


Figure 4.11: Flow distribution along the horizontal well model without friction loss consideration

With non-friction well model, the flow distribution is almost uniform due to uniform pressure profile. A little higher flow rates on heel and toe were generated because the flow ability around the heel and toe are higher due to the radial flow regime as shown in Figure 4.12.

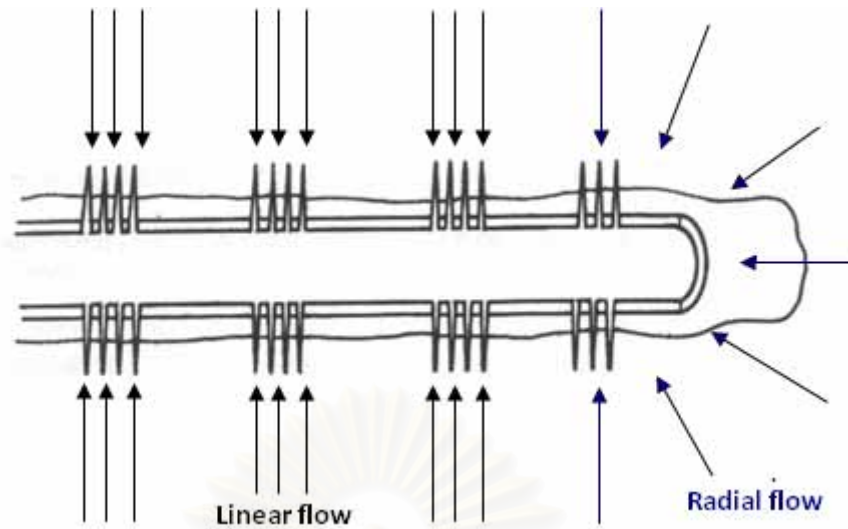


Figure 4.12: Flow regime along the horizontal wells

To emulate the flow distribution of the target, we need to adjust the opening interval for each segment. Note that our study uses 80 percent open interval as the maximum open interval.

The procedure to emulate the target flow distribution is as follows:

1. Model all horizontal wells **with friction** consideration along the horizontal wells with maximum open interval.
2. Simulate the waterflooding and record the average flow rate before breakthrough from all segments.
3. In order to even out the flow profile, use the ratio between segment flow rate obtained from the target and step 2 as the multiplier to adjust the open interval of each individual segment. For example,

The **target** flow distribution obtained from non-friction well model is

Node#	2	3	4	5	6	7	8	9	10	11
INJ rate(target)	688	613	581	564	556	556	564	581	613	683

The flow distribution of the injector obtained from maximum completion when accounting for friction is

Node#	2	3	4	5	6	7	8	9	10	11
INJ rate	1823	1023	668	481	378	323	301	302	324	377

Then, the multipliers for node 2 is $\frac{688.16}{1823.02} = 0.38$, and the multipliers for

other nodes are

Node#	2	3	4	5	6	7	8	9	10	11
Multiplier	0.38	0.60	0.87	1.17	1.47	1.72	1.87	1.93	1.89	1.81

After adjusting the open interval with these multipliers, then the new completion is

Node#	2	3	4	5	6	7	8	9	10	11
%Open (initial)	80.0	80.0	80.0	80.0	80.0	80.0	80.0	80.0	80.0	80.0
%Open (new)	30.2	47.9	69.5	93.8	117.8	137.6	150.0	154.0	151.3	145.1

4. Normalize the open interval of each segment by dividing by the maximum open interval. For example:

The maximum open interval is 154.03% at node 9th. So we normalize all open intervals by $\frac{80}{154.08}$. The normalized open intervals are

Node#	2	3	4	5	6	7	8	9	10	11
%Open (new)	30.2	47.9	69.5	93.8	117.8	137.6	150.0	154.0	151.3	145.1
%Open(normalized)	15.7	24.9	36.1	48.7	61.2	71.5	77.9	80.0	78.6	75.4

5. Simulate the waterflooding with completion obtained from step 4 then record the flow distribution again.
6. Repeat steps 3 to 5 until the flow distribution meets the target profile.

The iterations are performed until a flow distribution similar to the target is obtained. The results obtained from iterations are:

สถาบันวิทยบริการ
จุฬาลงกรณ์มหาวิทยาลัย

Iteration : 1

Node#	2	3	4	5	6	7	8	9	10	11
%open (INJ)	80.0	80.0	80.0	80.0	80.0	80.0	80.0	80.0	80.0	80.0
INJ rate ,RB/D	1823	1023	668	481	378	323	301	302	324	377
%open (PROD)	80.0	80.0	80.0	80.0	80.0	80.0	80.0	80.0	80.0	80.0
PROD rate ,RB/D	686	440	319	252	215	198	194	203	225	268

Iteration : 2

Node#	2	3	4	5	6	7	8	9	10	11
%open (INJ)	15.7	24.9	36.1	48.7	61.2	71.5	77.9	80.0	78.6	75.4
INJ rate ,RB/D	894	869	779	669	566	487	437	416	421	461
%open (PROD)	29.8	40.0	50.9	61.4	70.2	76.4	79.6	80.0	78.3	75.8
PROD rate ,RB/D	439	392	345	301	266	244	235	237	252	287

Iteration : 3

Node#	2	3	4	5	6	7	8	9	10	11
%open (INJ)	8.5	12.3	18.9	28.8	42.1	57.2	70.4	78.3	80.0	78.2
INJ rate ,RB/D	668	664	673	661	627	582	539	513	514	560
%open (PROD)	20.2	26.2	35.0	46.1	58.0	68.9	76.6	80.0	79.8	78.1
PROD rate ,RB/D	373	339	320	302	283	269	261	262	276	314

Iteration : 4

Node#	2	3	4	5	6	7	8	9	10	11
%open (INJ)	7.3	9.5	13.6	20.6	31.3	45.8	61.8	74.3	79.9	80.0
INJ rate ,RB/D	641	599	598	605	606	596	580	569	577	631
%open (PROD)	17.4	21.4	28.0	37.2	48.7	60.9	71.5	78.0	80.0	79.4
PROD rate ,RB/D	355	317	300	290	281	275	274	279	295	336

Iteration : 5

Node#	2	3	4	5	6	7	8	9	10	11
%open (INJ)	7.2	9.0	12.2	17.7	26.5	39.5	55.5	70.1	78.4	80.0
INJ rate ,RB/D	653	591	574	572	577	582	585	589	608	669
%open (PROD)	16.7	19.8	25.3	33.2	43.6	55.8	67.4	75.9	79.6	80.0
PROD rate ,RB/D	353	310	291	281	275	274	277	286	305	348

Iteration : 6

Node#	2	3	4	5	6	7	8	9	10	11
%open (INJ)	7.5	9.1	12.1	17.1	25.0	36.9	52.4	67.7	77.3	80.0
INJ rate ,RB/D	671	599	572	562	562	567	576	590	616	683
%open (PROD)	16.6	19.3	24.2	31.4	41.1	52.8	64.7	74.1	79.0	80.0
PROD rate ,RB/D	355	308	287	276	271	271	277	289	310	355

Iteration : 7

Node#	2	3	4	5	6	7	8	9	10	11
%open (INJ)	7.7	9.3	12.3	17.1	24.7	36.2	51.3	66.6	76.8	80.0
INJ rate ,RB/D	682	607	576	561	556	560	570	586	617	686
%open (PROD)	16.7	19.3	24.0	30.8	40.1	51.5	63.3	73.1	78.5	80.0
PROD rate ,RB/D	358	309	287	274	269	269	276	289	312	358

Iteration : 8

Node#	2	3	4	5	6	7	8	9	10	11
%open (INJ)	7.8	9.4	12.5	17.3	24.8	36.1	51.0	66.3	76.6	80.0
INJ rate ,RB/D	687	611	579	562	555	557	566	583	615	686
%open (PROD)	16.8	19.4	24.0	30.7	39.8	50.9	62.8	72.6	78.3	80.0
PROD rate ,RB/D	360	310	287	274	268	268	275	288	312	359

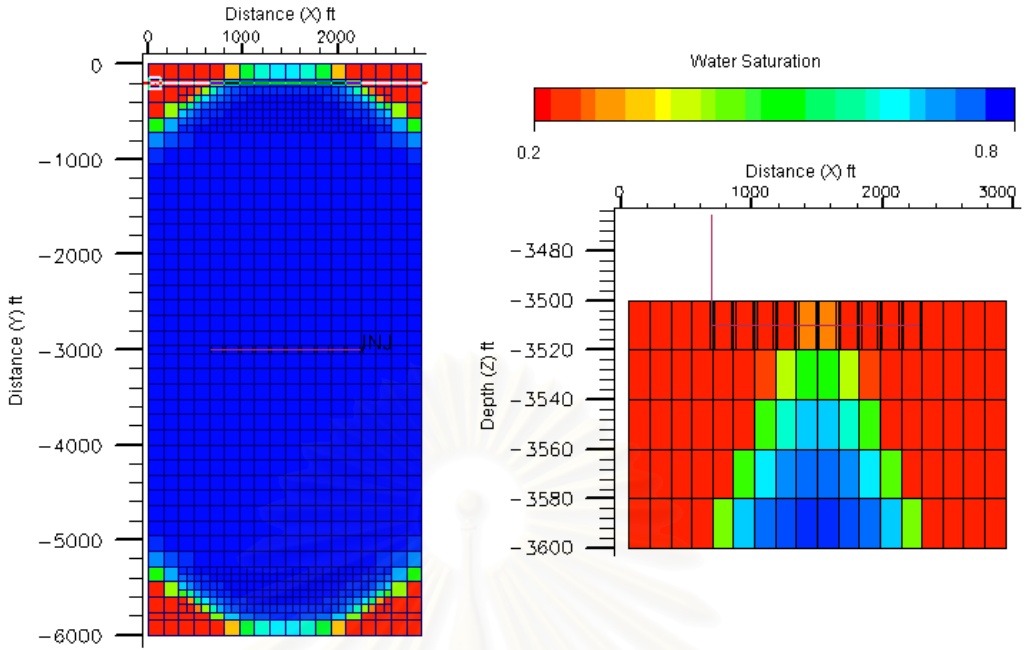
Iteration : 9

Node#	2	3	4	5	6	7	8	9	10	11
%open (INJ)	7.8	9.5	12.6	17.4	25.0	36.2	51.0	66.2	76.6	80.0
INJ rate ,RB/D	688	613	580	563	556	556	564	582	614	685
%open (PROD)	16.8	19.5	24.1	30.7	39.7	50.8	62.5	72.4	78.2	80.0
PROD rate ,RB/D	361	311	287	274	267	267	274	288	312	359

After 9 iterations, the most desirable flow distribution is obtained. Figures 4.13 and 4.14 compare the saturation distribution of the target profile and the saturation of the adjusted completion. The saturation distributions at breakthrough and sweep efficiency are the same. At 4,344 days which is the breakthrough time, a sweep efficiency of about 87% and recovery factor of 52.6%. are obtained. The water front is more parallel to the horizontal wells compared to the waterflooding using frictional horizontal wells without completion interval adjustment.



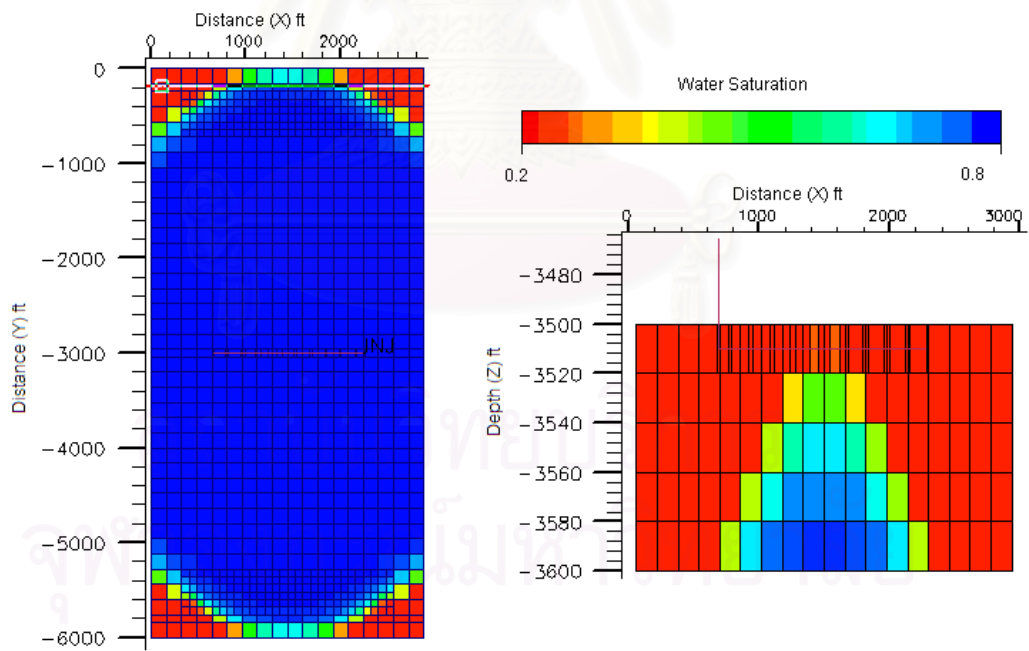
สถาบันวิทยบริการ
จุฬาลงกรณ์มหาวิทยาลัย



A) Top view of reservoir (bottom layer)

B) Side view of reservoir at producer

Figure 4.13: Saturation distribution at breakthrough when using non-friction well model



A) Top view of reservoir (bottom layer)

B) Side view of reservoir at producer

Figure 4.14: Saturation distribution at breakthrough when using frictional well with flow distribution emulating the non-friction well model

In any case, we can observe that the water front when flooding with non-ideal friction-free well model is not totally uniform like its flow distribution but moves faster in the middle section. Figure 4.15 shows the saturation distribution when flooding with non-friction well model at different time steps.

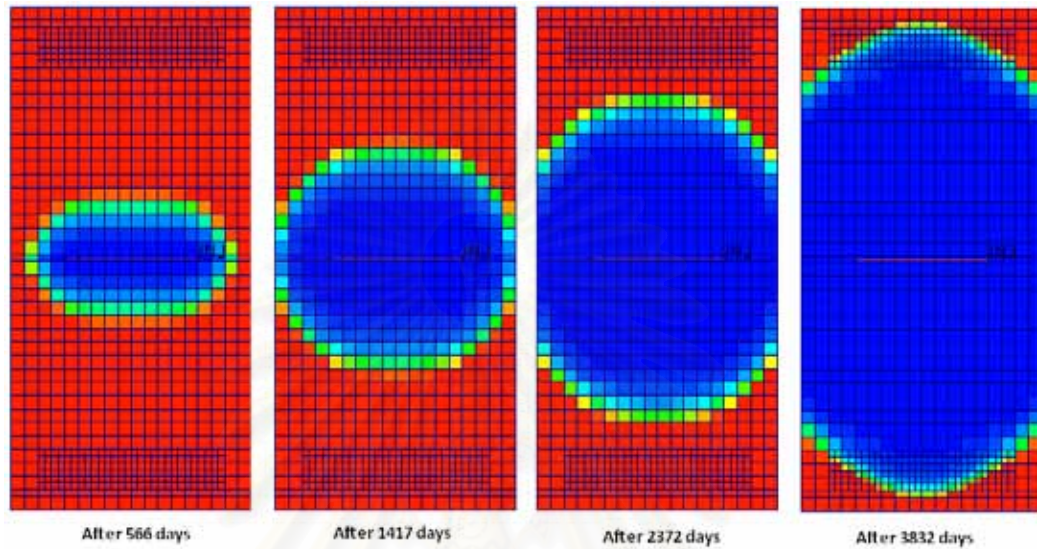
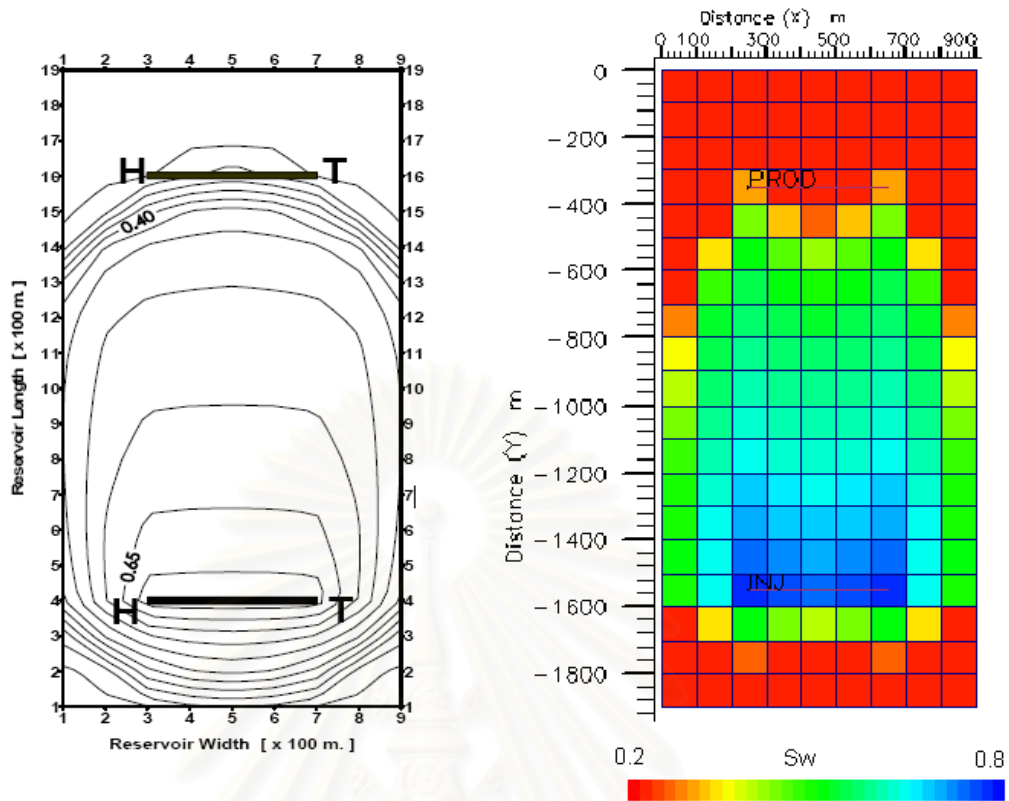


Figure 4.15: Development of water front by non-ideal friction-free well model

To generate a more uniform water front, the flow rate at the heel and the toe should be higher. The optimal completion will be established based on the concept of generating uniform water front.

When comparing the result comparison of this study with Popa's⁽²⁾, the sweep efficiencies at breakthrough obtained in this study were less than those obtained in Popa's study. The waterflooding using non-friction well model in this study does not generate the uniform water front like the one in Popa's work. The reason may be caused by different method of simulating, reservoir conditions, and determination method for sweep efficiency. Since Popa's study used a two dimension numerical model, one layer reservoir with the same dimension and conditions as used in Popa's study was used in our simulation in an attempt to match the results. However, the results are still different from those obtained in Popa's study. Figure 4.16 compares the saturation distribution at breakthrough from both studies.



A) Popa's study

B) This study

Figure 4.16: Comparison between saturation distribution at breakthrough obtained from two studies

Since the waterflooding using non-friction well model cannot generate a uniform water front as previously expected, further adjustment on the opening/closing fraction of each interval is needed in order to establish the flow distribution that generates the most uniform water front so called “Optimal Completion” to optimize water flooding performance.

The procedure to establish the optimal completion is similar to that used to obtain the completion which generates the flow distribution of non-friction well model previously described. But we need to set new candidate flow distributions as the targets and select the best one as the optimal completion after comparing the simulation result.

From the saturation distribution in Figure 4.13, when flooding with the flow distribution obtained from non-friction well model, the water breaks through at the middle segment of the producer, and some amount of oil still remains in the zones near the heel and the toe of the producers. Thus, the flow rates at the heel and the toe of the injector or producers should be increased to produce more oil from the remaining oil zones. New flow distributions were established from this concept, and the flow distribution obtained from non-friction well was used as the reference profile.

The reference flow distribution was normalized and plotted in term of flow fraction versus the node location in a unit horizontal length. All node flow rates were divided by the operating flow rate which is 6,000 RB/D for injector and 3,000 RB/D for producer. The location of each node is defined by the distance from the middle of the unit-length horizontal section. Table 4.5 compares the flow reference flow profiles before and after normalization, and Figure 4.17 illustrates the normalized reference flow fraction profile.

Table 4.5: Comparison of reference flow profiles between before and after normalization

Before normalization

Node	2	3	4	5	6	7	8	9	10	11
INJ rate (RB/D)	688	613	581	564	556	556	564	581	613	684
PROD rate (RB/D)	361	311	288	274	267	267	274	288	311	359

After normalization

Location	-0.45	-0.35	-0.25	-0.15	-0.05	0.05	0.15	0.25	0.35	0.45
INJ flow fraction	0.115	0.102	0.097	0.094	0.093	0.093	0.094	0.097	0.102	0.114
PROD flow fraction	0.120	0.104	0.096	0.091	0.089	0.089	0.091	0.096	0.104	0.120

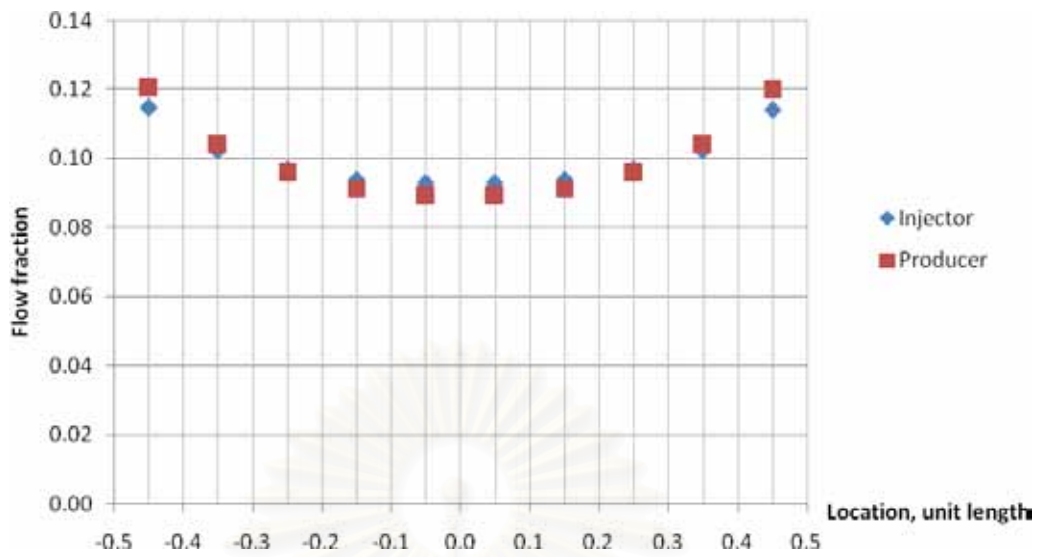


Figure 4.17: Normalized reference flow fraction profile

The flow fraction profiles shown in Figure 4.17 were adjusted to be perfectly symmetrical curves by averaging each flow fraction with its respective node in the opposite direction. After adjusting, the symmetry flow fraction profiles were obtained as shown in Table 4.6.

Table 4.6: The normalized reference flow fraction profiles after symmetrical adjustment

Location	-0.45	-0.35	-0.25	-0.15	-0.05	0.05	0.15	0.25	0.35	0.45
INJ flow fraction	0.114	0.102	0.097	0.094	0.093	0.093	0.094	0.097	0.102	0.114
PROD flow fraction	0.120	0.104	0.096	0.091	0.089	0.089	0.091	0.096	0.104	0.120

In order to establish the new flow distribution, the increasing of the flow rates at the heel and the toe must relate to the decreasing of the flow rates in the middle nodes. The flow fraction profile in Table 4.6 was rewritten in term of flow fraction offset to the average flow fraction by subtracting all flow fractions by 0.1 which is the average value for flow fraction. The result is shown in Table 4.7 and can be plotted as Figure 4.18.

Table 4.7: The normalized reference flow fraction profiles after subtracting by 0.1

Location	-0.45	-0.35	-0.25	-0.15	-0.05	0.05	0.15	0.25	0.35	0.45
INJ offset	0.014	0.002	-0.003	-0.006	-0.007	-0.007	-0.006	-0.003	0.002	0.014
PROD offset	0.020	0.004	-0.004	-0.009	-0.011	-0.011	-0.009	-0.004	0.004	0.020

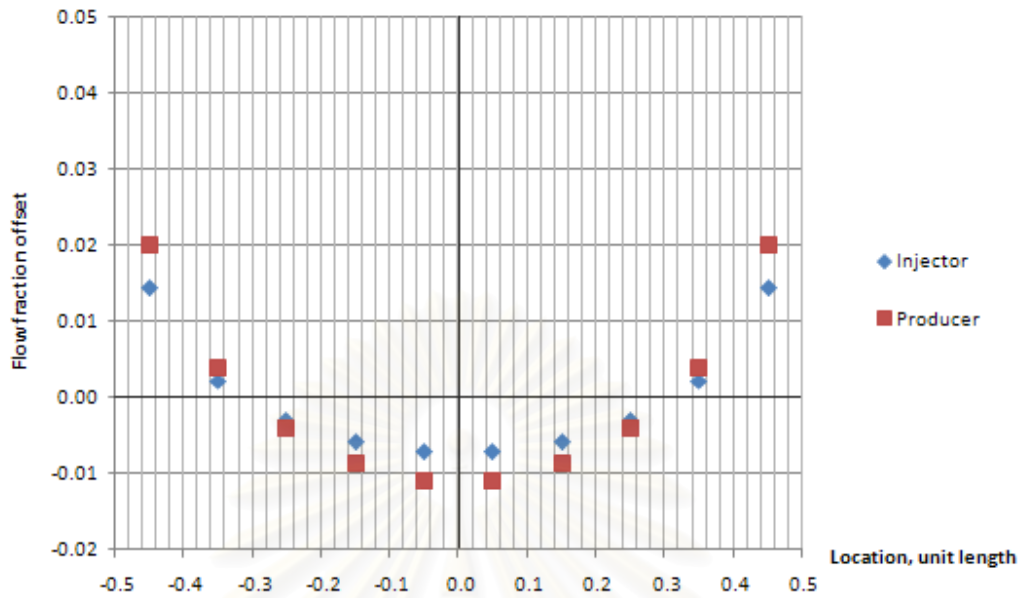
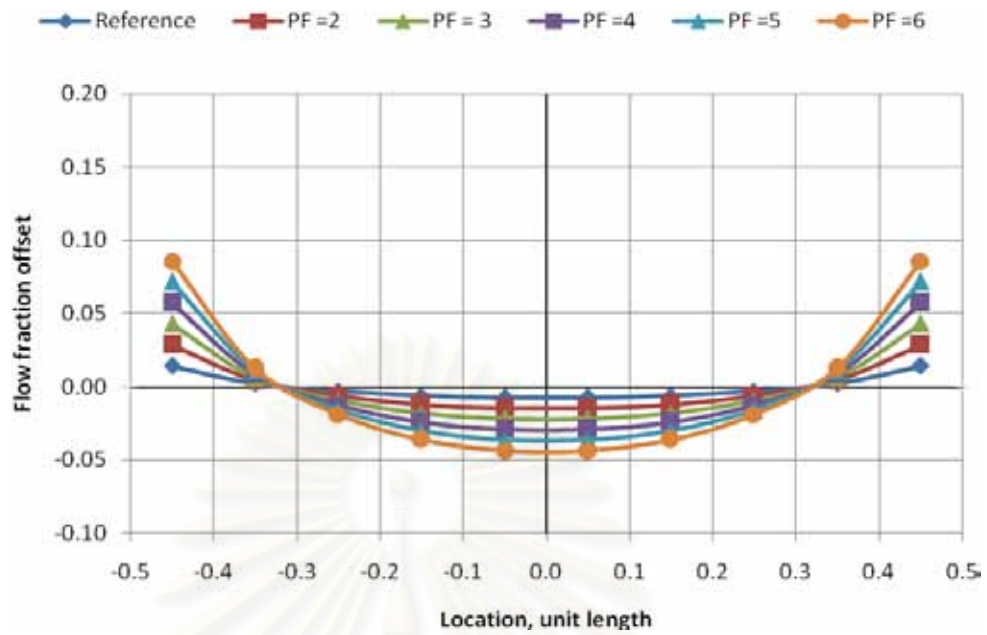


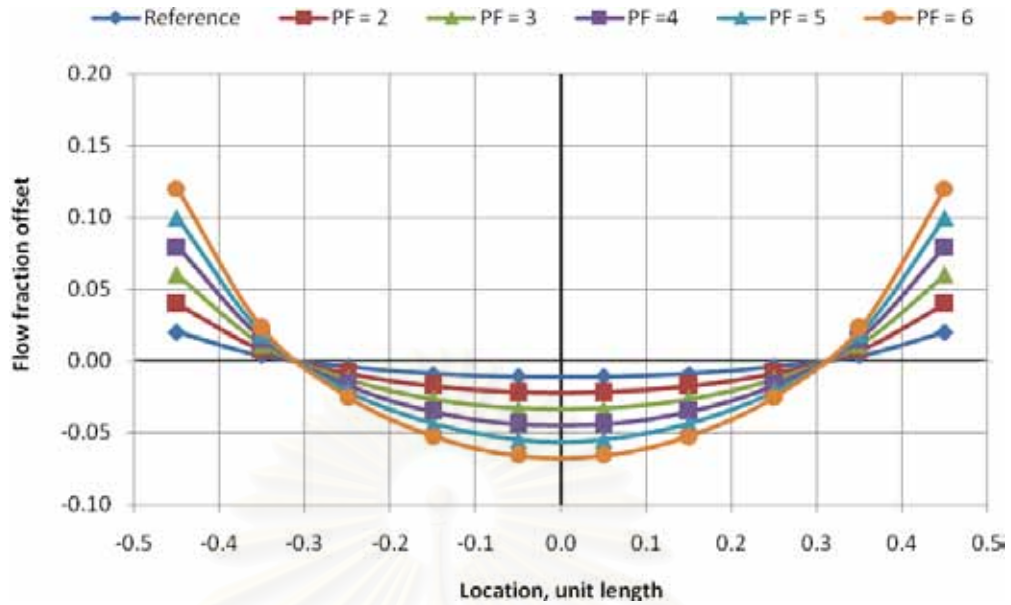
Figure 4.18: The plots of flow fraction offset versus location in a unit-length horizontal section for injector and producer

In order to establish the target flow fraction profiles, the flow fraction profiles in Table 4.7 were multiplied by the “Profile Factor” (PF). This parameter is used to indicate the increasing degree of the flow rate at the heel and the toe. Figures 4.19 and 4.20 compare the reference and new flow fraction profiles for the producer and injector, respectively. Note that for the reference flow profile, the profile factor is equal to 1.



Location	Flow fraction offset									
	-0.45	-0.35	-0.25	-0.15	-0.05	0.05	0.15	0.25	0.35	0.45
Reference	0.014	0.002	-0.003	-0.006	-0.007	-0.007	-0.006	-0.003	0.002	0.014
PM = 2	0.029	0.004	-0.006	-0.012	-0.015	-0.015	-0.012	-0.006	0.004	0.029
PM = 3	0.043	0.006	-0.009	-0.018	-0.022	-0.022	-0.018	-0.009	0.006	0.043
PM = 4	0.057	0.008	-0.013	-0.024	-0.029	-0.029	-0.024	-0.013	0.008	0.057
PM = 5	0.072	0.011	-0.016	-0.030	-0.036	-0.036	-0.030	-0.016	0.011	0.072
PM = 6	0.086	0.013	-0.019	-0.036	-0.044	-0.044	-0.036	-0.019	0.013	0.086

Figure 4.19: Comparison of flow fraction offset profiles for the injector between different profile factors



Location	Flow fraction offset									
	-0.45	-0.35	-0.25	-0.15	-0.05	0.05	0.15	0.25	0.35	0.45
Reference	0.020	0.004	-0.004	-0.009	-0.011	-0.011	-0.009	-0.004	0.004	0.020
PM = 2	0.040	0.008	-0.008	-0.017	-0.022	-0.022	-0.017	-0.008	0.008	0.040
PM = 3	0.060	0.011	-0.012	-0.026	-0.033	-0.033	-0.026	-0.012	0.011	0.060
PM = 4	0.080	0.015	-0.017	-0.035	-0.044	-0.044	-0.035	-0.017	0.015	0.080
PM = 5	0.100	0.019	-0.021	-0.044	-0.055	-0.055	-0.044	-0.021	0.019	0.100
PM = 6	0.120	0.023	-0.025	-0.052	-0.066	-0.066	-0.052	-0.025	0.023	0.120

Figure 4.20: Comparison of flow fraction offset profiles for the producer between different profile factors

In order to establish new target flow distribution for specific profile factor, the flow rate for each node can be calculated by multiplying the operating flow rate by the flow fraction offset shown in Figures 4.19 and 4.20 for injector and producer, respectively. Then, we add all flow rates by the average segment flow rate. For example, in order to establish the new target flow distributions for the injector with an injection rate of 6,000 RB/D, we need to multiply all flow fractions by 6,000 RB/D and add by 600 RB/D to the result. After that, we specify the location in term of node number. The new target flow distributions for the injector and producer are obtained as shown in Table 4.8 and 4.9, respectively.

Table 4.8: Comparison of the target flow distribution for injection rate of 6,000 RB/D with different profile factors

Node#	Node injection rate, RB/D									
	2	3	4	5	6	7	8	9	10	11
PF = 2	772	625	562	528	513	513	528	562	625	772
PF = 3	858	638	543	492	469	469	492	543	638	858
PF = 4	943	651	524	456	425	425	456	524	651	943
PF = 5	1029	664	505	420	382	382	420	505	664	1029
PF = 6	1115	676	486	384	338	338	384	486	676	1115

Table 4.9: Comparison of the target flow distribution for production rate of 3,000 RB/D with different profile factors

Node#	Node production rate, RB/D									
	2	3	4	5	6	7	8	9	10	11
PF = 2	420	323	275	248	234	234	248	275	323	420
PF = 3	480	334	263	222	201	201	222	263	334	480
PF = 4	540	346	250	195	169	169	195	250	346	540
PF = 5	600	357	238	169	136	136	169	238	357	600
PF = 6	660	368	225	143	103	103	143	225	368	660

The simulations are performed and iterated using the same procedure used to emulate the non-friction well model. New target flow distributions are achieved by adjusting the fraction of the open interval. Figures 4.21 to 4.25 show the saturation distribution at breakthrough obtained by simulating with these flow distributions.

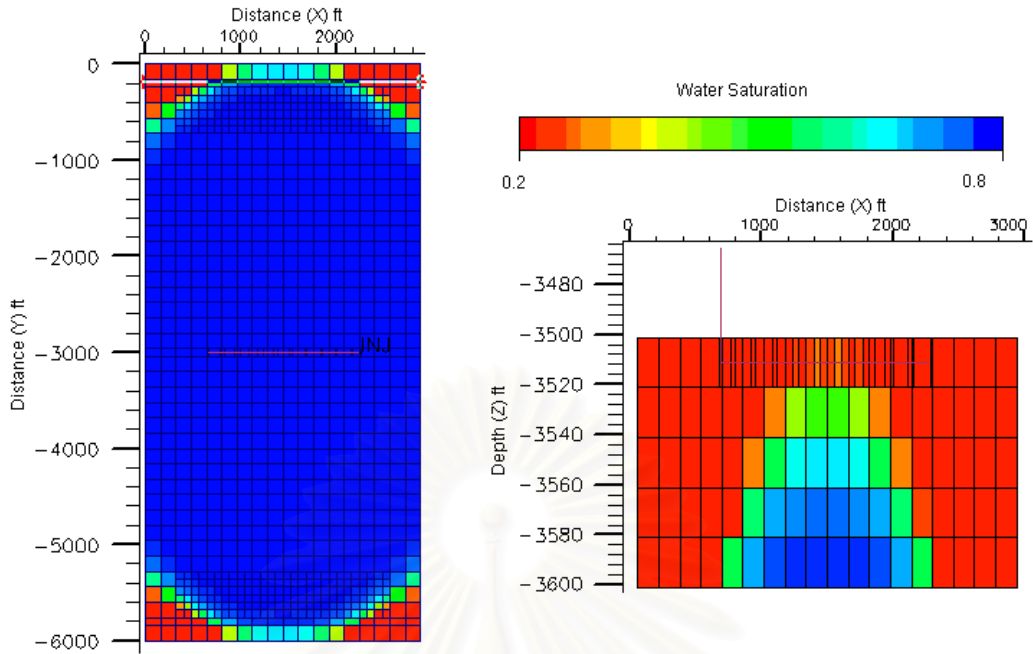


Figure 4.21: Saturation distribution at breakthrough for profile factor of 2

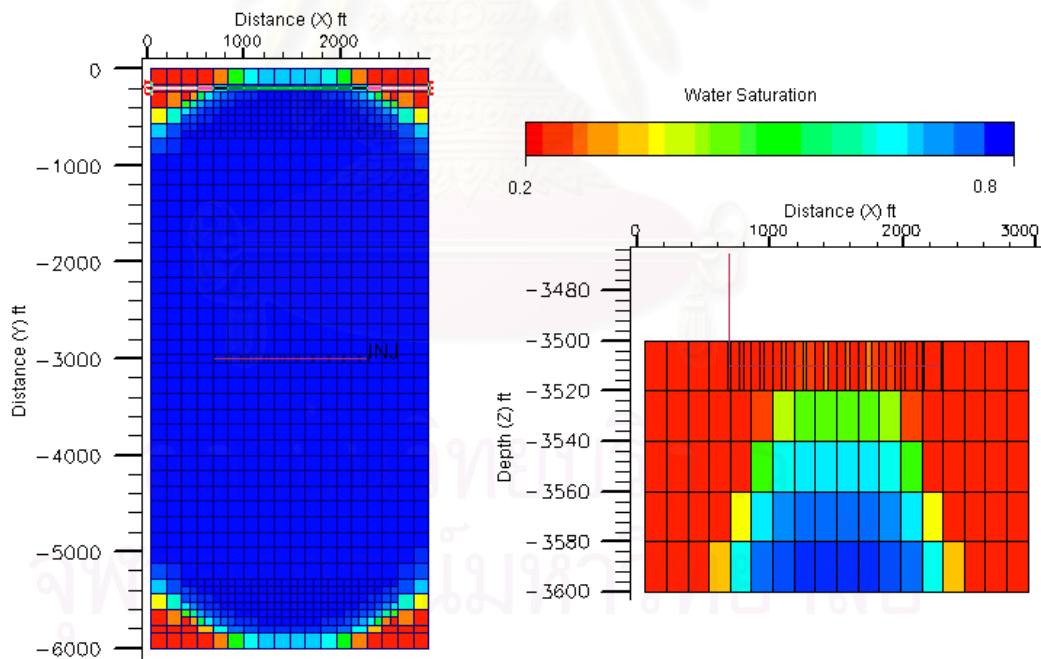


Figure 4.22: Saturation distribution at breakthrough for profile factor of 3

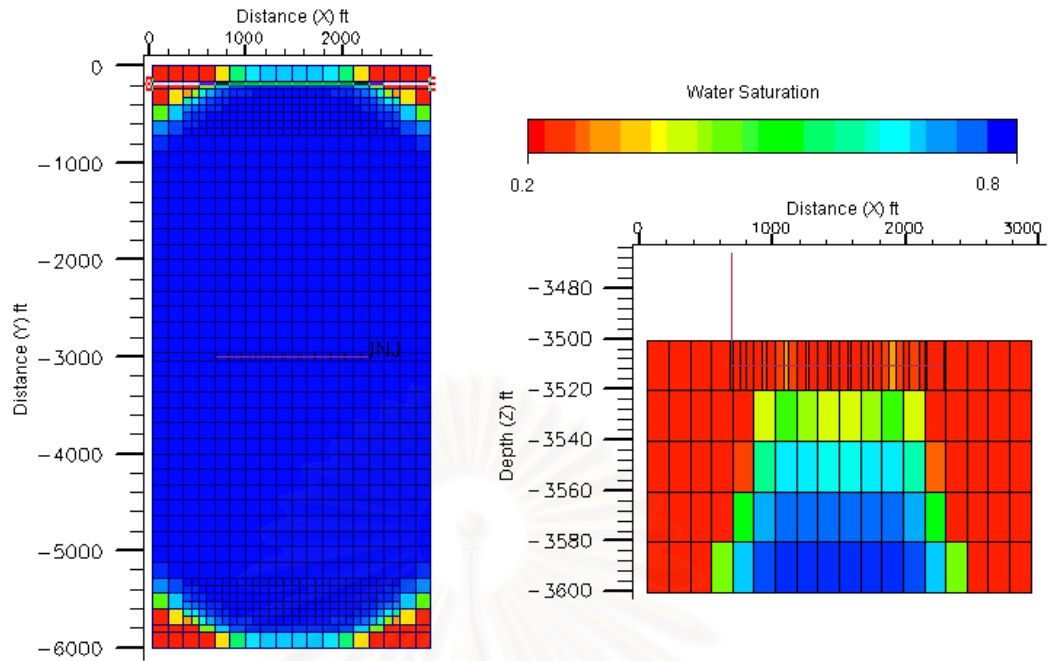


Figure 4.23: Saturation distribution at breakthrough for profile factor of 4

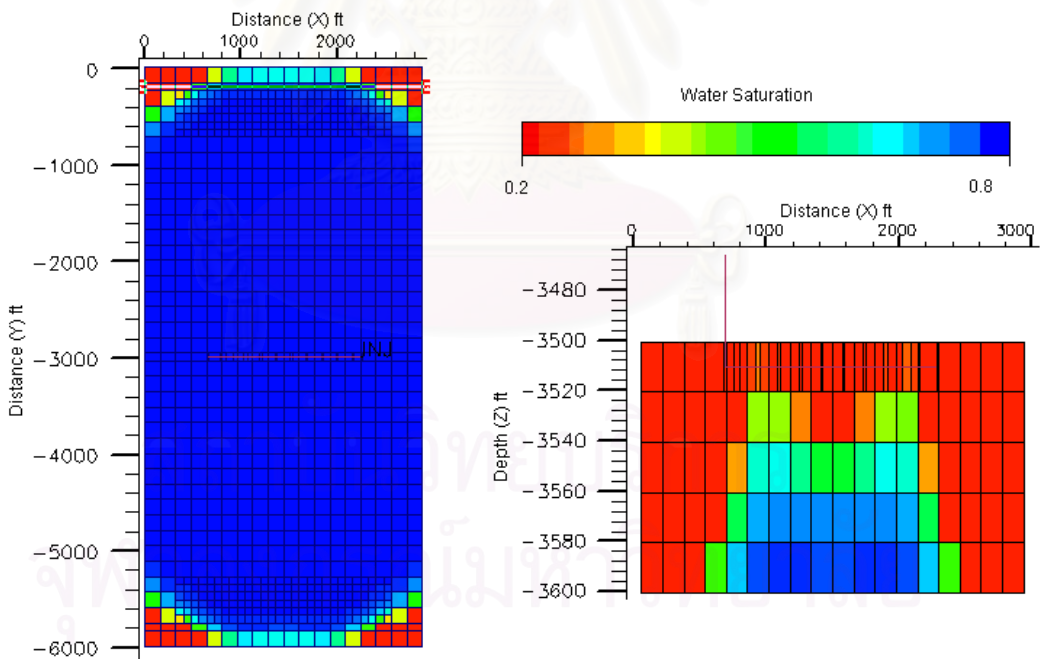


Figure 4.24: Saturation distribution at breakthrough for profile factor of 5

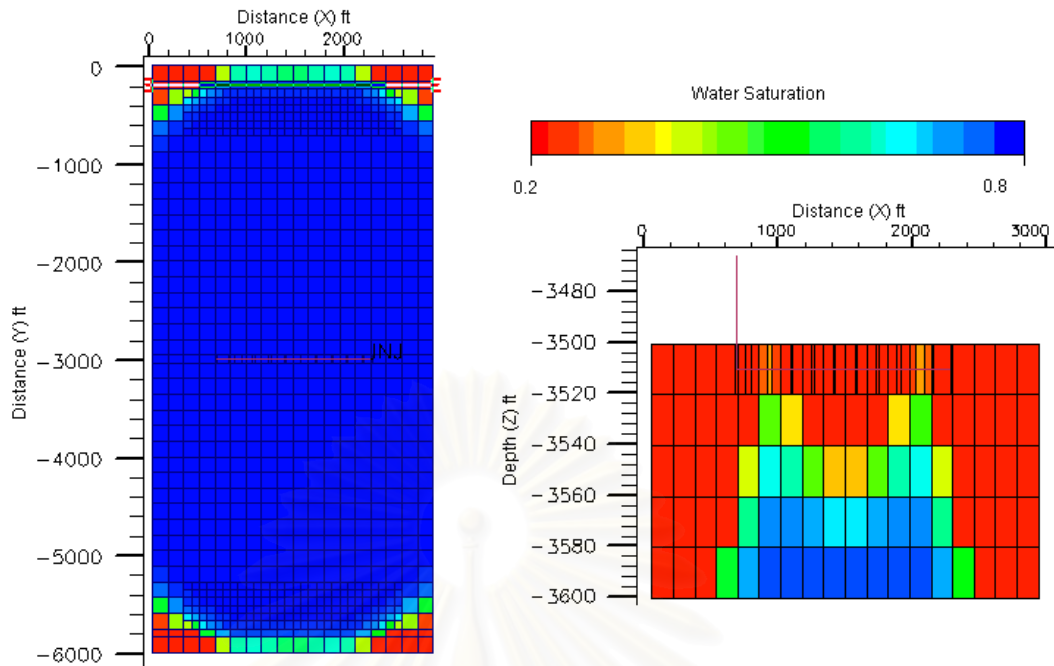


Figure 4.25: Saturation distribution at breakthrough for profile factor of 6

The breakthrough time and saturation distribution at breakthrough are the initial criteria used to compare waterflooding performance. Table 4.10 compares the results for different flow distributions. The flow distributions with profile factor of 4, 5 and 6 have the best sweep efficiency (90%). The breakthrough time generally increases as the profile factor increases until there are excessive flow rates at the heel and the toe for profile factor of 6 which breaks through faster than profile factor of 5. For these reasons, the profile factor of 5 was selected to be the optimal completion. Appendix B illustrates the saturation distributions at breakthrough in every layer of reservoir model for different completion strategies.

Table 4.10: Waterflooding performance at breakthrough
for different flow profiles

Profile factor	Sweep efficiency (%)	Breakthrough time (days)	Recovery factor (%)
2	88	4,436	53.69
3	89	4,525	54.78
4	90	4,557	55.16
5	90	4,587	55.53
6	90	4,557	55.16

Figure 4.26 illustrates the development of water front for the optimal completion case. The high flow rates at the heel and the toe cause non-uniform water front at the beginning. However, the water front becomes more and more uniform as it reaches the producer.

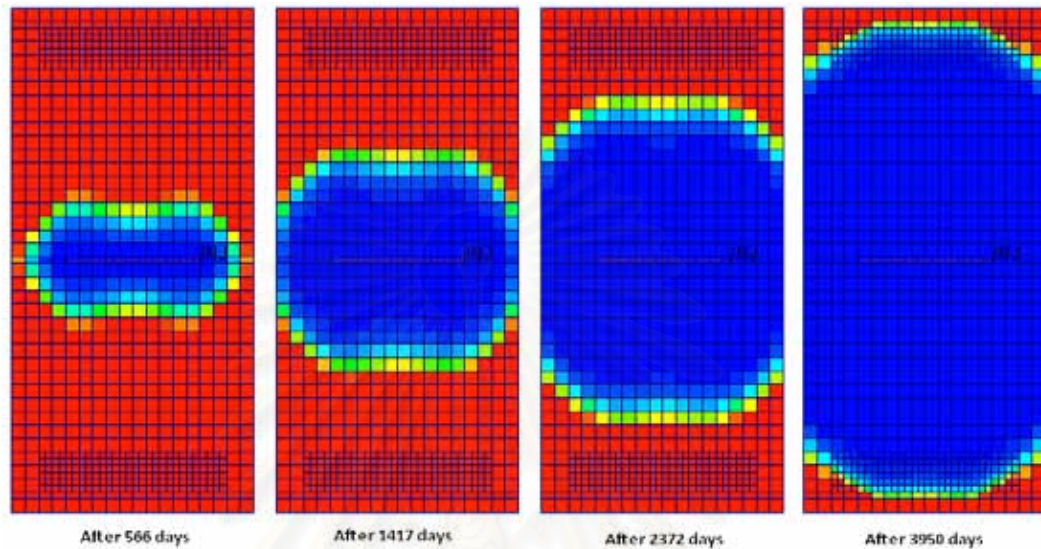


Figure.4.26: Development of water front by optimal completion

Since the optimal completion generates a more or less uniform flood front, the orientation of the horizontal well should not make any difference. To prove this, a case with direct line drive pattern was simulated. With the same optimal completion, i.e., the same perforation profile from heel to toe, the direct line drive pattern yields the same saturation distribution, breakthrough time, and flow distribution along the horizontal wells as those obtained with inverted line drive. So, the same results are obtained whether using inverted or direct line drive pattern. Figure 4.27 shows the saturation distribution of optimal completion using the direct line drive pattern.

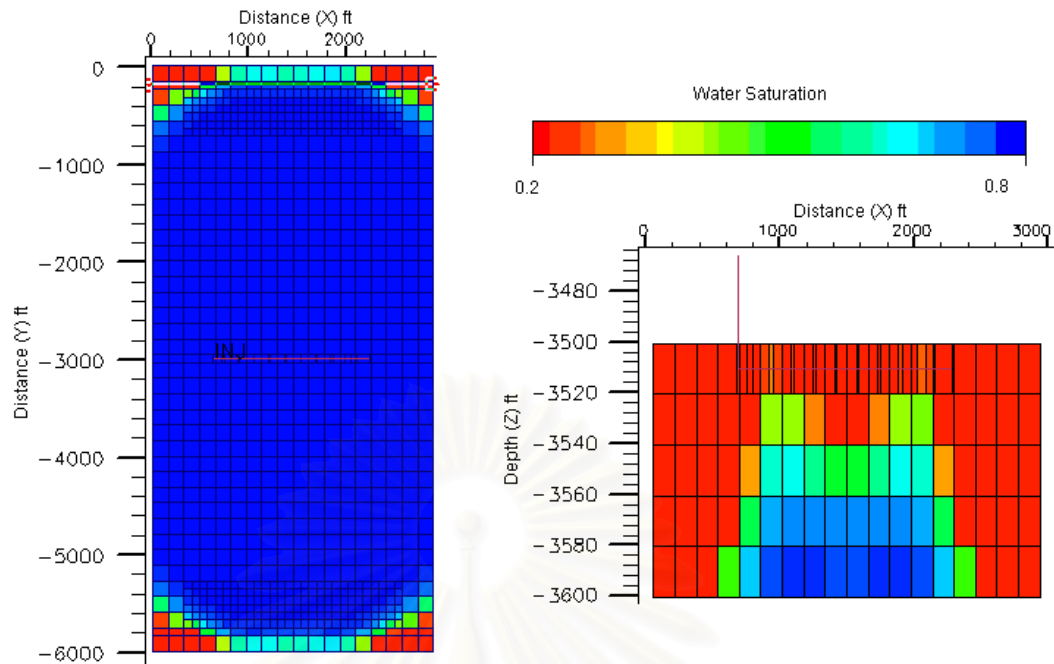


Figure 4.27: Saturation distribution at breakthrough for profile factor of 5 in direct line drive pattern

4.2.3 Comparison of Optimal Completion and Equally Open Completion

In this section, the comparison between optimal completion and equally open completion (the completion used in base case) is discussed. The objective is to study the advantages of optimal completion over equal open interval completion. The two types of completion are listed in Table 4.11.

Table 4.11: Summary of compared case conditions

Completion	Pattern	Friction consideration	Perforation
Equally open completion	Inverted	Yes	Default
Optimal completion	Inverted	Yes	Optimal

Since the optimal completion is created in order to generate uniform water front at breakthrough, it changes the flow distribution, creating higher drawdown near the heel and the toe. Figure 4.28 compares the flow distributions of the optimal and the equally open completion for the producer.

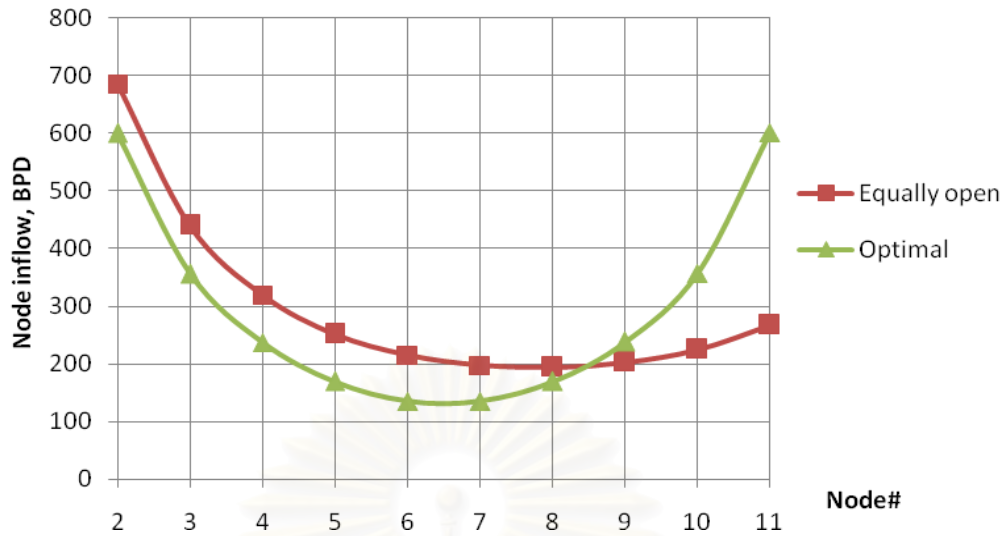


Figure 4.28: Comparison of flow distributions at the producer for equally open and optimal completions

Since the horizontal well does not fully penetrate the entire reservoir, the water injected at the heel and the toe has to sweep the un-penetrated areas in order to create a uniform water front. It requires more flow rate at the heel and the toe to sweep oil in these columns. This explains why the optimal completion has higher flow rate at the heel and the toe.

Table 4.12: Comparison of waterflooding performance for different completions

Result	Equally open	Optimal
Breakthrough time, days	4,436	4,587
Sweep efficiency, %	87	90
Recovery at BT, %	53.7	55.5
Producer BHP at BT, psia	1,426	1,389
Injector BHP at BT, psia	1,710	1,855

Table 4.12 summarizes the results from each case. The breakthrough time is an important factor to see the improvement. Obviously, the optimal completion can delay water breakthrough by 151 days (from 4,436 to 4,587 days) compared to the equally open completion. The sweep efficiency and recovery factor at breakthrough are improved due to the delay of breakthrough.

Generally, the watercut limit may be used as the economic limit especially in waterflooding. Excessive water production may cause the operation to become uneconomic. Assuming a watercut limit of 0.9, we can observe the water production and recovery efficiency comparison in Figures 4.29 and 4.30.

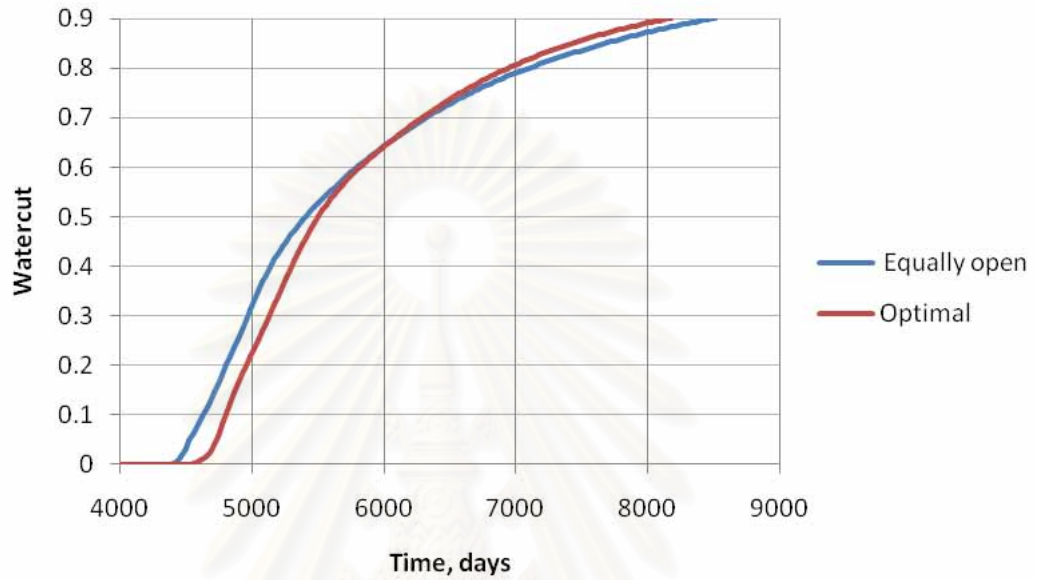


Figure 4.29: Comparison between watercut profiles for different completions

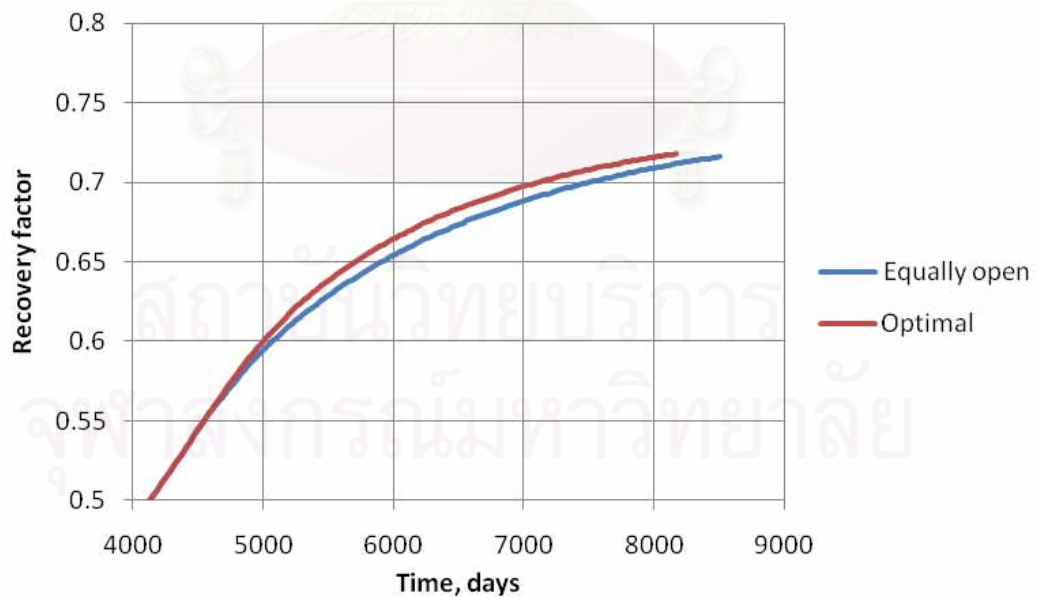


Figure 4.30: Comparison between recovery efficiency profiles for different completions

From the comparison, the watercut for the optimal completion increases faster than that for the equally open completion and becomes equal at around 6,000 days with 0.65 watercut. After that, the watercut for the optimal completion is higher than that for the equally open completion. The recovery factors at abandonment for the optimal completion and the equally open completion are 71.70% and 71.61%, respectively. The recovery factors at abandonment obtained from the two completions are not much different. The optimal completion can recover the oil faster than the equally open completion due to delay of the breakthrough time. However, it improves only small amount of recovery factor at abandonment.

Table 4.13: Comparison of open interval fraction for different completions

Completion	% open interval at segment:										
	2	3	4	5	6	7	8	9	10	11	Avg.
Equally open	80	80	80	80	80	80	80	80	80	80	80
Optimal (INJ)	12.0	9.7	9.2	9.5	10.8	13.6	19.1	29.2	47.3	80.0	24.1
Optimal (PROD)	26.8	18.3	13.3	10.3	9.04	10.2	14.8	24.9	44.5	80.0	25.2

Table 4.13 shows the open intervals for the two cases. The optimal completion has smaller open intervals between the wells and the reservoir. This causes reduction in productivity or injectivity of the horizontal wells, increases the required BHP for the injector, and decreases the required BHP for the producer. Figure 4.31 compares the BHP history of the two completions.

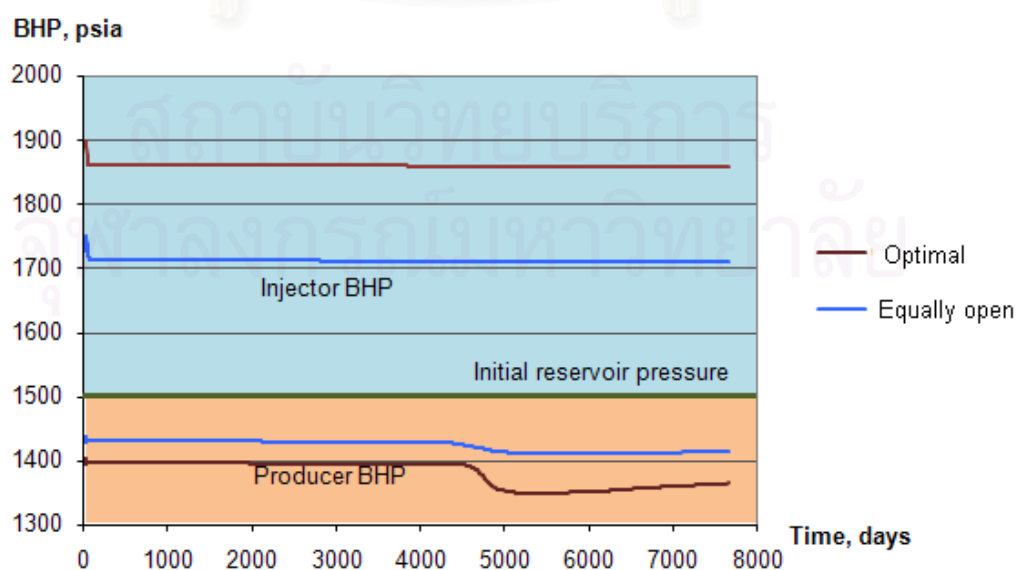


Figure 4.31: Comparison between BHP history for different completions

The injector BHP for optimal completion is 150 psi higher than that for equally open completion. Thus, it requires more compressor power to inject water into the reservoir. For the producer, the BHP of the optimal completion is lower than that for equally open completion. After breakthrough, detected by a drop in BHP of the producer, the BHP curve for the optimal completion drops more than that for the equally open completion and may cause problem in vertical lift.

Another parameter that relates to the BHP history is the watercut. The BHP of the producer drops after breakthrough due to change in water saturation around the wellbore. The relative permeability of oil reduces rapidly while the relative permeability of water increases at a slower rate. This condition requires more difference between formation and wellbore pressures to maintain the liquid production rate. Furthermore, the hydrostatic head in the vertical section increases rapidly due to water production. A low BHP may not be able to lift the reservoir fluid to the surface, thus requiring downhole pump. These are the disadvantages of optimal completion.

The efficiency of optimal completion should be compared when variables such as flow rate and mobility ratio are changed. The breakthrough time, sweep efficiency, recovery efficiency, and BHP may give different results when these variables are different.

CHAPTER V

EFFECT OF FLOW RATE AND MOBILITY RATIO

This chapter studies the performance of the optimal completion with different conditions such as flow rate and mobility ratio. With different operating flow rates, the friction losses along the horizontal section are different. This causes the flow distribution to be changed and may affect the sweep efficiency. For different mobility ratios, the preference of water to displace oil in the reservoir is changed. It actually affects the sweep efficiency of waterflooding. We studied how much it affects the optimal completion and compare the performance when using different completions.

5.1 Optimal Completion with Different Flow Rates

As shown in Section 4.2, the sweep efficiency of waterflooding using horizontal wells depends on the flow distribution along the horizontal section. The frictional pressure loss is the most important factor which affects the flow distribution. One of the factor causing a change in friction along the horizontal well is the flow rate. This chapter presents the effect of various flow rates to the waterflooding performance.

The completion with maximum open interval with inverted line drive pattern and the optimal completion were simulated with various injection and production rates. Four operating flow rates of 6000, 8,000, 10000, and 12000 RB/D were considered. The results such as flow distribution, sweep efficiency, breakthrough time, BHP, water cut and recovery efficiency are compared to illustrate the advantages and disadvantages of optimal completion in different conditions.

Since the operating flow rates of four cases are different, the reference flow distribution for each operating flow rate had to be determined from the non-friction well model separately. Figure 5.1 illustrates the normalized reference flow profile for different operating flow rates. The figure shows that the flow profiles are similar for all flow rates. Then, we use the same set of target flow distribution mentioned in section 4.2.2 to determine the optimal completion for different operating flow rates.

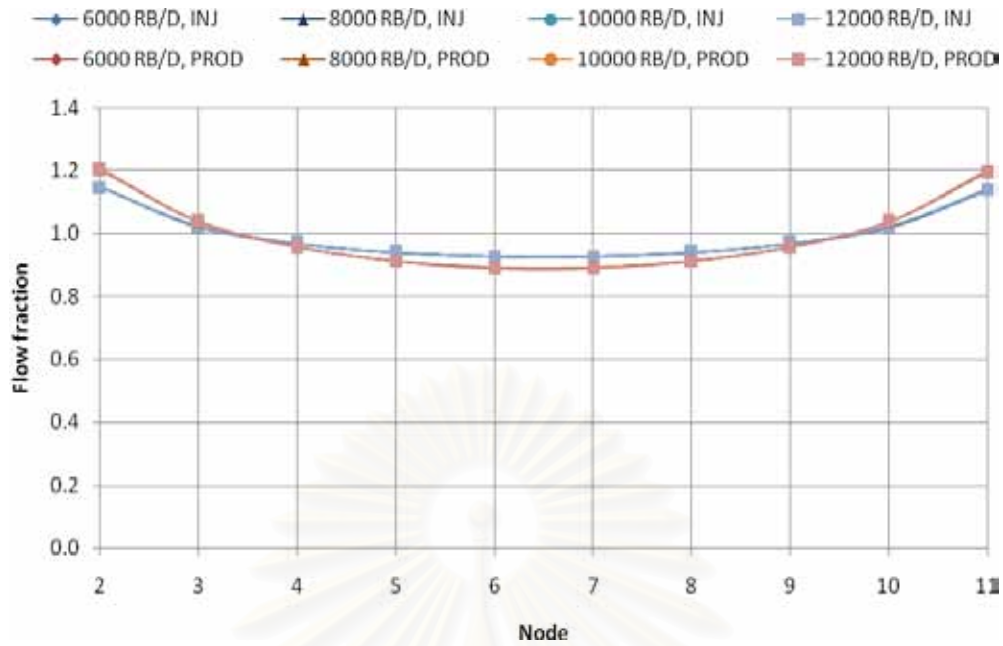


Figure 5.1: The normalized reference flow fraction profiles for different operating flow rates

5.1.1 Effect on Optimal Flow Distribution and Open Interval

After running a numerous number of simulations for different profiles as mentioned in Section 4.2.2, the optimal completions for the considered flow rates were obtained. Interestingly, the optimal completion was achieved by the profile factor of 5 for all considered flow rates. Figures 5.2 and 5.3 compare the optimal flow distributions before breakthrough and the completions strategy of producers for all cases, respectively.

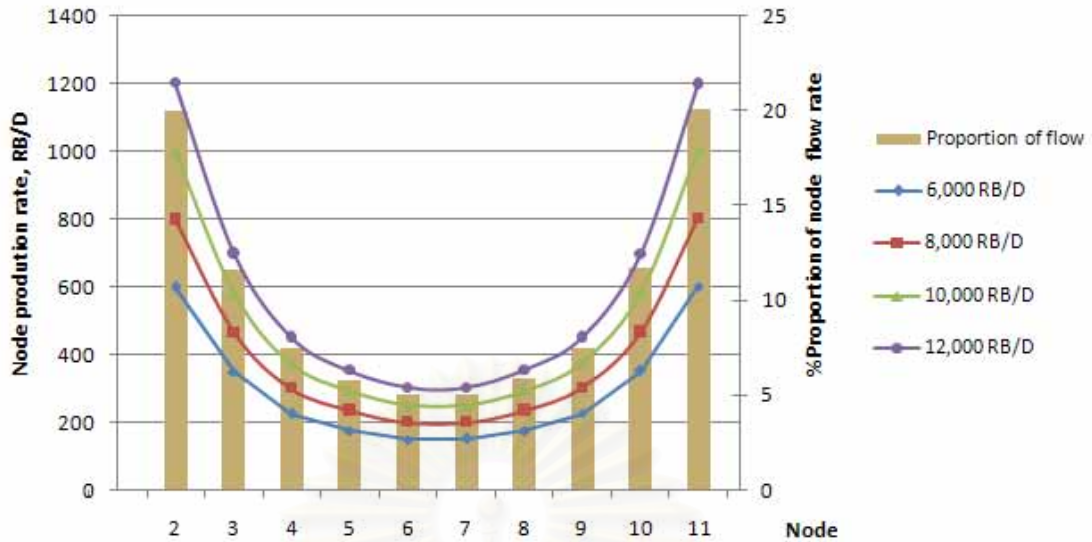


Figure 5.2: Comparison between optimal flow distributions at the producers for different flow rates

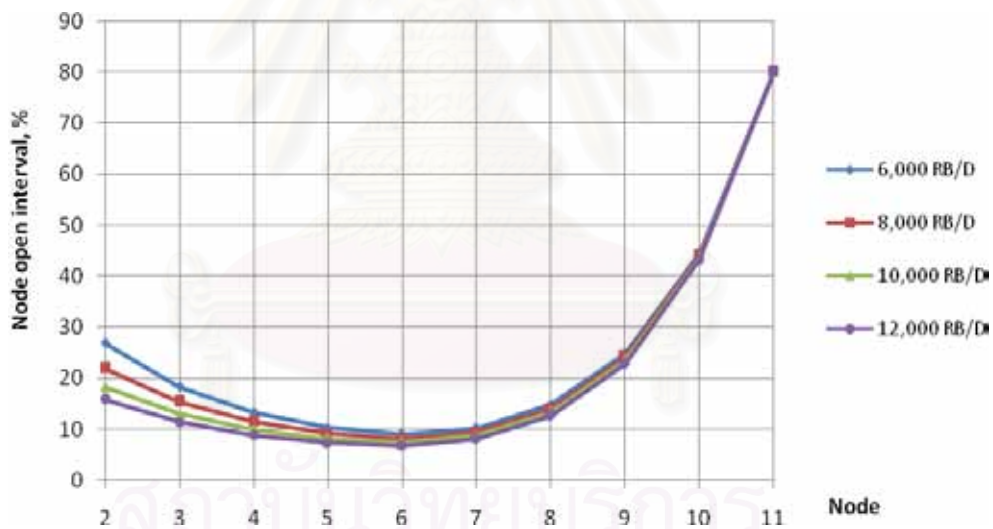


Figure 5.3: Comparison between optimal completion strategies at the producers for different flow rates

The results show that the optimal flow distribution of every case is achieved by a profile factor of 5. This means that changing the operating rate does not affect the proportion of optimal flow distribution along the horizontal section. However, the optimal completion strategies are different. With a higher operating rate, the open interval near the heel is less in order to keep the flood front uniform, which causes the productivity to slightly decrease. This is the disadvantage when using the optimal

completion as mentioned in Section 4.2.3. The effect of optimal completion to the BHP will be discussed in Section 5.1.4.

Considering before breakthrough, the average pressure profiles of optimal completion for different operating flow rates for the producer are illustrated in Figure 5.4. The pressure loss due to friction can be determined by the pressure difference between nodes 1 and 11. At high operating flow rate, the pressure drop due to friction increases due to high fluid velocity.

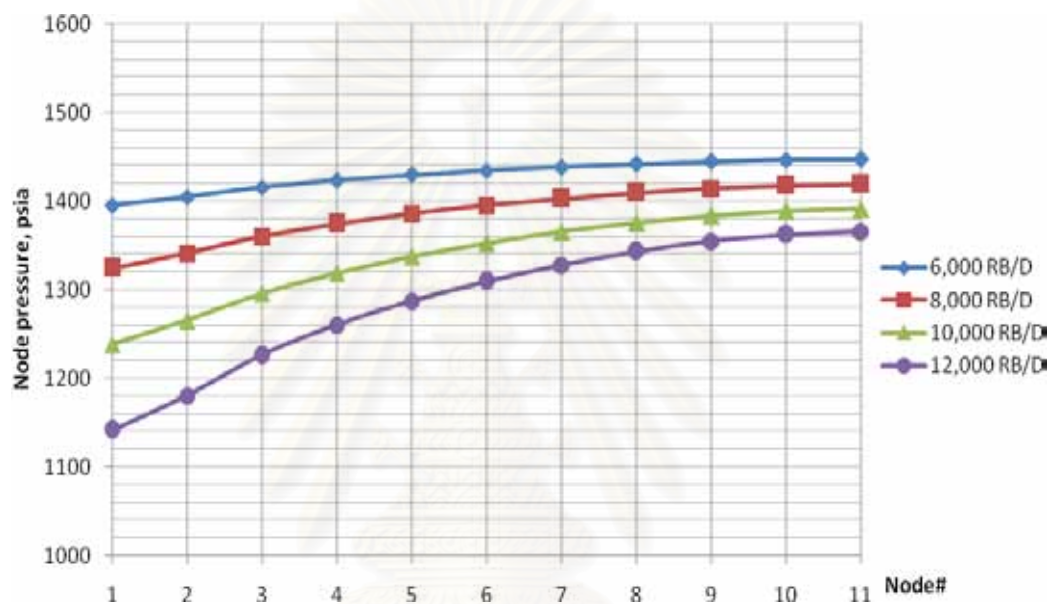


Figure 5.4: Comparison between average pressure profiles for different operating flow rates

5.1.2 Effect on Sweep Efficiency at Breakthrough

The breakthrough times for waterflooding with optimal completion are 4587, 3493, 2811, and 2352 days for the operating flow rate of 6000, 8000, 10000, and 12000 RB/D, respectively. Since the operating rate for each case is different, the breakthrough time cannot be compared to indicate which flow rate is better than the others. Then, the recovery and sweep efficiency at breakthrough are used to compare the performance for different operating flow rates. Figure 5.5 compares the recovery factor at breakthrough for all operating flow rates.

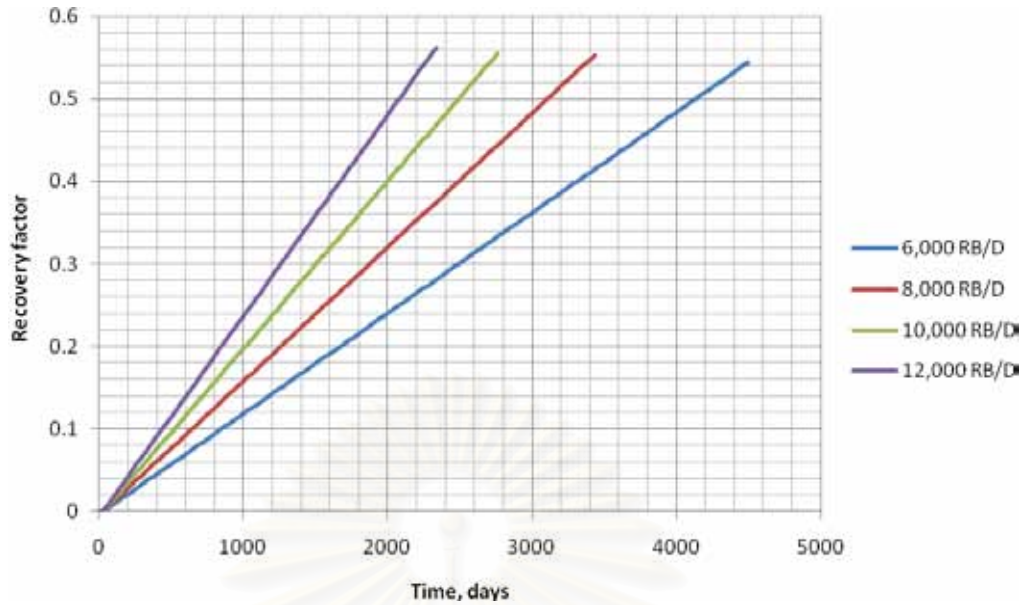


Figure 5.5: Comparison of recovery factors at breakthrough for different operating flow rates

The recovery factors at breakthrough obtained from optimal completion are around 55% for all considered operating flow rates. This results show that optimal completion gives only a small difference in the oil recovery factor for different operating flow rates. From Figure 5.5, we can see that operating with high flow rate is more preferable because it can recover oil faster than other operating flow rates.

The sweep efficiency at breakthrough obtained from waterflooding with optimal completion for different operating flow rates are related to the recovery factor at breakthrough. A sweep efficiency of 90% can be obtained from every operating flow rate as shown in Figures 5.6 to 5.9.

สถาบันวิทยบริการ
จุฬาลงกรณ์มหาวิทยาลัย

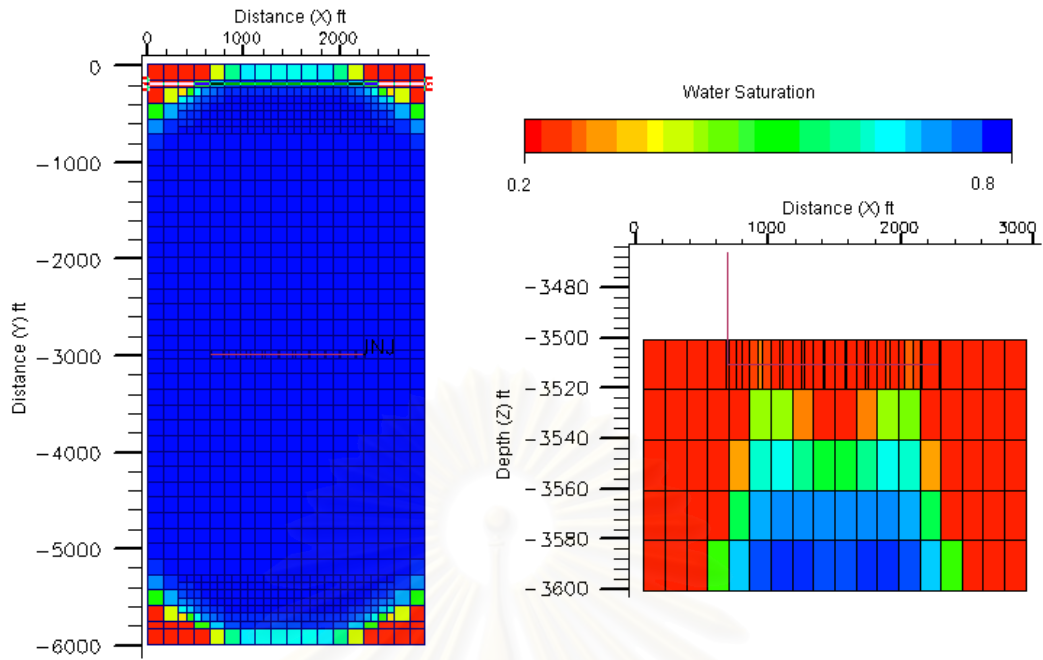


Figure 5.6: Saturation distribution at breakthrough using optimal completion for operating rate of 6,000 RB/D

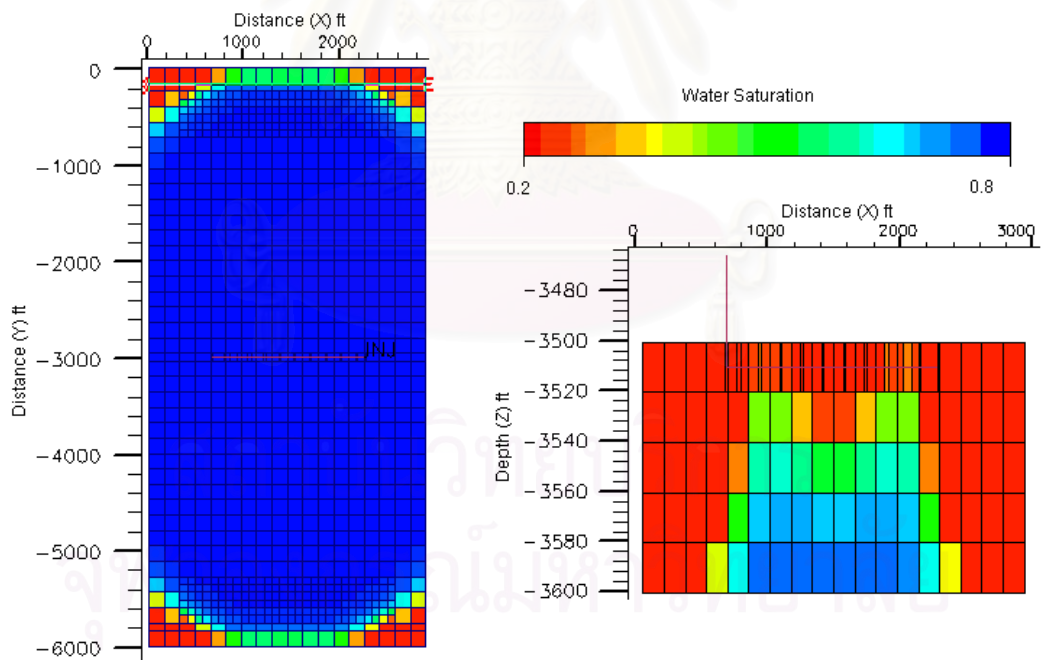


Figure 5.7: Saturation distribution at breakthrough using optimal completion for operating rate of 8,000 RB/D

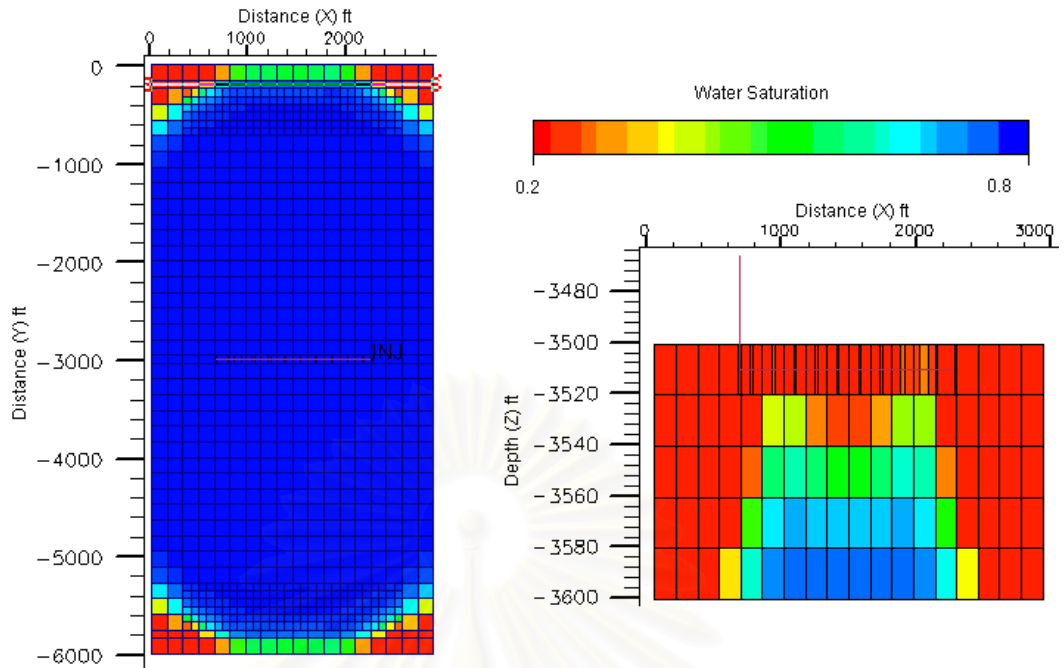


Figure 5.8: Saturation distribution at breakthrough using optimal completion for operating rate of 10,000 RB/D

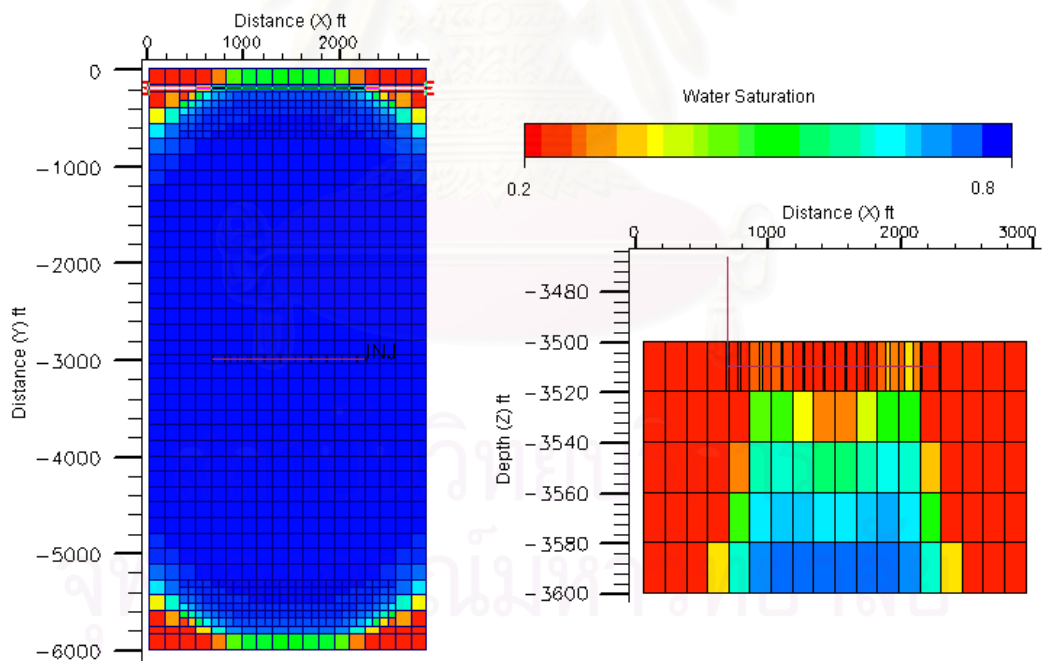


Figure 5.9: Saturation distribution at breakthrough using optimal completion for operating rate of 12,000 RB/D

As previously shown in Section 4.2.3, the sweep efficiency at breakthrough when using optimal completion is more than that of the equally open interval completion. Table 5.1 summarizes the sweep efficiency at breakthrough obtained from different completions and operating flow rates.

Table 5.1: Summary of the sweep efficiency at breakthrough for different completions and operating flow rates

Completion	Sweep efficiency (%)			
	6,000 RB/D	8,000 RB/D	10,000 RB/D	12,000 RB/D
Equally open	87	85	84	81
Optimal	90	90	90	90

The sweep efficiency at breakthrough decreases as the operating flow rate increases when using the equally open interval completion but does not change when using optimal completions. Higher operating flow rate causes more friction in the horizontal injector and producers. Then, the water tends to move from the heel of the injector to the heel of the producer. This causes lower sweep efficiency when using equally open completion. The optimal completion is more preferable when operating at high flow rate due to a large increase in sweep efficiency. Figure 5.10 compares the saturation distribution at breakthrough when operating at 12,000 RB/D for the two types of completion.

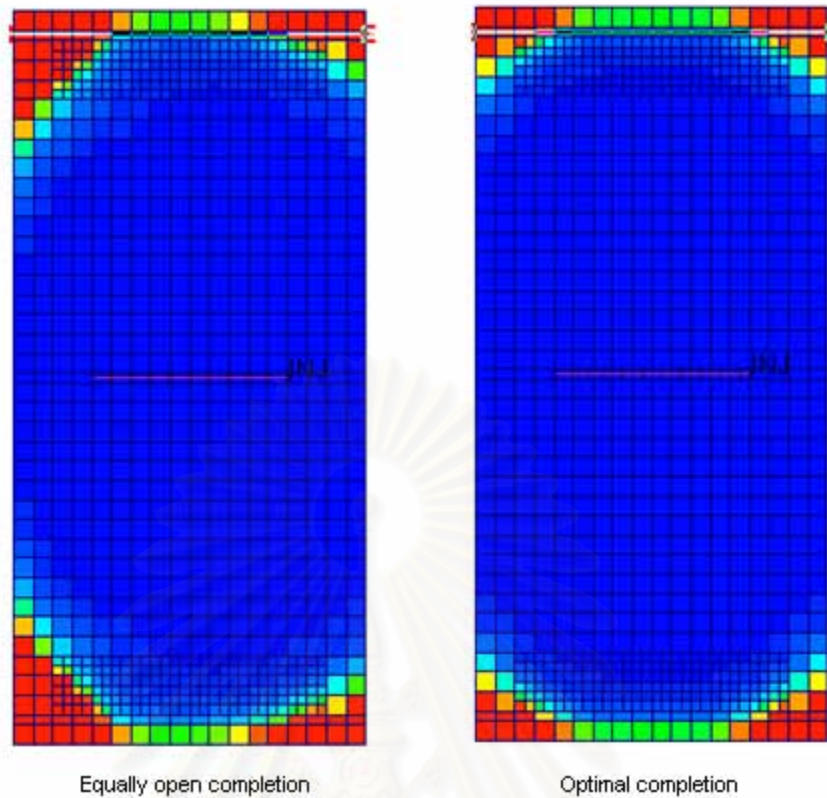


Figure 5.10: Comparison of saturation distribution at breakthrough when operating at 12,000 RB/D for different completions

5.1.3 Effect on Watercut and Recovery Efficiency at Abandonment

In economic analysis, oil and water production profiles are used to calculate the cash flow and NPV of the project. Watercut is typically used to determine the economic limit in waterflooding project. Assuming the abandonment condition to be 0.9 watercut, the watercut profile and recovery factor at abandonment obtained from waterflooding with the optimal completion for different operating flow rates are shown in Figures 5.11 and 5.12, respectively.

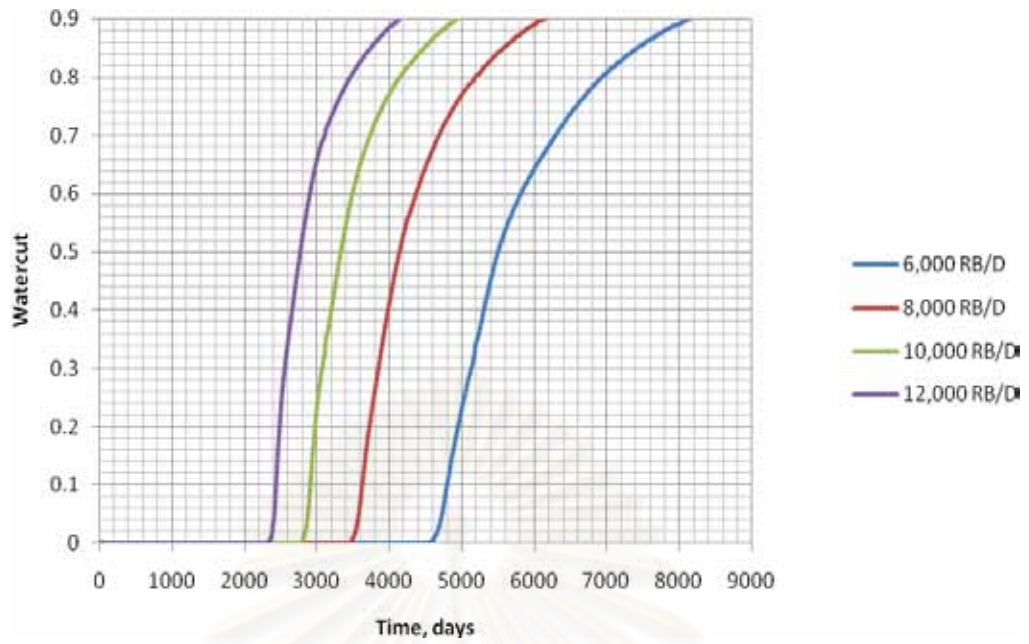


Figure 5.11: Watercut profile obtained from optimal completion for different operating flow rates

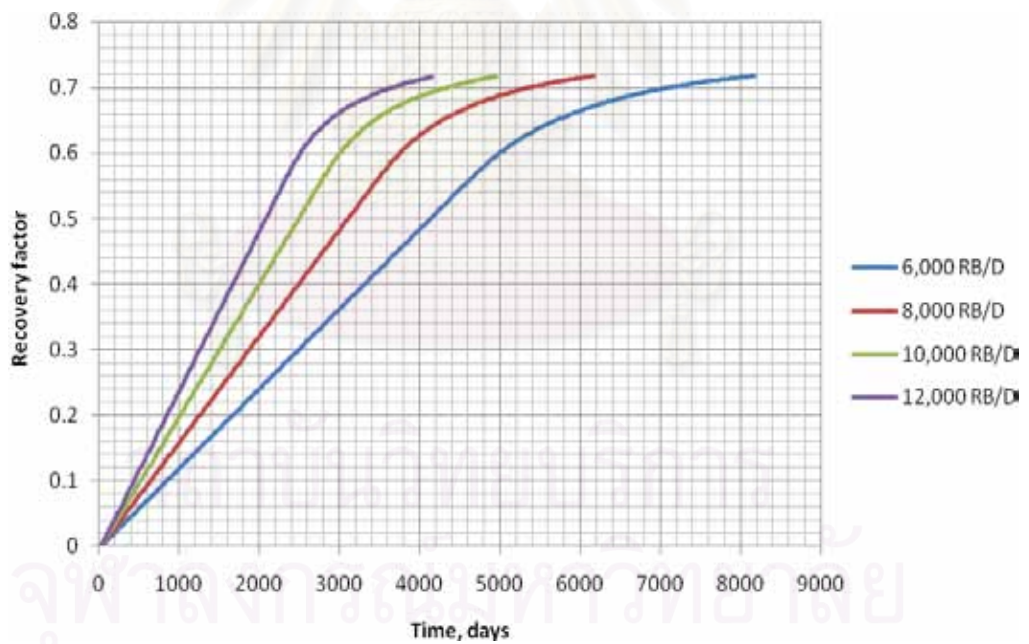


Figure 5.12: Recovery efficiency obtained from optimal completion for different operating flow rates

The recovery efficiency at 0.9 watercut is about 0.72 for all operating flow rates. The operating flow rate does not affect the recovery efficiency obtained from optimal completions.

As mentioned in Section 4.2.3, the recovery factor when using optimal completion is more than that of the equally open interval completion. Figure 5.13 compares the recovery factor at abandonment for the two completions. The recovery factors for the optimal completion are a bit more than those for the equally open completion for all operating flow rates. Using the optimal completion, the water breaks through at all sections along the horizontal producer. Then, the watercut increases faster than that using the equally open completion. Even though, there is a small increase in recovery efficiency, the optimal completion can recover oil faster than the equally open completion. The time spent to recover oil greatly affects financial status of the project. The faster we can recover the, the better the net present value and other economic indicator. The watercut and production profiles for different completions and operating flow rates are shown in Appendix B.

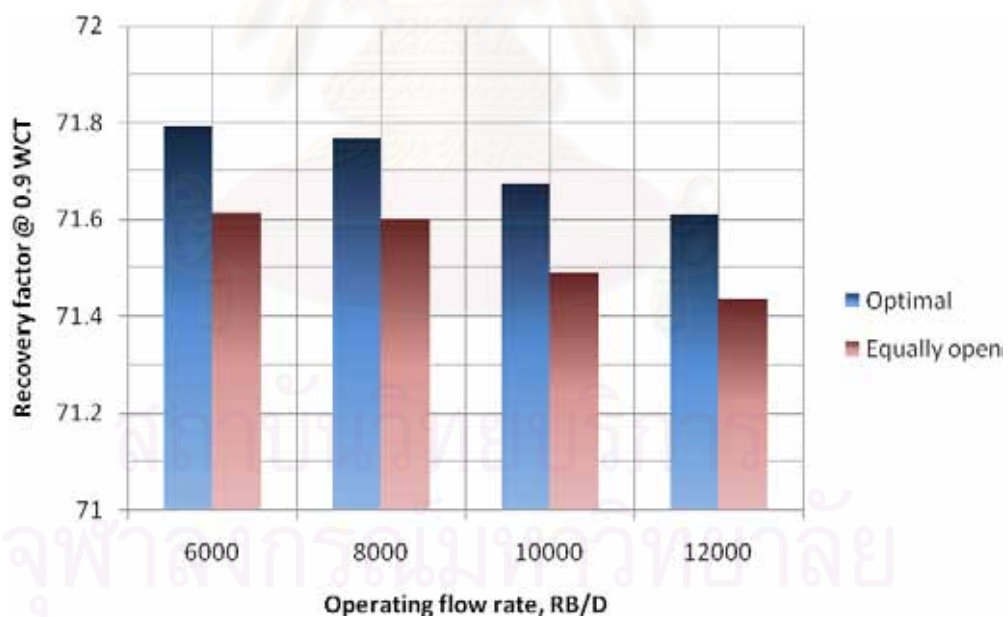


Figure 5.13: Comparison of recovery factor at abandonment for different completions at various operating flow rates

5.1.4 Effect on Bottomhole Pressure

As mentioned in Section 5.1.1, the open interval of optimal completion is less than the equally open completion. This causes more pressure drop along the horizontal wells. In addition, operating at a high rate causes more friction loss along the horizontal well. Thus, water flooding with optimal completion at high flow rate may encounter the limitation of insufficient BHP.

For the producer, the minimum BHP to produce the fluid from the bottom hole to the surface depends on the operating flow rate and hydrostatic head in the vertical section. Too low BHP may cause insufficient pressure to produce the reservoir fluid to the surface. The disadvantage of optimal completion is that it needs a small BHP to allow reservoir fluid to flow into the producer wellbore. This problem can be solved by installing downhole pump in the producer. This requires more investment on the equipment. The optimal completions for different operating rates require different BHPs. Figure 5.14 compares BHP of the producer for different operating flow rates when using optimal completion profile.

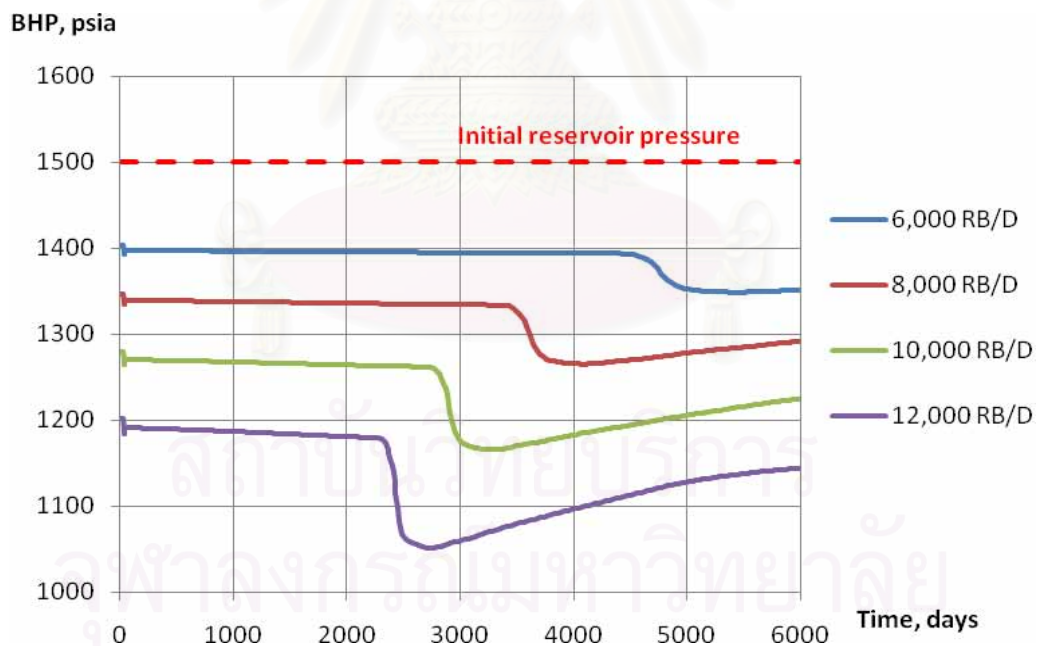


Figure 5.14: Comparison of producer's BHP history for different operating flow rates

Obviously, a higher operating flow rate requires less BHP than the lower operating flow rate to allow inflow to the wellbore. Typically, the minimum BHP to allow vertical flow from the bottom hole to the surface depends on the flow rate. Upward flow with higher flow rate requires more BHP.

The limitation of operating with high flow rate must also be considered at the injector. Figure 5.15 compares the BHP of optimal completed injector for different operating flow rates. Higher flow rate requires more BHP to inject water into the reservoir. The limit of BHP depends on the fracture pressure of the reservoir and the pump power used to inject the water.

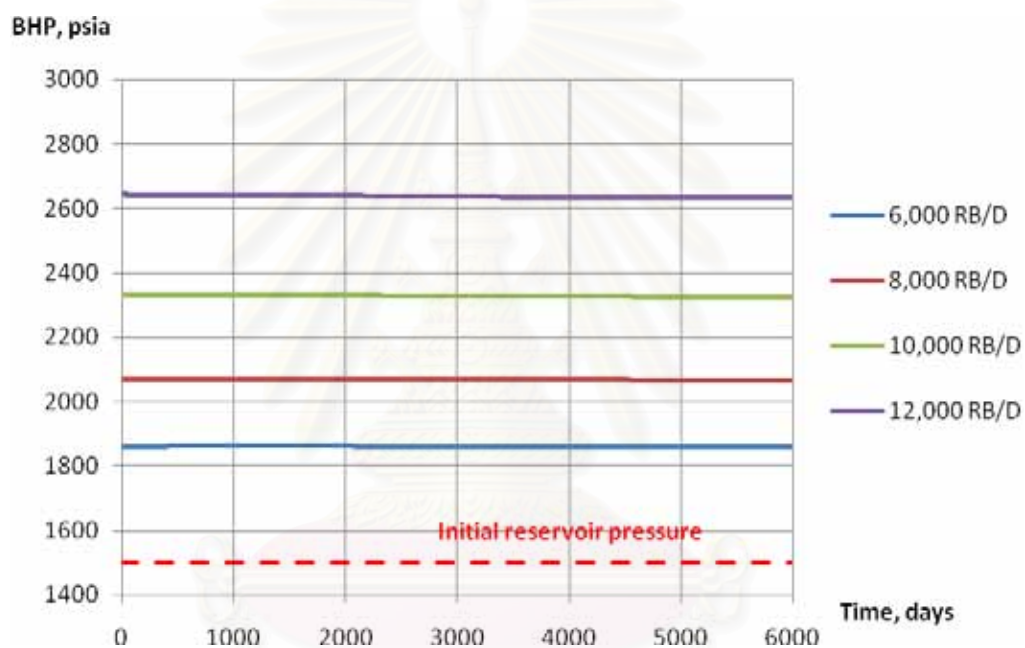


Figure 5.15: Comparison of producer's BHP history for different operating flow rates

The sweep efficiency is the criteria to decide whether the optimal completion or the equally open interval is more preferable to use. However, the reduction in BHP for the producer with optimal completion due to less open interval may cause insufficient BHP to lift fluid to the surface. Figure 5.16 compares the difference of producer's BHP before breakthrough between the two completions for different operating flow rates. From Figure 5.16, the difference of producer's BHP is higher at a high operating flow rate.

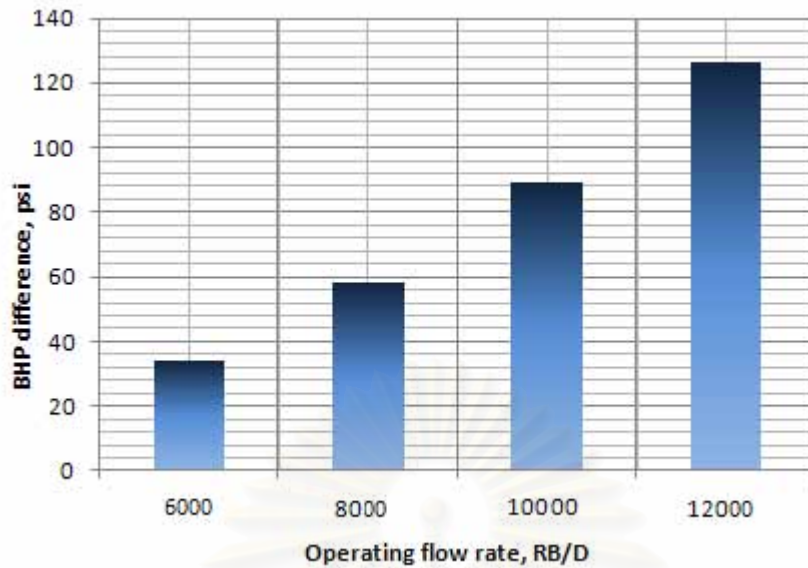


Figure 5.16: Difference of producer's BHP before breakthrough between equally open completion and optimal completion for different flow rates

5.2 Optimal Completion with Different Mobility Ratios

Mobility ratio affects the preference of water to move and displace oil in the reservoir. Different mobility ratios give different sweep and displacement efficiencies. This section studies the effect of different mobility ratio by varying the oil viscosity in each case.

Four mobility ratios of 1, 3, 5 and 10 were considered. An operating flow rate of 6,000 RB/D was used for all cases. Reference flow profiles for different mobility ratios were determined from the non-friction well model. Figure 5.17 shows that different flow fraction profiles were obtained for different mobility ratios. However, the difference is quite small. Therefore, we selected only one reference flow profile that gives the most sweep efficiency to represent the reference flow distributions for all mobility ratios.

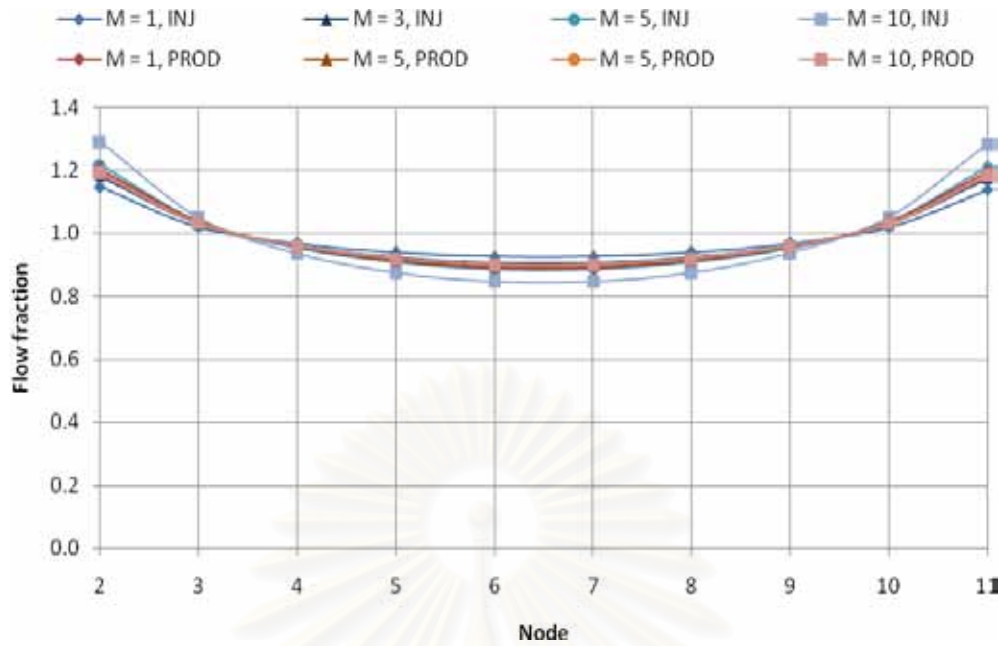


Figure 5.17: The normalized reference flow fraction profiles for different mobility ratios

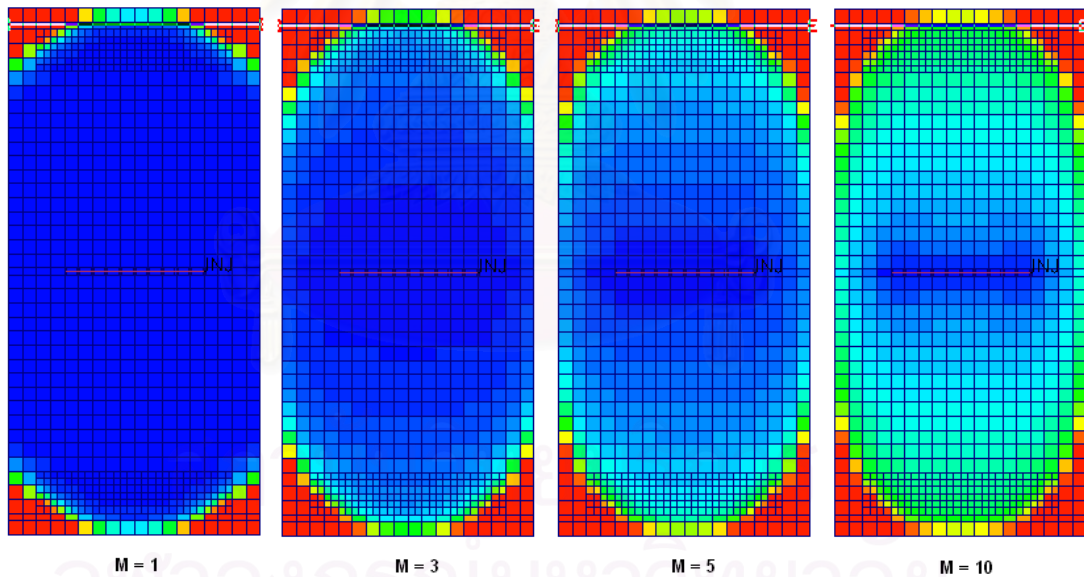


Figure 5.18: Comparison between saturation distributions at breakthrough obtained from non-friction well model for different mobility ratios

Figure 5.18 compares the sweep efficiencies obtained from the non-friction well model for different mobility ratios. The non-friction well model at mobility ratio of 1 gives the most sweep efficiency. Thus, the reference flow profile for mobility ratio of 1 was selected to determine the target flow distributions. Then, the same set of target

flow distributions as mentioned in Section 4.2.2 was used to determine the optimal completion for different mobility ratios. The results such as flow distribution, sweep efficiency, breakthrough time, BHP, water cut and recovery efficiency are compared to see the efficiency of optimal completion under different conditions.

5.2.1 Effect on Flow Distribution and Open Interval

After running a numerous number of simulations and several iterations, the optimal completions for different mobility ratios were obtained. The optimal flow distributions for mobility ratio of 1, 3, 5 and 10 were achieved with profile factor of 5, 4, 4 and 3 respectively. This means that mobility ratio affects the profile of optimal flow distribution. For a high mobility ratio, the optimal completion requires less flow rate at the heel and the toe than the case with low mobility ratio because the high mobility ratio causes the water to move faster through the reservoir. In order to create a uniform water front, the flow rate at the heel and the toe should be lower at higher mobility ratio. Figures 5.19 compares optimal flow distributions before breakthrough for different mobility ratios.

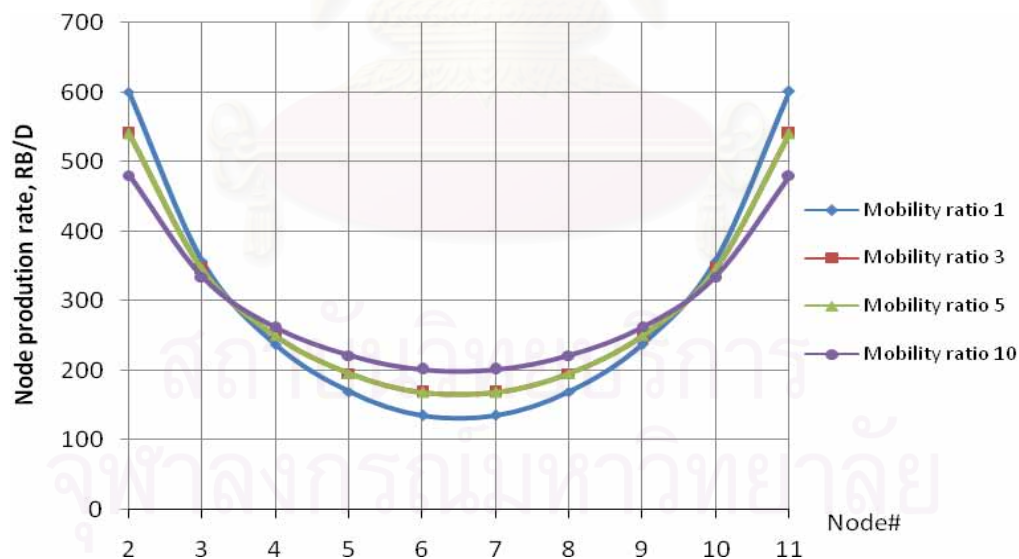


Figure 5.19: Comparison between optimal flow distributions at producers for different mobility ratios

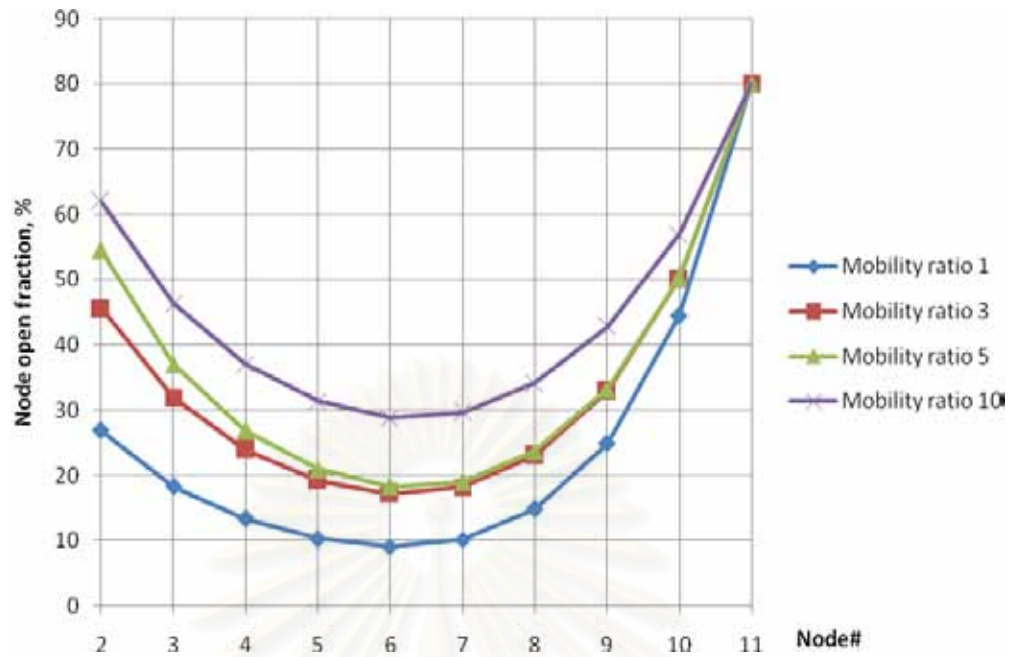


Figure 5.20: Comparison between optimal completion strategies at producers for different mobility ratios

Figure 5.20 compares the optimal completions strategies of producers for different mobility ratios. The open intervals of the optimal completion for a high mobility ratio are larger than those for a low mobility ratio due to higher drawdown at the producer. The change in drawdown pressure due to high oil viscosity has more effect than the change in friction loss inside the well as shown in Figure 5.21. Note that the mobility ratios of 3 and 5 have the same optimal flow profile which is profile factor of 4. When the drawdown pressure between the well and the reservoir is much more than the friction loss in the well, the friction loss has less effect. This is the reason why the difference between open interval fractions at the heel and the toe for high oil viscosity is less than that for low oil viscosity.

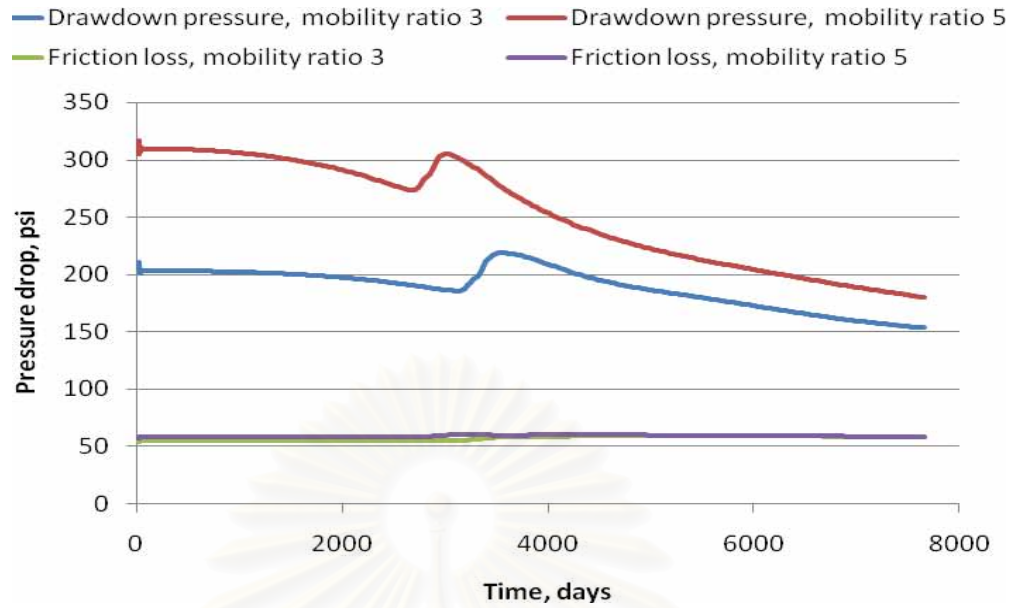


Figure 5.21: Comparison of pressure drop components at producers for different mobility ratios

5.2.2 Effect on Sweep Efficiency at Breakthrough

From the simulation result, the breakthrough time of waterflooding with optimal completions is 4587, 3219, 2763, and 2245 days for the mobility ratio of 1, 3, 5 and 10, respectively. We can see that the higher the mobility ratio, the faster the breakthrough time. Since the mobility ratio of each case is different, the breakthrough time and recovery factor at breakthrough cannot be compared to indicate which mobility ratio is better than the others. Then, the sweep efficiency at breakthrough is used to compare the performance of optimal completions for different mobility ratios. The saturation distributions at breakthrough obtained from waterflooding with optimal completion for different mobility ratios are shown in Figures 5.22 to 5.25. The sweep efficiency obtained from optimal completion decreases when the mobility ratio increases.

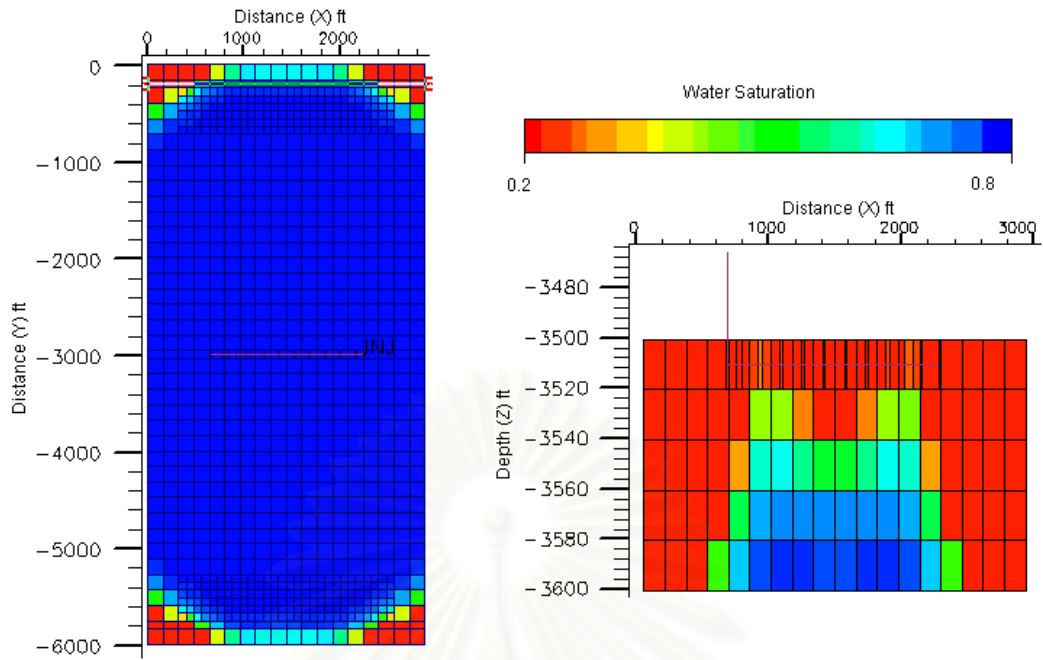


Figure 5.22: Saturation distribution at breakthrough using optimal completion for mobility ratio of 1

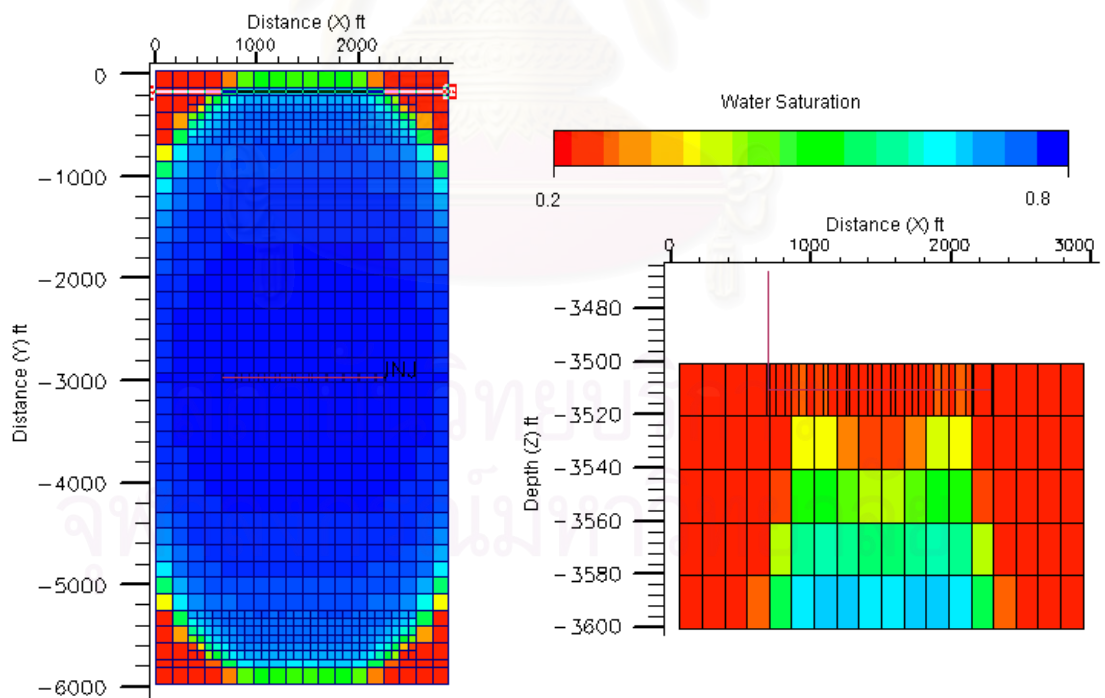


Figure 5.23: Saturation distribution at breakthrough using optimal completion for mobility ratio of 3

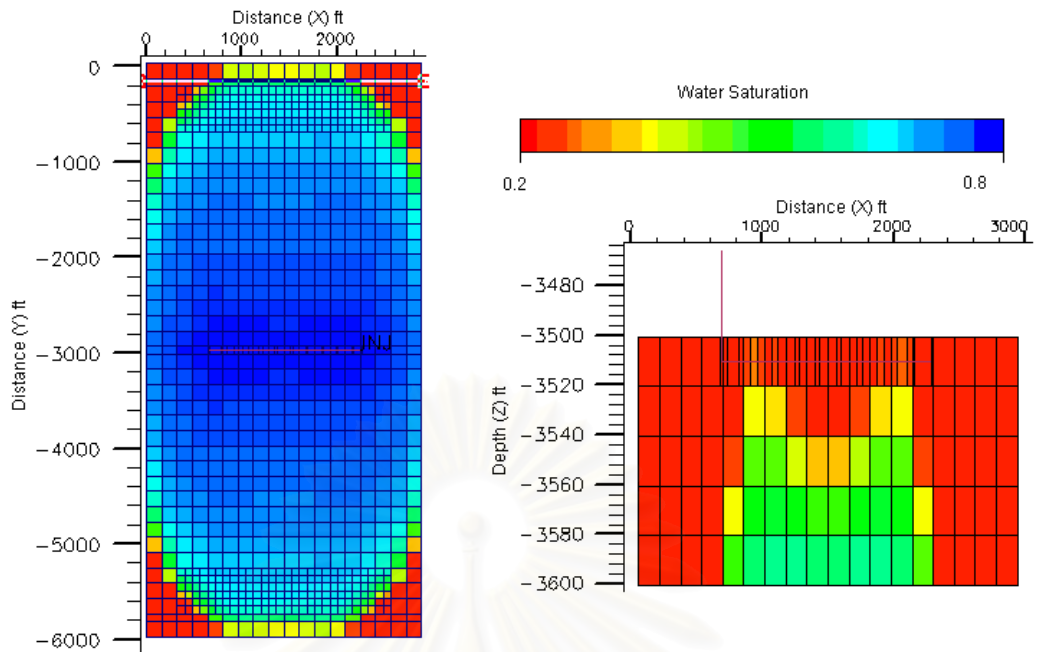


Figure 5.24: Saturation distribution at breakthrough using optimal completion for mobility ratio of 5

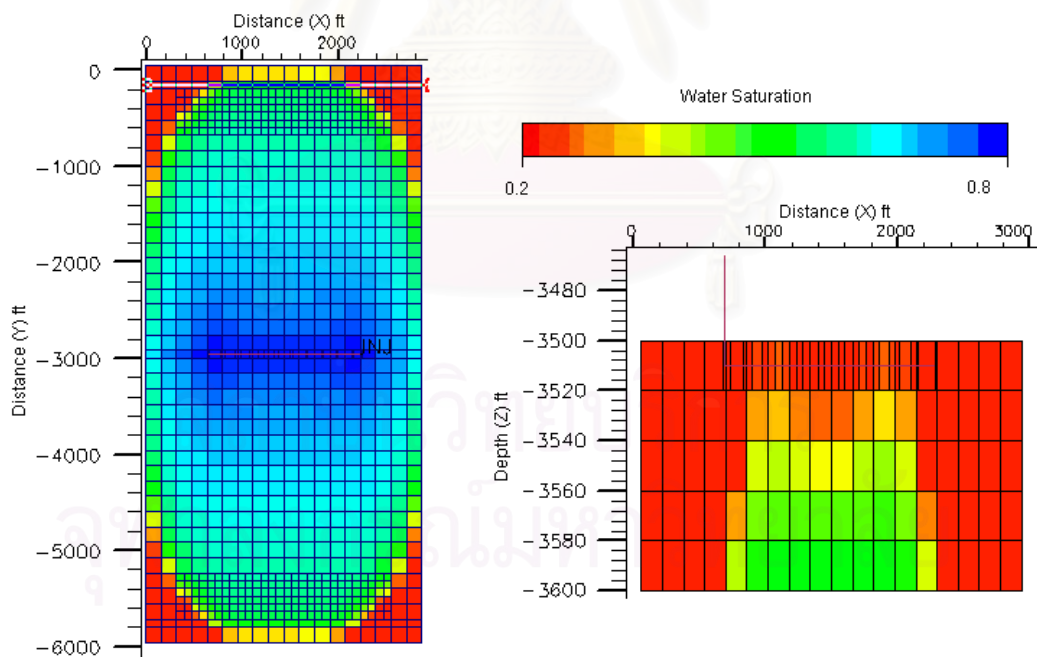


Figure 5.25: Saturation distribution at breakthrough using optimal completion for mobility ratio of 10

Table 5.2: Summary of sweep efficiency at breakthrough for different completions and mobility ratios

Completion	Sweep efficiency (%)			
	M = 1	M = 3	M = 5	M = 10
Equally open	87	81	77	68
Optimal	90	86	84	77

Table 5.2 summarizes the sweep efficiency at breakthrough for different completions and mobility ratios. The difference in sweep efficiency of both cases decreases rapidly as the mobility ratio increases. The sweep efficiencies between the two cases become more pronounced as the mobility ratio increases. The optimal completion is more preferable when operating at high mobility ratio due to a much better sweep efficiency. Figure 5.26 compares the saturation distribution at breakthrough when mobility ratio is 10 for different completions.

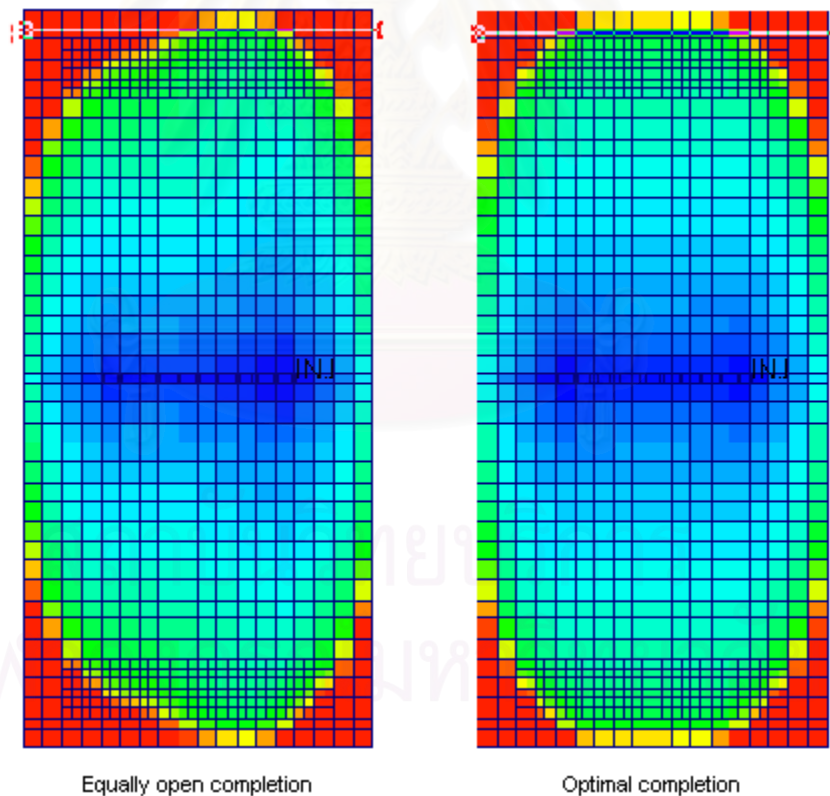


Figure 5.26: Comparison of saturation distribution at breakthrough when mobility ratio is 10 for different completions

5.2.3 Effect on Watercut and Recovery Efficiency at Abandonment

In economic analysis, oil and water production profiles are used to calculate the cash flow and NPV of the project. Watercut is typically used to determine the economic limit in waterflooding project. Assuming the abandonment condition to be 90% watercut, Figures 5.27 and 5.28 compare the watercut profiles and the recovery factors at abandonment for different mobility ratios. The recovery factors for the mobility ratio of 1, 3, 5 and 10 are 71.79%, 66.45%, 61.21% and 52.40%, respectively.

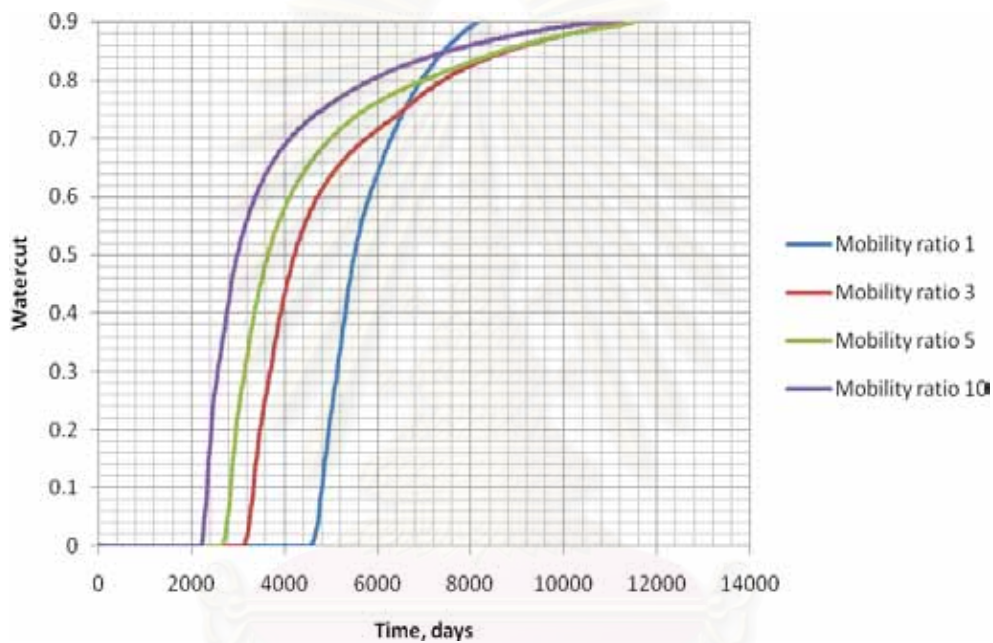


Figure 5.27: Watercut profiles for different mobility ratios

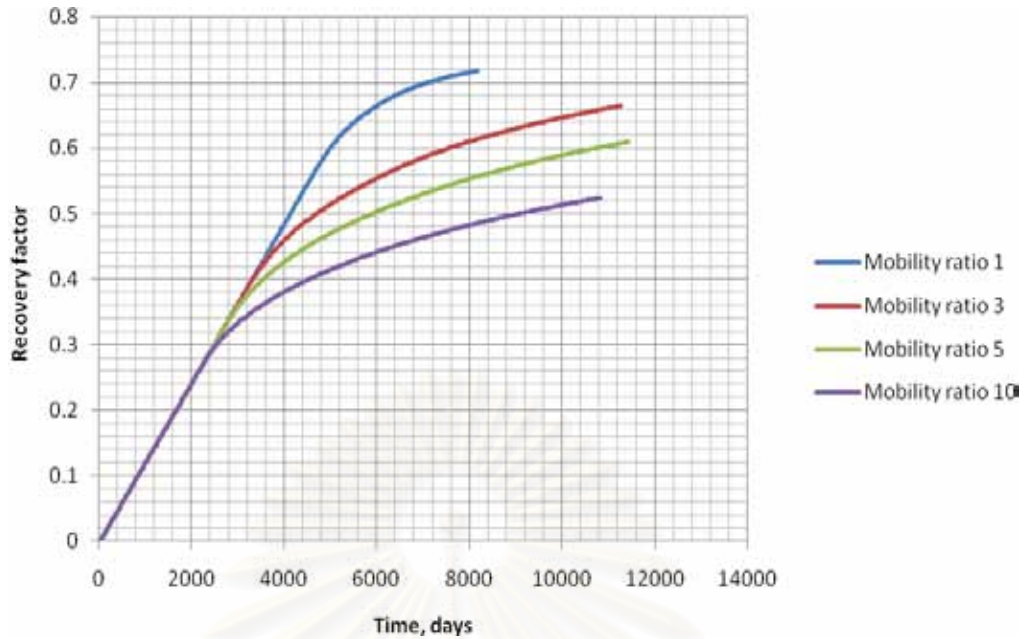


Figure 5.28: Recovery factors at 90% watercut for different mobility ratios

Figure 5.29 compares the recovery factor at abandonment for the two completions. The recovery factors for the optimal completion are a bit more than that for the base case for all mobility ratios. Using the optimal completion, the water breaks through at all sections along the horizontal producer. Then, the watercut increases faster than that for equally open completion. Even though, there is a small increase in recovery efficiency, the optimal completion can recover oil faster than the equally open completion. The time spent to recover oil greatly affects financial status of the project. The faster we can recover the, the better the net present value and other economic indicator. The watercut and production profiles for different completions and mobility ratios are shown in Appendix B.

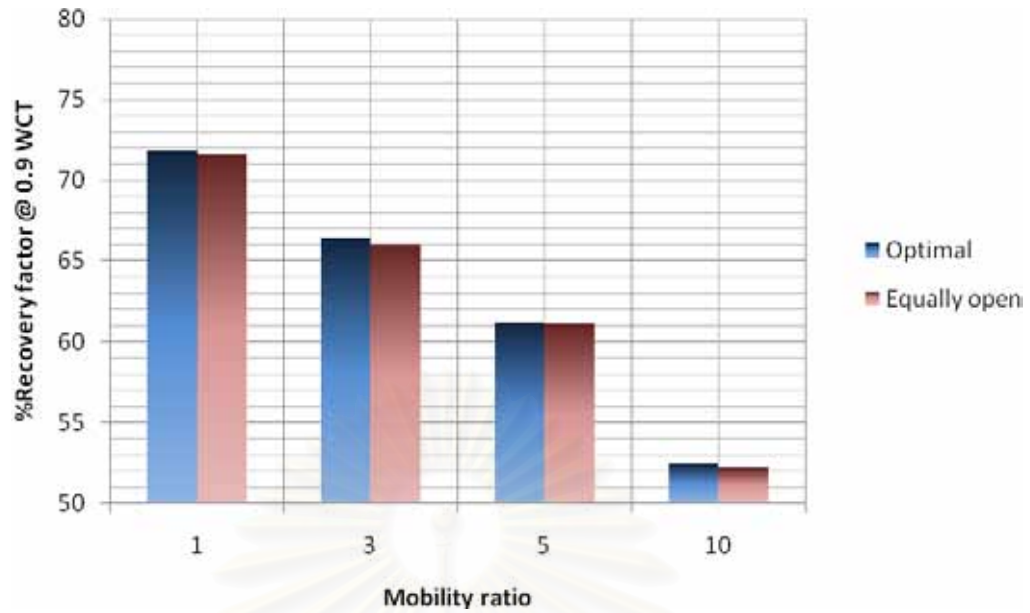


Figure 5.29: Comparison of recovery factor at abandonment for different completions at various mobility ratios

5.2.4 Effect on Bottomhole Pressure

The mobility ratio not only affects the sweeping of water the reservoir, but also affects pressure drop in the reservoir. Since the mobility ratio is varied by changing the oil viscosity, the effect of the oil viscosity to the BHP is determined. A high oil viscosity causes a large pressure drop, thus requiring a low BHP to allow oil to flow into the wellbore. This may cause insufficient pressure to produce the reservoir fluid to the surface. Using optimal completion in the reservoir where the oil is viscous has more limitation. Figure 5.30 compares the BHP of optimal completed producer for different oil viscosities.

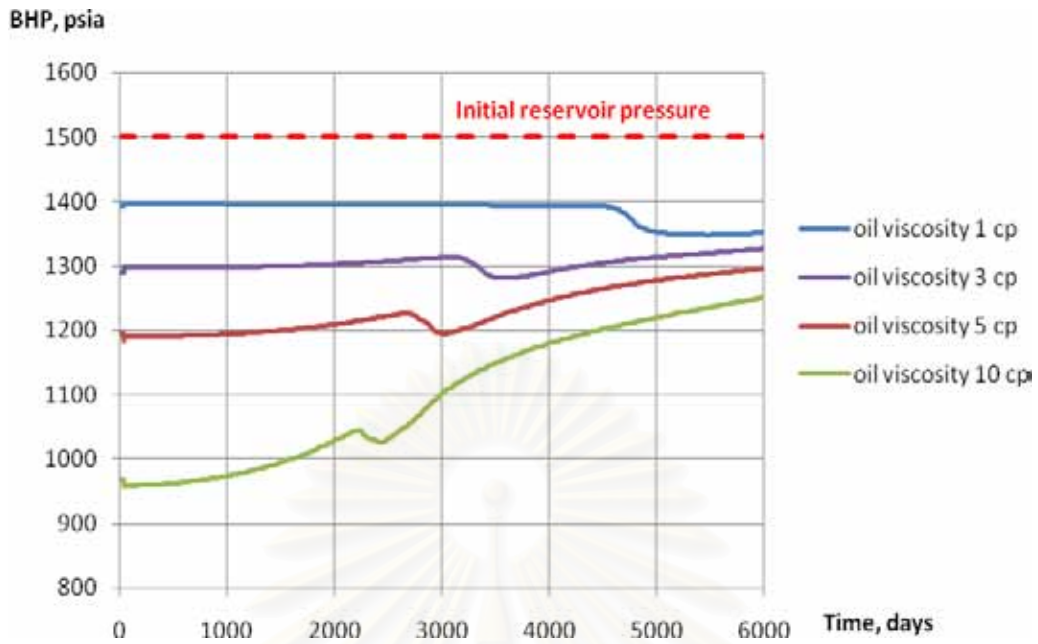


Figure 5.30: Comparison of producer's BHP history for different mobility ratios

As seen in Figure 5.30, a high oil viscosity requires less BHP than a low oil viscosity to flow into the wellbore. The BHP after breakthrough increases since more water which has less viscosity flows into the wellbore. Insufficient BHP can be solved by installing a downhole pump or producing at a lower flow rate.

Compared to the equally open completion, the optimal completion requires less BHP to allow reservoir fluid to flow into the producer. Figure 5.31 shows the reduction of producer's BHP before breakthrough due to the optimal completion compared to the equally open completion for different oil viscosities. From Figure 5.31, the difference of BHP is more pronounced at high mobility ratio.

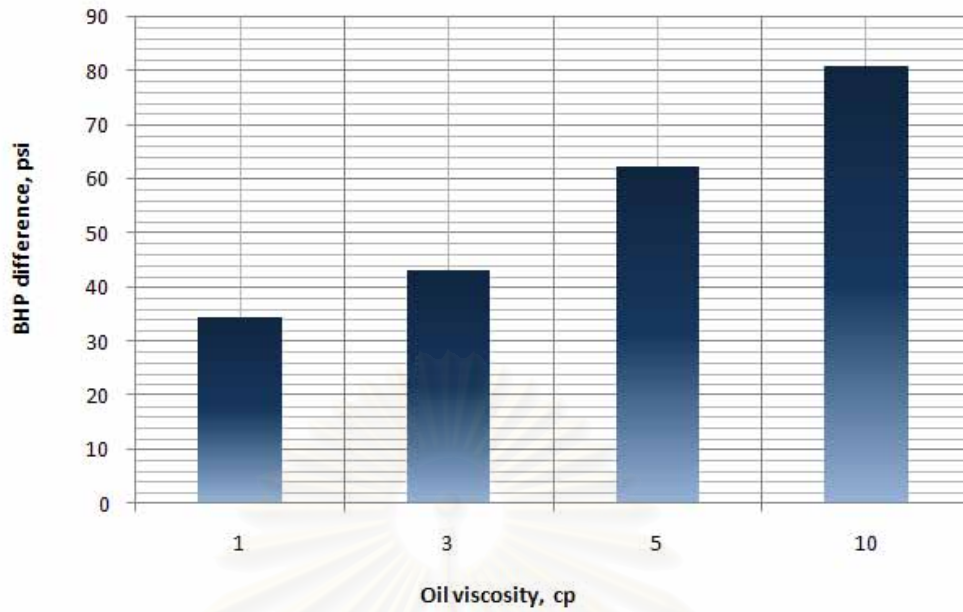


Figure 5.31: Difference of producer's BHP before breakthrough between equally open completion and optimal completions for different mobility ratios

CHAPTER VI

CONCLUSIONS AND REMARKS

This chapter concludes the waterflooding performance when using the optimal completion for different operating flow rates and mobility ratios. The performances such as sweep efficiency, recovery factor and BHP requirement are compared between using the equally open interval completion and optimal completion. Then, some remarks for this thesis are noted.

6.1 Conclusions

In this study, the performance of waterflooding with different completions and conditions were simulated. Two flooding patterns, direct and inverted line drive are concerned when using horizontal injector and producer. Waterfloodings with equally open interval using both patterns were simulated in order to compare their performances. The result shows that the inverted line drive pattern gives more sweep efficiency, so this pattern was selected for developing the optimal completion.

The horizontal injector and producers were modeled by using the multi-segment well model. The horizontal section of the well was divided into 10 segments. With this well model, the segment's parameters such as pressure and flow rate can be monitored. We can also adjust the open interval of each segment in the model in order to accommodate segment flow rates needed in the establishment of uniform flood front. Thus, we can iterate the process of changing the completion strategy and monitoring the segment's flow rate until obtaining the target flow distribution.

In this study, the optimal completion was developed to generate the most uniform water front. A flow distribution with high flow rate at the toe and the heel was obtained as the optimal completion. This optimal completion improves the sweep efficiency and delays the breakthrough time. Compared to the equally open completion, the advantages and disadvantages of the optimal completion can be listed as follows:

1. The optimal completion can generate more uniform water front than the equally open completion.

2. Before breakthrough, the overall efficiency of the optimal completion is generally better than that for the equally open completion. The optimal completion gives a better sweep efficiency, longer time before breakthrough, and a higher recovery factor at breakthrough.
3. Although the optimal completion can improve only a little recovery factor at abandonment (90% watercut), the optimal completion can recover oil faster than the equally open completion. This means that a small amount of water needed to be injected in order to recover the oil.
4. The optimal completion requires less BHP for the producer. In some cases, the downhole pump might be required to lift the fluids to the surface.

The performances of the optimal completion for different operating flow rates and mobility ratios are compared. The effect of the operating flow rate and the mobility ratio summarized as follows:

1. The operating flow rate does not affect the sweep efficiency of the optimal completion but affect that for the equally open completion by reducing the sweep efficiency at high operating flow rates.
2. A higher mobility ratio gives less sweep efficiency for both optimal completion and the equally open completion. However, the mobility ratio has more effect to the sweep efficiency for the equally open completion than that for the optimal completion.

6.2 Remarks

1. In this study, we assumed the skin factor for all completion to be zero. The variation of skin factor may affect the completion strategy of the optimal completion.
2. The optimal flow distributions obtained from the simulation can be applied to any completion techniques.
3. The heterogeneity of the reservoir can reduce the sweep efficiency of the optimal completion.
4. A higher flow rate is more preferable due to faster recovery. However, the BHP requirement should be considered, especially when using the optimal completion.

5. This study did not include the consideration of the vertical flow performance in the simulations. All BHP results were obtained from the inflow performance only.
6. The other factors such as dip angle of the reservoir, the ratio of the well length to the pattern width, wellbore diameter, wellbore roughness, pattern geometry, etc. should be investigated for their effects on the waterflooding performance.



สถาบันวิทยบริการ
จุฬาลงกรณ์มหาวิทยาลัย

References

- [1] Ferreira, H.; Mamora, D.D.; and Startzman, R.A. Simulation Studies of Waterflood Performance with Horizontal Wells, paper SPE 35208, Presented at the Permian Basin in Oil and Gas Recovery Conference, Calgary, Texas, 1996.
- [2] Popa, C.G.; and Clipea, M. Improve Waterflooding Efficiency by Horizontal Wells, paper SPE 50400, Presented at the 1998 SPE International Conference on Horizontal Well Technology, Alberta, Canada, 1998.
- [3] Mukminov, I.R. Influence of the Horizontal Well Length upon Production Rate and Water-cut Performance in Regular Field Development System with Horizontal Wells, paper SPE 77827, Presented at the SPE Asia Pacific Oil and Gas Conference and Exhibition, Melbourne, Australia, 2002.
- [4] Watermark, R.V.; Schmelting, J.; Duaben, D.L.; Robinowitz, S.; and Weyland, H.V. Application of Horizontal Waterflooding to Improve Oil Recovery from Old Oil Fields, paper SPE 99668, Presented at the 2006 SPE/DOE Symposium on Improve Oil Recovery, Tulsa, Oklahoma, 2006.
- [5] Furul, K.; Zhu, D.; Hill, A.D.; Davis, E.R.; and Buck, B.R. Optimization of Horizontal Well Completion Design with Cased/Perforated or Slotted Liner Completions, paper SPE 90579, Presented at the 2004 SPE Annual Technical Conference and Exhibition, Houston, 2006.
- [6] Asheim, and Harald, "Determination of Perforation Schemes To Control Production and Injection Profiles Along Horizontal Wells," Journal of SPE Drilling & Completion Journal 12, No.1 (March 1997): 13-18.

- [7] Ratterman, E.E.; Voll, B.A.; and Augustine; J.R. New Technology Applications to Increase Oil Recovery by Creating Uniform Flow Profiles in Horizontal Wells: Case Studies and Technology Overview, paper SPE 10177, Presented at the International Petroleum Technology Conference, Qatar, 2005.
- [8] ECLIPSE Technical Description Manual [Computer file]. Schlumberger, 2006.
- [9] Moen, T.; Reslink, A.S.; and Asheim, H.; Inflow Control Device and Near-Wellbore Interaction, paper SPE 112471, Presented at the SPE International Symposium and Exhibition on Formation Damage Control, Louisiana, 2008.
- [10] Michael, G.; and Curtis, H.W.; Well Performance, 2 nd ed. New Jersey: Prentice Hall, 1991.
- [11] Sada, D.J.; Horizontal Well Technology. Oklahoma: PennWell Books, 1991.
- [12] Aguilera, R.; Artindale, J.S.; Cordell, G.M.; Ng, M.C.; Nicholl, G.W.; and Runions, G.A.; Horizontal Wells. Vol. 9: Contributions in Petroleum Geology & Engineering. Texas: Gulf, 1991.
- [13] Jahn, F.; Cook, M.; and Ghaham, M.; Hydrocarbon Exploration and Production. Netherlands, Elsevier Science B.V., 1998.
- [14] Willhite, G.P.; Waterflooding. Society of Petroleum Engineers, 1986.
- [15] Aronofsky, J.S.; and Dallas; Mobility Ratio-Its Influence on Flood Patterns During Water Encroachment. Paper SPE 132-G, Presented at the Fall Meeting of Petroleum Branch, Oklahoma, 1951.



APPENDICES

สถาบันวิทยบริการ
จุฬาลงกรณ์มหาวิทยาลัย

APPENDIX A

ECLIPSE script for optimal completion case with operating flow rate of 6,000 RB/D and mobility ratio of 1

RUNSPEC section

```

START
  1 'JAN' 2000 /

FIELD

GAS

OIL

WATER

NSTACK
  150 /

ENDSCALE
  'NODIR' 'REVERS' 1 20 /

MSGFILE
  1 /

LGR
  6 840 0 2 2 10 'NOINTERP' 0 /

WSEGDIMS
  3 12 2 /

DISPDIMS
  1 2 1 /

DIMENS
  18 39 5 /

SCDPDIMS
  0 0 0 0 0 /

EQLDIMS
  1 100 100 1 20 /

REGDIMS
  1 1 0 0 /

TABDIMS
  1 1 20 20 1 20 20 1 /

WELLDIMS
  4 32 2 4 /

```

Grid section

ECHO

GRIDUNIT

-- Grid data units

'FEET' /

MAPAXES

-- Grid Axes wrt Map Coordinates

0 0 0 0 0 0 /

ECHO

CARFIN

-- Cartesian Local Grid Refinement

'PROD1' 3 16 3 5 1 5 28 6 5 1* /

ENDFIN

CARFIN

-- Cartesian Local Grid Refinement

'WPROD1' 4 14 2 2 1 1 32 1 1 1* /

ENDFIN

REFINE

'WPROD1' /

NXFIN

2 3 3 3 3 3 3 3 3 3 /

ENDFIN

REFINE

'WPROD1' /

HXFIN

90 10 27.19 45.63 27.19 34.03 31.94 34.03 38.01 23.97 38.01 40.4 19.2 40.4

41.42 17.17 41.42 40.88 18.24 40.88 38.46 23.08 38.46 33.57 32.87 33.57 24.92

50.15 24.92 10 80 10 /

ENDFIN

CARFIN

-- Cartesian Local Grid Refinement

'PROD2' 3 16 35 37 1 5 28 6 5 1*/

ENDFIN

CARFIN

-- Cartesian Local Grid Refinement

'WPROD2' 4 14 38 38 1 1 32 1 1 1*/

ENDFIN

REFINE

'WPROD2' /

NXFIN

2 3 3 3 3 3 3 3 3 3 /

ENDFIN

REFINE

'WPROD2' /

HXFIN

90 10 27.19 45.63 27.19 34.03 31.94 34.03 38.01 23.97 38.01 40.4 19.2 40.4

41.42 17.17 41.42 40.88 18.24 40.88 38.46 23.08 38.46 33.57 32.87 33.57 24.92

50.15 24.92 10 80 10 /

ENDFIN

AMALGAM

-- LGR Amalgamations

'PROD1' 'WPROD1' /

'PROD2' 'WPROD2' /

/

CARFIN

-- Cartesian Local Grid Refinement

'INJ' 5 15 20 20 5 5 32 1 1 1*/

ENDFIN

REFINE

'INJ' /

NXFIN

3 3 3 3 3 3 3 3 3 2 /

ENDFIN

REFINE

'INJ' /

HXFIN

10 80 10 23.41 53.17 23.41 32.04 35.92 32.04 37.67 24.65 37.67 41.15

17.69476225 41.15 43.2 13.6 43.19963572 44.36 11.27423636 44.36288182 44.96

10.08117841 44.95941079 45.12 9.768768917 45.11561554 44.52 10.97 44.52 10 90

/

EQUALS

PORO 0.2 /

/

EQUALS

PERMI 1000 /

/

EQUALS

PERMJ 1000 /

/

EQUALS

PERMK 100 /

/



สถาบันวิทยบริการ
จุฬาลงกรณ์มหาวิทยาลัย

PVT section

PVTW

-- Water PVT Properties

--	P _{ref}	B _w	c _w	μ	Viscosity
	1450	1.01	0	1	4.437172e-06

/

PVDO

-- Dead Oil PVT Properties (No Dissolved Gas)

--	Pressure	B _o	Viscosity
	14.7	1.05787	1
	293.3	1.048232	1
	434.2	1.048068	1
	644	1.047956	1
	853.7	1.0479	1
	1063.5	1.047846	1
	1273.2	1.047843	1
	1483	1.047826	1
	1620	1.047812	1
	1902.5	1.047804	1
	2112.2	1.047796	1
	2322	1.04779	1
	2531.7	1.047785	1
	2741.5	1.04778	1
	2951.2	1.047776	1
	3161	1.047773	1
	3370	1.04777	1
	3580.5	1.047767	1
	3790.2	1.047765	1
	4000	1.047763	1

/

DENSITY

-- Fluid Densities at Surface Conditions

Oil API	Water S.G.	Gas S.G.
54.9	62.430	0.0561851 /

ROCK

-- Rock Properties

Pressure	Compressibility
1450	1.52989e-06 /

SCAL section

SWOF

-- Water/Oil Saturation Functions

Sw	krw	kro	Pc
0.2	0	0.5	0
0.26666667	0.00068587106	0.41902624	0
0.33333333	0.0054869684	0.34296776	0
0.4	0.018518519	0.27216553	0
0.46666667	0.043895748	0.20704333	0
0.53333333	0.085733882	0.14814815	0
0.6	0.14814815	0.096225045	0
0.66666667	0.23525377	0.05237828	0
0.73333333	0.35116598	0.018518519	0
0.8	0.5	0	0
1	0.5	0	0

/

สถาบันวิทยบริการ
จุฬาลงกรณ์มหาวิทยาลัย

Schedule section

WELSPECL

'INJ' '1' 'INJ' 2 1 5080 'WATER' 1* 'STD' 'SHUT' 'YES' 1* 'AVG' 3* 'STD' /

/

COMPDATL

'INJ' 'INJ' 31 1 1 1 'SHUT' 2* 0.164 3* 'X' 1* /

/

COMPDATL

'INJ' 'INJ' 30 1 1 1 'SHUT' 2* 0.164 3* 'X' 1* /

/

COMPDATL

'INJ' 'INJ' 29 1 1 1 'OPEN' 2* 0.164 3* 'X' 1* /

/

COMPDATL

'INJ' 'INJ' 28 1 1 1 'SHUT' 2* 0.164 3* 'X' 1* /

/

COMPDATL

'INJ' 'INJ' 27 1 1 1 'SHUT' 2* 0.164 3* 'X' 1* /

/

COMPDATL

'INJ' 'INJ' 26 1 1 1 'OPEN' 2* 0.164 3* 'X' 1* /

/

COMPDATL

'INJ' 'INJ' 25 1 1 1 'SHUT' 2* 0.164 3* 'X' 1* /

/

COMPDATL

'INJ' 'INJ' 24 1 1 1 'SHUT' 2* 0.164 3* 'X' 1* /

/

COMPDATL

'INJ' 'INJ' 23 1 1 1 'OPEN' 2* 0.164 3* 'X' 1* /

/

COMPDATL

'INJ' 'INJ' 22 1 1 1 'SHUT' 2* 0.164 3* 'X' 1* /
/

COMPDATL

'INJ' 'INJ' 21 1 1 1 'SHUT' 2* 0.164 3* 'X' 1* /
/

COMPDATL

'INJ' 'INJ' 20 1 1 1 'OPEN' 2* 0.164 3* 'X' 1* /
/

COMPDATL

'INJ' 'INJ' 19 1 1 1 'SHUT' 2* 0.164 3* 'X' 1* /
/

COMPDATL

'INJ' 'INJ' 18 1 1 1 'SHUT' 2* 0.164 3* 'X' 1* /
/

COMPDATL

'INJ' 'INJ' 17 1 1 1 'OPEN' 2* 0.164 3* 'X' 1* /
/

COMPDATL

'INJ' 'INJ' 16 1 1 1 'SHUT' 2* 0.164 3* 'X' 1* /
/

COMPDATL

'INJ' 'INJ' 15 1 1 1 'SHUT' 2* 0.164 3* 'X' 1* /
/

COMPDATL

'INJ' 'INJ' 14 1 1 1 'OPEN' 2* 0.164 3* 'X' 1* /
/

COMPDATL

'INJ' 'INJ' 13 1 1 1 'SHUT' 2* 0.164 3* 'X' 1* /
/

COMPDATL

'INJ' 'INJ' 12 1 1 1 'SHUT' 2* 0.164 3* 'X' 1* /
/

COMPDATL

'INJ' 'INJ' 11 1 1 1 'OPEN' 2* 0.164 3* 'X' 1* /
/

COMPDATL

'INJ' 'INJ' 10 1 1 1 'SHUT' 2* 0.164 3* 'X' 1* /
/

COMPDATL

'INJ' 'INJ' 9 1 1 1 'SHUT' 2* 0.164 3* 'X' 1* /
/

COMPDATL

'INJ' 'INJ' 8 1 1 1 'OPEN' 2* 0.164 3* 'X' 1* /
/

COMPDATL

'INJ' 'INJ' 7 1 1 1 'SHUT' 2* 0.164 3* 'X' 1* /
/

COMPDATL

'INJ' 'INJ' 6 1 1 1 'SHUT' 2* 0.164 3* 'X' 1* /
/

COMPDATL

'INJ' 'INJ' 5 1 1 1 'OPEN' 2* 0.164 3* 'X' 1* /
/

COMPDATL

'INJ' 'INJ' 4 1 1 1 'SHUT' 2* 0.164 3* 'X' 1* /
/

COMPDATL

'INJ' 'INJ' 3 1 1 1 'SHUT' 2* 0.164 3* 'X' 1* /
/

COMPDATL

'INJ' 'INJ' 2 1 1 1 'OPEN' 2* 0.164 3* 'X' 1* /
/

COMPDATL

'INJ' 'INJ' 1 1 1 1 'SHUT' 2* 0.164 3* 'X' 1* /
/

WELSEGS

'INJ' 5090 2* 'INC' 'HFA' 'DF' 2* /

2 2 1 1 90 0 0.164 0.001 4* /

3 11 1 2 160 0 0.164 0.001 4* /

/

COMPSEGL

'INJ' /

'INJ' 31 1 1 1 2* 'X' 1 2* /

/

WCONINJE

'INJ' 'WATER' 'SHUT' 'RATE' 6000 1* 7000 3* /

/

WELSPECL

'PROD1' '1' 'WPROD1' 2 1 5000 'OIL' 1* 'STD' 'SHUT' 'YES' 1* 'AVG' 3* 'STD' /

/

COMPDATL

'PROD1' 'WPROD1' 2 1 1 1 'SHUT' 2* 0.164 3* 'X' 1* /

/

COMPDATL

'PROD1' 'WPROD1' 3 1 1 1 'SHUT' 2* 0.164 3* 'X' 1* /

/

COMPDATL

'PROD1' 'WPROD1' 4 1 1 1 'OPEN' 2* 0.164 3* 'X' 1* /

/

COMPDATL

'PROD1' 'WPROD1' 5 1 1 1 'SHUT' 2* 0.164 3* 'X' 1* /

/

COMPDATL

'PROD1' 'WPROD1' 6 1 1 1 'SHUT' 2* 0.164 3* 'X' 1* /

/

COMPDATL

'PROD1' 'WPROD1' 7 1 1 1 'OPEN' 2* 0.164 3* 'X' 1* /

/

COMPDATL

'PROD1' 'WPROD1' 8 1 1 1 'SHUT' 2* 0.164 3* 'X' 1* /
/

COMPDATL

'PROD1' 'WPROD1' 9 1 1 1 'SHUT' 2* 0.164 3* 'X' 1* /
/

COMPDATL

'PROD1' 'WPROD1' 10 1 1 1 'OPEN' 2* 0.164 3* 'X' 1* /
/

COMPDATL

'PROD1' 'WPROD1' 11 1 1 1 'SHUT' 2* 0.164 3* 'X' 1* /
/

COMPDATL

'PROD1' 'WPROD1' 12 1 1 1 'SHUT' 2* 0.164 3* 'X' 1* /
/

COMPDATL

'PROD1' 'WPROD1' 13 1 1 1 'OPEN' 2* 0.164 3* 'X' 1* /
/

COMPDATL

'PROD1' 'WPROD1' 14 1 1 1 'SHUT' 2* 0.164 3* 'X' 1* /
/

COMPDATL

'PROD1' 'WPROD1' 15 1 1 1 'SHUT' 2* 0.164 3* 'X' 1* /
/

COMPDATL

'PROD1' 'WPROD1' 16 1 1 1 'OPEN' 2* 0.164 3* 'X' 1* /
/

COMPDATL

'PROD1' 'WPROD1' 17 1 1 1 'SHUT' 2* 0.164 3* 'X' 1* /
/

COMPDATL

'PROD1' 'WPROD1' 18 1 1 1 'SHUT' 2* 0.164 3* 'X' 1* /
/

COMPDATL

'PROD1' 'WPROD1' 19 1 1 1 'OPEN' 2* 0.164 3* 'X' 1* /
/

COMPDATL

'PROD1' 'WPROD1' 20 1 1 1 'SHUT' 2* 0.164 3* 'X' 1* /
/

COMPDATL

'PROD1' 'WPROD1' 21 1 1 1 'SHUT' 2* 0.164 3* 'X' 1* /
/

COMPDATL

'PROD1' 'WPROD1' 22 1 1 1 'OPEN' 2* 0.164 3* 'X' 1* /
/

COMPDATL

'PROD1' 'WPROD1' 23 1 1 1 'SHUT' 2* 0.164 3* 'X' 1* /
/

COMPDATL

'PROD1' 'WPROD1' 24 1 1 1 'SHUT' 2* 0.164 3* 'X' 1* /
/

COMPDATL

'PROD1' 'WPROD1' 25 1 1 1 'OPEN' 2* 0.164 3* 'X' 1* /
/

COMPDATL

'PROD1' 'WPROD1' 26 1 1 1 'SHUT' 2* 0.164 3* 'X' 1* /
/

COMPDATL

'PROD1' 'WPROD1' 27 1 1 1 'SHUT' 2* 0.164 3* 'X' 1* /
/

COMPDATL

'PROD1' 'WPROD1' 28 1 1 1 'OPEN' 2* 0.164 3* 'X' 1* /
/

COMPDATL

'PROD1' 'WPROD1' 29 1 1 1 'SHUT' 2* 0.164 3* 'X' 1* /
/

COMPDATL

'PROD1' 'WPROD1' 30 1 1 1 'SHUT' 2* 0.164 3* 'X' 1* /
/

COMPDATL

'PROD1' 'WPROD1' 31 1 1 1 'OPEN' 2* 0.164 3* 'X' 1* /
/

COMPDATL

'PROD1' 'WPROD1' 32 1 1 1 'SHUT' 2* 0.164 3* 'X' 1* /
/

WELSPECL

'PROD2' '1' 'WPROD2' 2 1 5000 'OIL' 1* 'STD' 'SHUT' 'YES' 1* 'AVG' 3* 'STD' /
/

COMPDATL

'PROD2' 'WPROD2' 2 1 1 1 'SHUT' 2* 0.164 3* 'X' 1* /
/

COMPDATL

'PROD2' 'WPROD2' 3 1 1 1 'SHUT' 2* 0.164 3* 'X' 1* /
/

COMPDATL

'PROD2' 'WPROD2' 4 1 1 1 'OPEN' 2* 0.164 3* 'X' 1* /
/

COMPDATL

'PROD2' 'WPROD2' 5 1 1 1 'SHUT' 2* 0.164 3* 'X' 1* /
/

COMPDATL

'PROD2' 'WPROD2' 6 1 1 1 'SHUT' 2* 0.164 3* 'X' 1* /
/

COMPDATL

'PROD2' 'WPROD2' 7 1 1 1 'OPEN' 2* 0.164 3* 'X' 1* /
/

COMPDATL

'PROD2' 'WPROD2' 8 1 1 1 'SHUT' 2* 0.164 3* 'X' 1* /
/

COMPDATL

'PROD2' 'WPROD2' 9 1 1 1 'SHUT' 2* 0.164 3* 'X' 1* /
/

COMPDATL

'PROD2' 'WPROD2' 10 1 1 1 'OPEN' 2* 0.164 3* 'X' 1* /
/

COMPDATL

'PROD2' 'WPROD2' 11 1 1 1 'SHUT' 2* 0.164 3* 'X' 1* /
/

COMPDATL

'PROD2' 'WPROD2' 12 1 1 1 'SHUT' 2* 0.164 3* 'X' 1* /
/

COMPDATL

'PROD2' 'WPROD2' 13 1 1 1 'OPEN' 2* 0.164 3* 'X' 1* /
/

COMPDATL

'PROD2' 'WPROD2' 14 1 1 1 'SHUT' 2* 0.164 3* 'X' 1* /
/

COMPDATL

'PROD2' 'WPROD2' 15 1 1 1 'SHUT' 2* 0.164 3* 'X' 1* /
/

COMPDATL

'PROD2' 'WPROD2' 16 1 1 1 'OPEN' 2* 0.164 3* 'X' 1* /
/

COMPDATL

'PROD2' 'WPROD2' 17 1 1 1 'SHUT' 2* 0.164 3* 'X' 1* /
/

COMPDATL

'PROD2' 'WPROD2' 18 1 1 1 'SHUT' 2* 0.164 3* 'X' 1* /
/

COMPDATL

'PROD2' 'WPROD2' 19 1 1 1 'OPEN' 2* 0.164 3* 'X' 1* /
/

COMPDATL

'PROD2' 'WPROD2' 20 1 1 1 'SHUT' 2* 0.164 3* 'X' 1* /
/

COMPDATL

'PROD2' 'WPROD2' 21 1 1 1 'SHUT' 2* 0.164 3* 'X' 1* /
/

COMPDATL

'PROD2' 'WPROD2' 22 1 1 1 'OPEN' 2* 0.164 3* 'X' 1* /
/

COMPDATL

'PROD2' 'WPROD2' 23 1 1 1 'SHUT' 2* 0.164 3* 'X' 1* /
/

COMPDATL

'PROD2' 'WPROD2' 24 1 1 1 'SHUT' 2* 0.164 3* 'X' 1* /
/

COMPDATL

'PROD2' 'WPROD2' 25 1 1 1 'OPEN' 2* 0.164 3* 'X' 1* /
/

COMPDATL

'PROD2' 'WPROD2' 26 1 1 1 'SHUT' 2* 0.164 3* 'X' 1* /
/

COMPDATL

'PROD2' 'WPROD2' 27 1 1 1 'SHUT' 2* 0.164 3* 'X' 1* /
/

COMPDATL

'PROD2' 'WPROD2' 28 1 1 1 'OPEN' 2* 0.164 3* 'X' 1* /
/

COMPDATL

'PROD2' 'WPROD2' 29 1 1 1 'SHUT' 2* 0.164 3* 'X' 1* /
/

COMPDATL

'PROD2' 'WPROD2' 30 1 1 1 'SHUT' 2* 0.164 3* 'X' 1* /
/

COMPDATL

'PROD2' 'WPROD2' 31 1 1 1 'OPEN' 2* 0.164 3* 'X' 1* /
/

COMPDATL

'PROD2' 'WPROD2' 32 1 1 1 'SHUT' 2* 0.164 3* 'X' 1* /
/

WELSEGS

'PROD1' 5010 2* 'INC' 'HFA' 'DF' 2* /
2 2 1 1 90 0 0.164 0.001 4* /
3 11 1 2 160 0 0.164 0.001 4* /
/

WELSEGS

'PROD2' 5010 2* 'INC' 'HFA' 'DF' 2* /
2 2 1 1 90 0 0.164 0.001 4* /
3 11 1 2 160 0 0.164 0.001 4* /
/

COMPSEGL

'PROD1' /
'WPROD1' 2 1 1 1 2* 'X' 32 2* /
/

COMPSEGL

'PROD2' /
'WPROD2' 2 1 1 1 2* 'X' 32 2* /
/

WCONPROD

'PROD1' 'SHUT' 'LRAT' 3* 3000 1* 100 3* /
/

WCONPROD

'PROD2' 'SHUT' 'LRAT' 3* 3000 1* 100 3* /
/

WSEGITER

50 50 2* /

RPTSCHED

'PRES' 'SOIL' 'SWAT' 'SGAS' 'RS' 'RV' 'RESTART=2' /

RPTRST

'BASIC=2' /

TUNING

10* /

11* /

2* 150 7* /

TSTEP

29.4166666666667 /

WCONINJE

'INJ' 'WATER' 'OPEN' 'RESV' 6000 6000 7000 3* /

/

WCONPROD

'PROD1' 'OPEN' 'RESV' 3* 3000 3000 100 3* /

/

WECON

'PROD1' 2* 0.5 2* 'NONE' 'YES' 1* 'RATE' 1* 'NONE' 2* /

/

WCONPROD

'PROD2' 'OPEN' 'RESV' 3* 3000 3000 100 3* /

/

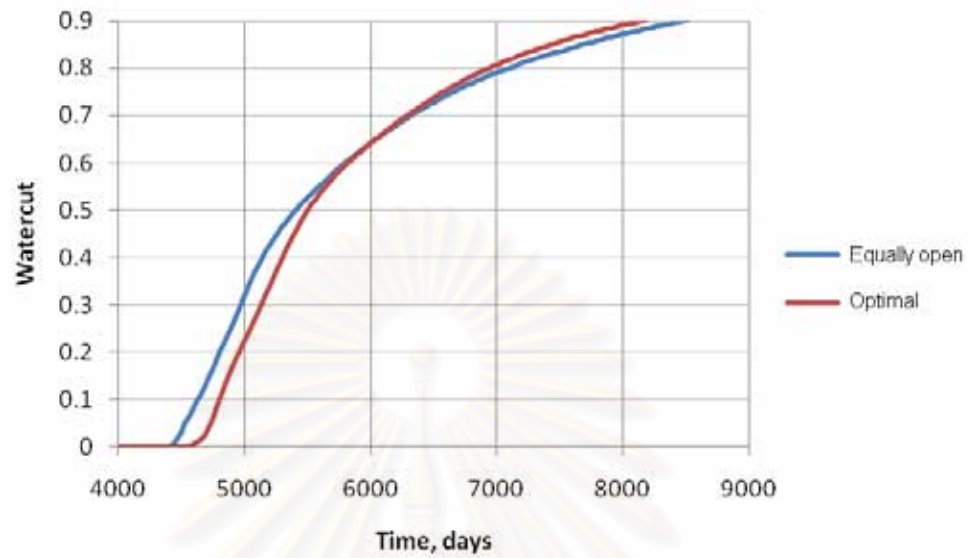
WECON

'PROD2' 2* 0.5 2* 'NONE' 'YES' 1* 'RATE' 1* 'NONE' 2* /

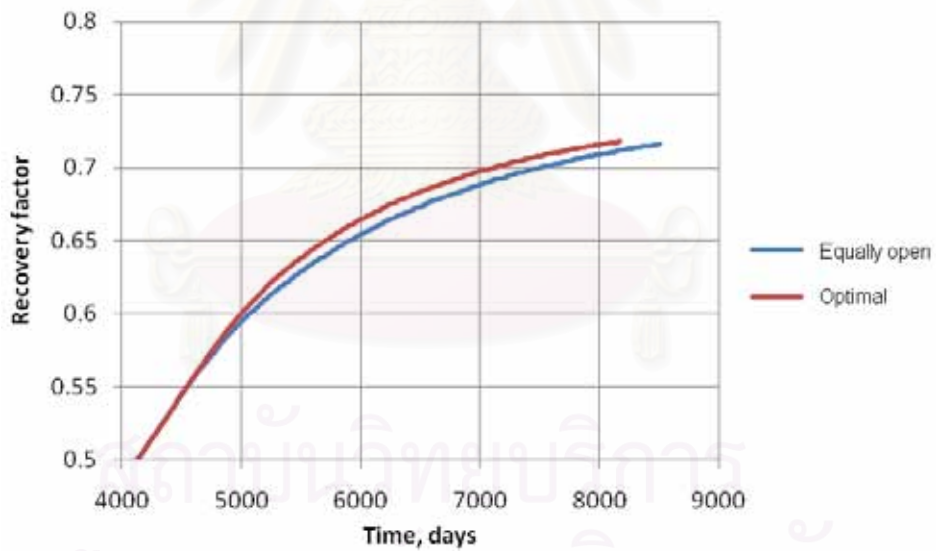
/

สงวนลิขสิทธิ์
จุฬาลงกรณ์มหาวิทยาลัย

APPENDIX B

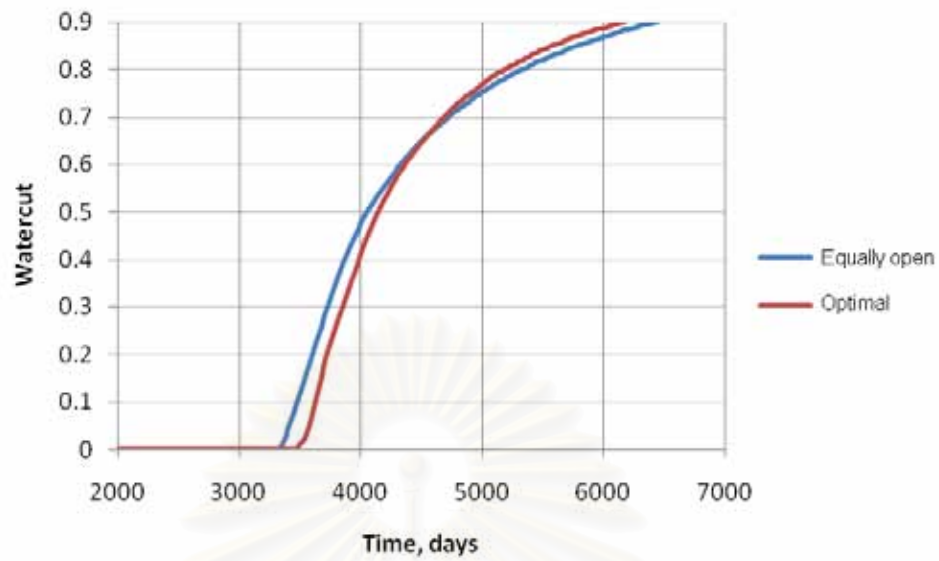


(a) Watercut profile

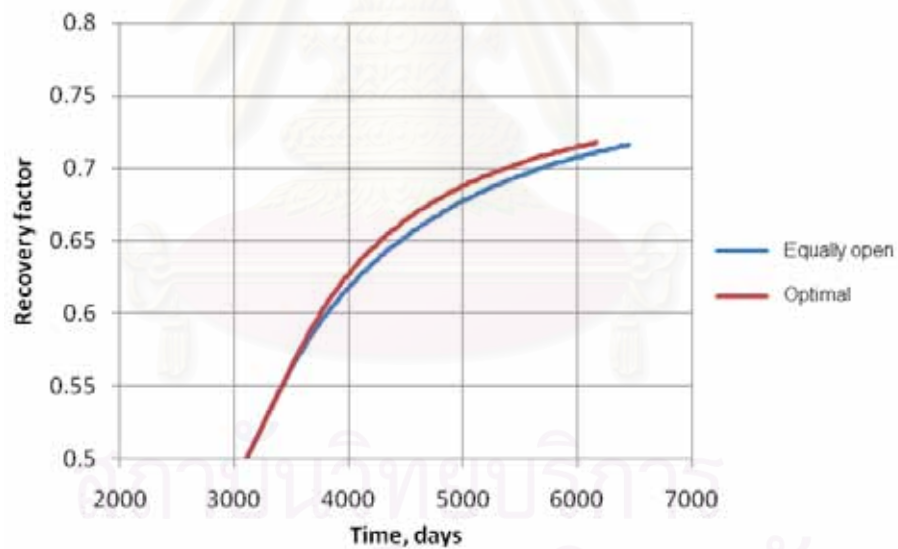


(b) Recovery factor profile

Figure B1: Comparison of watercut and recovery profile obtained from the base case and the optimal completion for the operating flow rate of 6,000 RB/D and mobility ratio of 1.

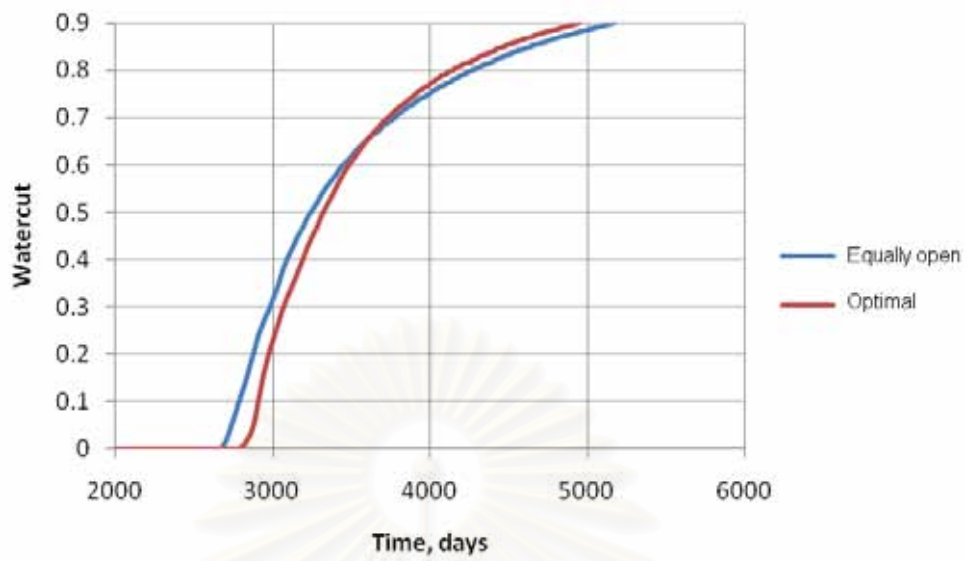


(a) Watercut profile

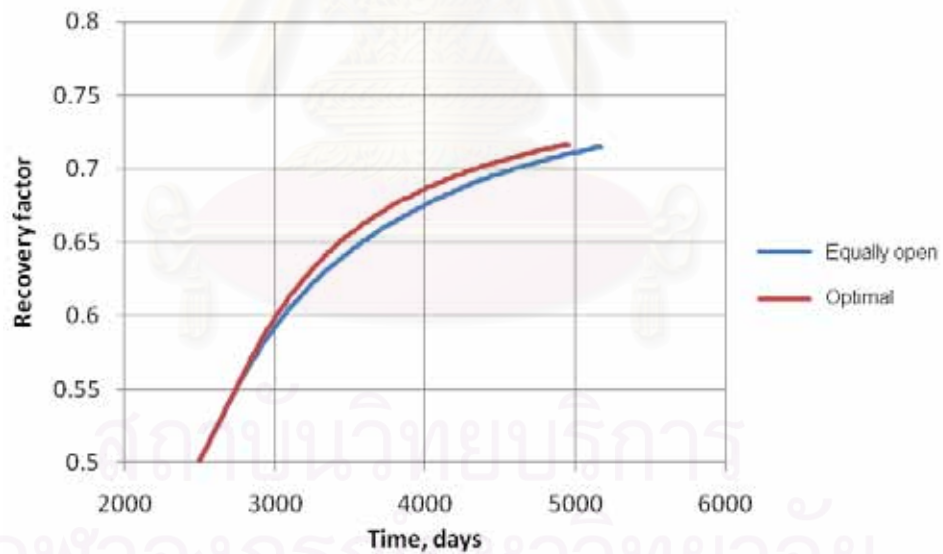


(b) Recovery factor profile

Figure B2: Comparison of watercut and recovery profile obtained from the base case and the optimal completion for the operating flow rate of 8,000 RB/D and mobility ratio of 1.

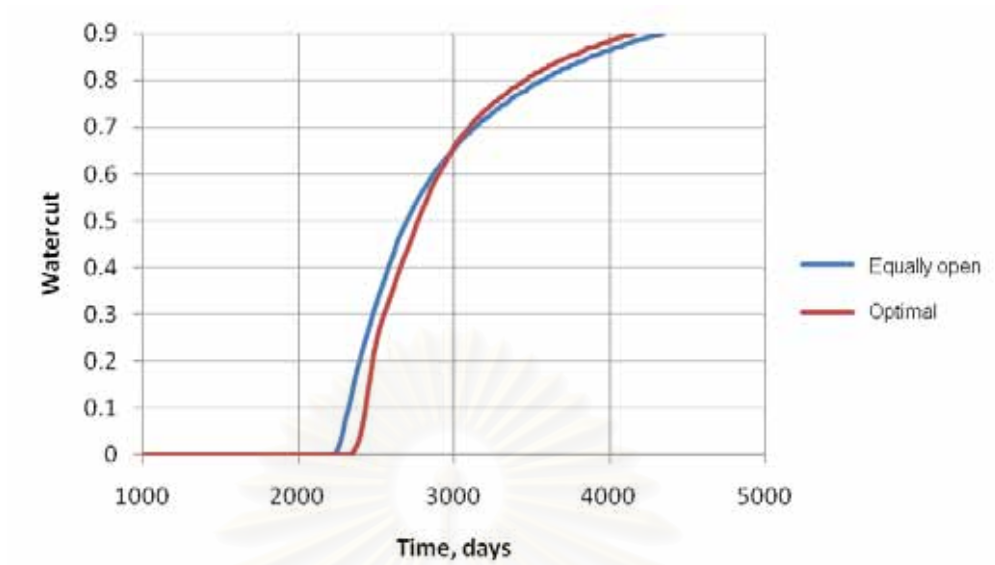


(a) Watercut profile

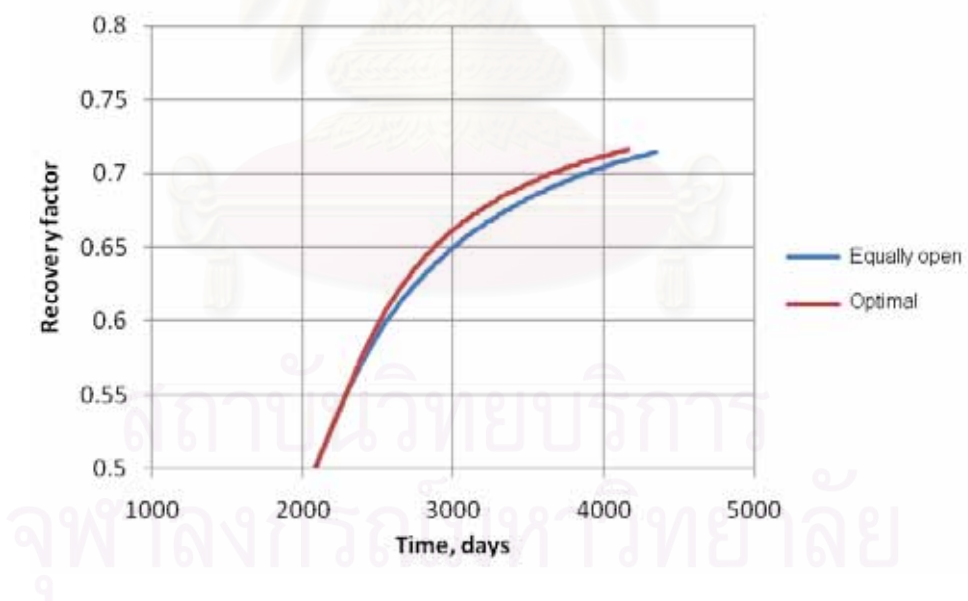


(b) Recovery factor profile

Figure B3: Comparison of watercut and recovery profile obtained from the equally open and the optimal completion for the operating flow rate of 10,000 RB/D and mobility ratio of 1.

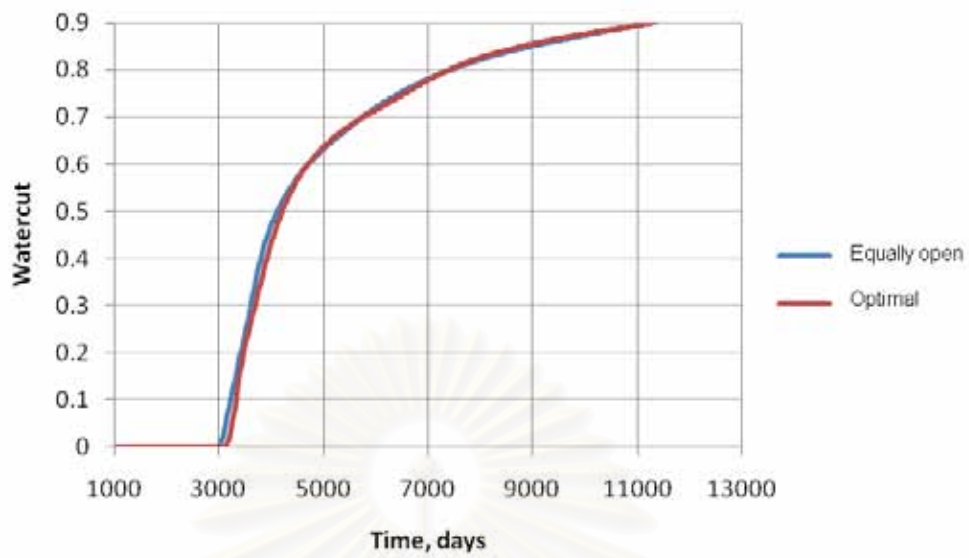


(a) Watercut profile

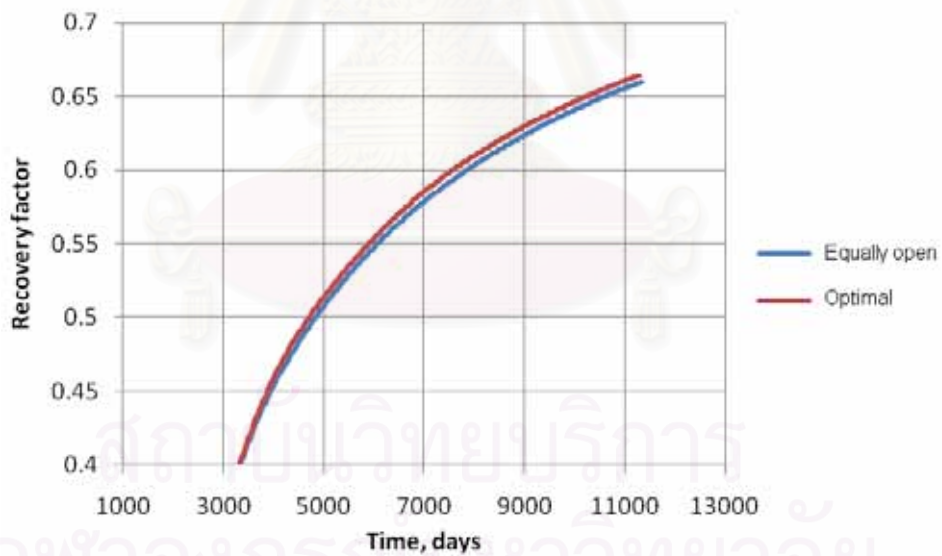


(b) Recovery factor profile

Figure B4: Comparison of watercut and recovery profile obtained from the equally open and the optimal completion for the operating flow rate of 12,000 RB/D and mobility ratio of 1.

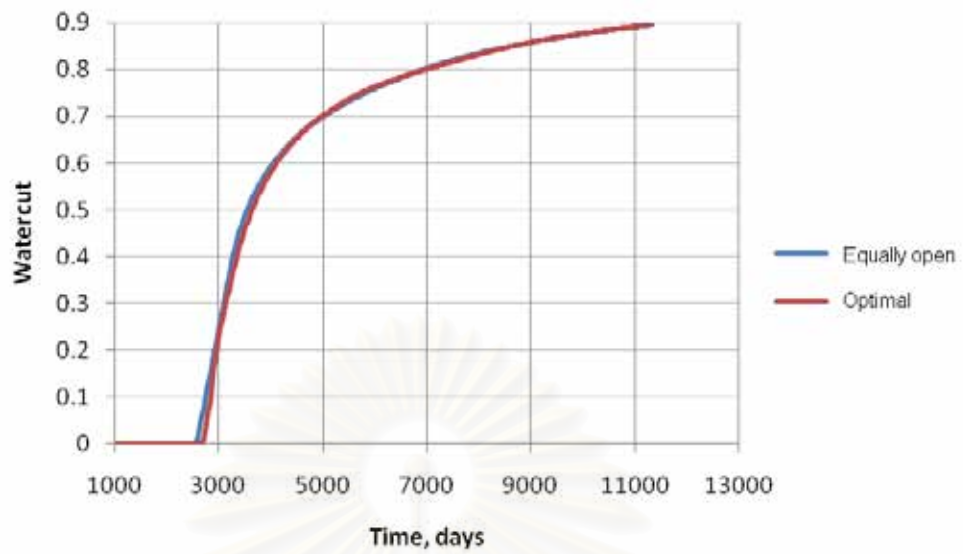


(a) Watercut profile

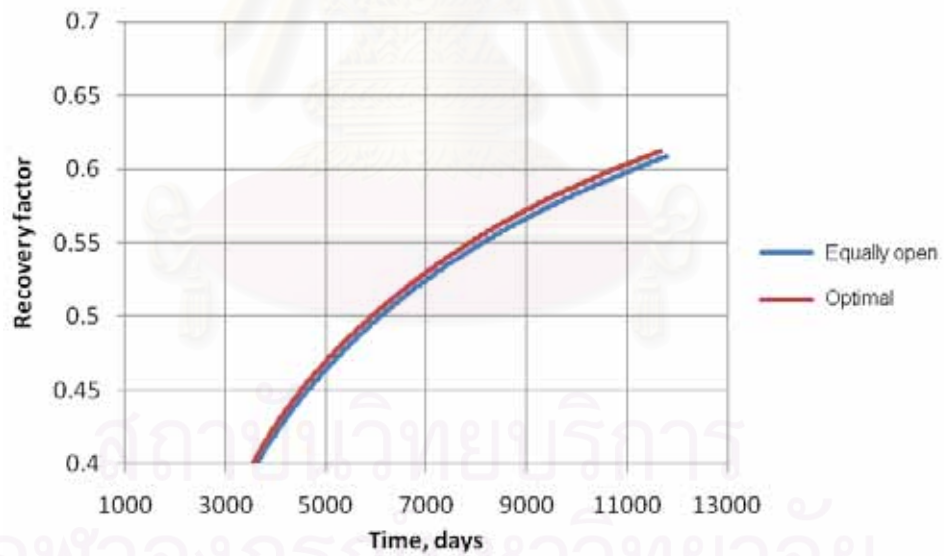


(b) Recovery factor profile

Figure B5: Comparison of watercut and recovery profile obtained from the equally open and the optimal completion for the operating flow rate of 6,000 RB/D and mobility ratio of 3.

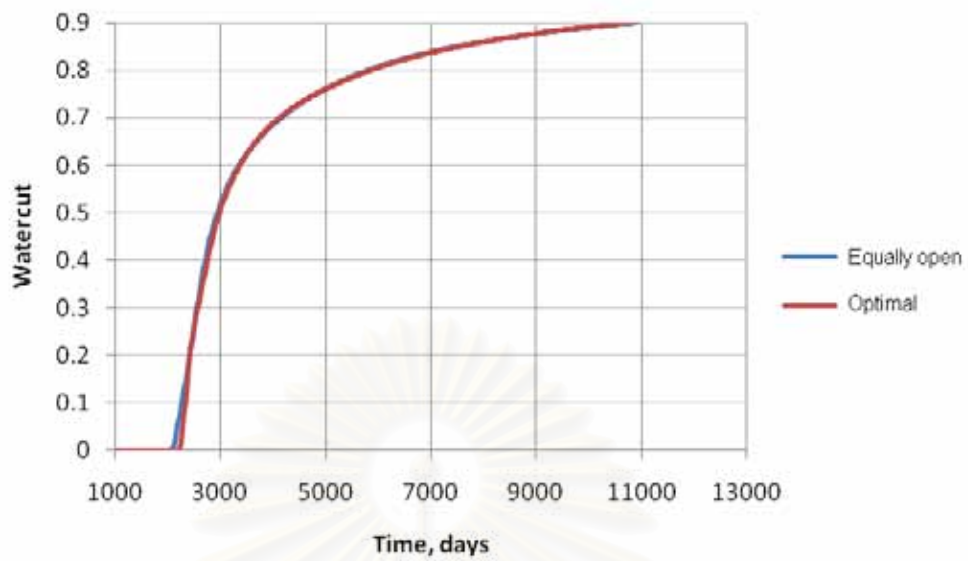


(a) Watercut profile

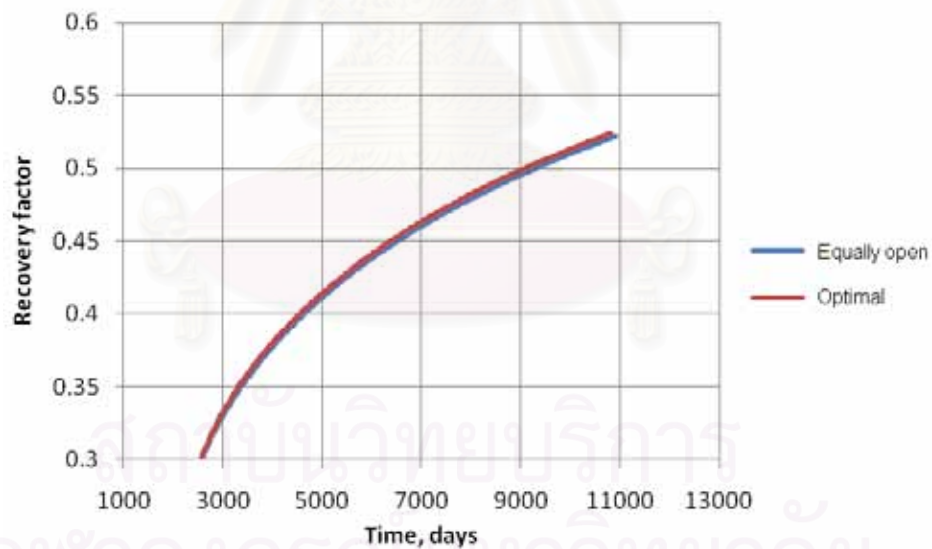


(b) Recovery factor profile

Figure B6: Comparison of watercut and recovery profile obtained from the equally open and the optimal completion for the operating flow rate of 6,000 RB/D and mobility ratio of 5.



(a) Watercut profile



(b) Recovery factor profile

Figure B7: Comparison of watercut and recovery profile obtained from the equally open and the optimal completion for the operating flow rate of 6,000 RB/D and mobility ratio of 10.

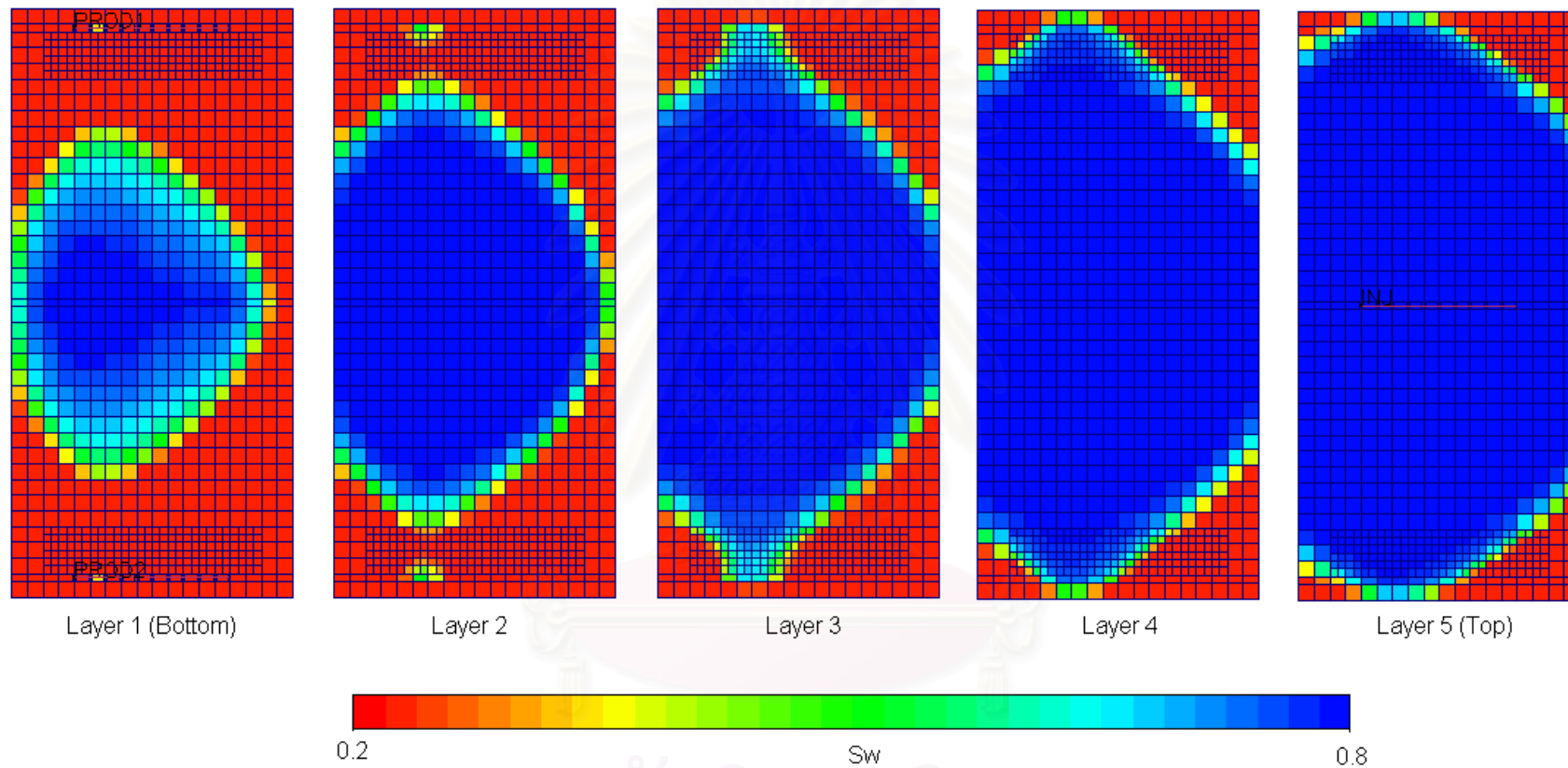


Figure B8: Saturation distribution at breakthrough time for equally open completion in direct line drive pattern with operating flow rate of 6,000 RB/D and mobility ratio of 1.

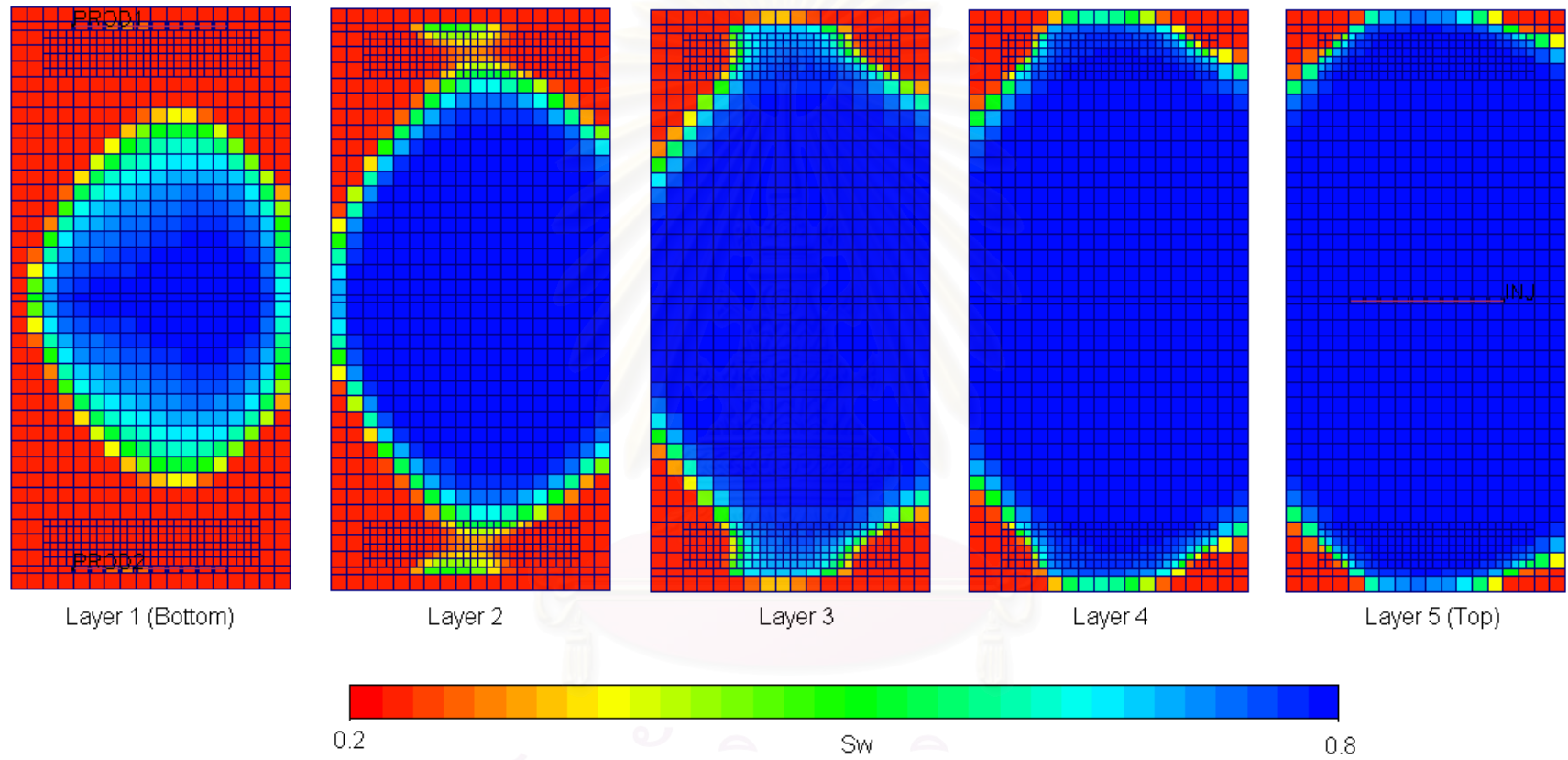


Figure B9: Saturation distribution at breakthrough time for equally open completion in inverted line drive pattern with operating flow rate of 6,000 RB/D and mobility ratio of 1.

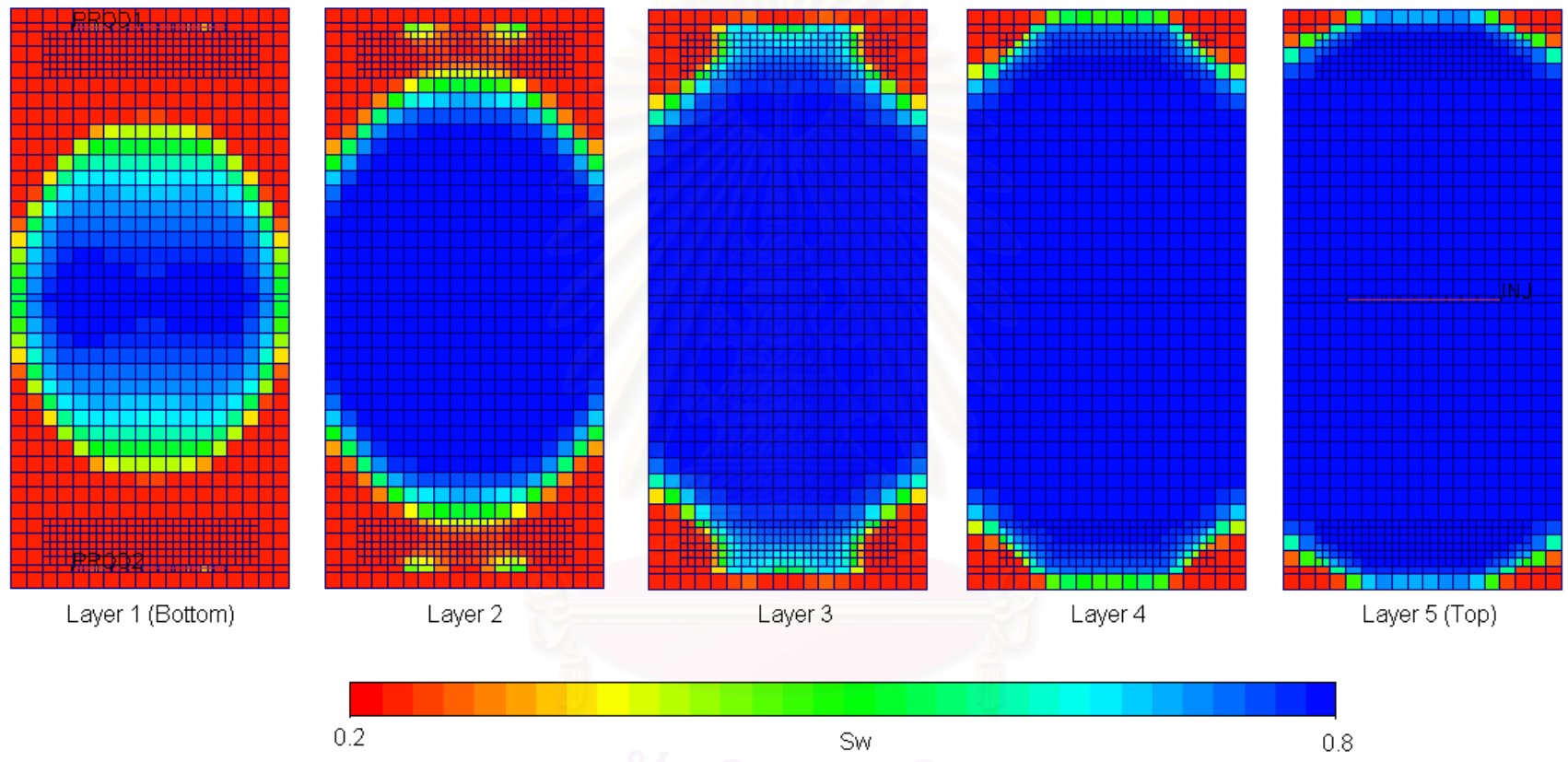


Figure B10: Saturation distribution at breakthrough time for optimal completion in inverted line drive pattern with operating flow rate of 6,000 RB/D and mobility ratio of 1.

VITAE

Komsant Suriyawutithum was born on March, 1982 in Bangkok, Thailand. He received his B.Eng. in Aerospace Engineering from the Faculty of Engineering, Kasetsart University in 2004. After graduating, he worked for Denso (Thailand) company for one and half year and then he resigned his work to study the Master of Petroleum Engineering at the Department of Mining and Petroleum Engineering, Faculty of Engineering, Chulalongkorn University.



สถาบันวิทยบริการ
จุฬาลงกรณ์มหาวิทยาลัย